THE STRUCTURE OF COESITE
AND THE
CLASSIFICATION OF TETRAHEDRAL STRUCTURES.

by

Tibor Zoltai
B.A.Sc. University of Toronto
(1955)

Submitted in partial fulfillment of the
requirements for the degree of Doctor
of Philosophy
at the
Massachusetts Institute of Technology
(1959)

Signature of author ....
May 4th, 1959. Department of Geology and Geophysics

Certified by ....
Thesis Superviser

Accepted by ....
Chairman, Departmental Comitee on Graduate Students

Preface.

This thesis investigation began with the structure determination of coesite but, once the structure was obtained, the study of its characteristics led to the investigation of various topics. The presence of 4-membered rings of tetrahedra in coesite as opposed to larger rings in low pressure silicas indicated a possible connection between the size of the rings and the energy of the structures. Consequently this relationship was studied. Once the size of the rings was found to be a function of energy, this appeared to be a natural basis for the subclassification of the tetrahedral structures. During the improvement of the classification several other characteristics of tetrahedral structures were noticed and incorporated in the new classification. Due to the mineralogical importance of the silicates the latters were described separately. A large number of structure models were constructed during the course of the improvement of the classification of tetrahedral structures. A novel technique was developed for their construction which appears to be interesting enough for publication. The thesis is, thus, the report of a coherent study, although separated into five publishable sections.

Abstract.

I. The crystal structure of coesite, the dense, high-pressure form of silica.

Coesite is monoclinic, and described in the first setting by the dimensions a= 7.17 Å, b= 7.17 Å, c= 12.38 Å, $\gamma = 120^{\circ}$, space group B2/b, Z= 16 SiO_2 per cell. Three-dimensional intensity data were obtained from precession photographs using MoKα radiation. The full three-dimensional Patterson function was computed and this was solved for an approximation to the electron density by use of minimum functions. The analysis was started with the aid of a new theoretical device for the location of inversion peaks.

In coesite, Si is tetrahedrally surrounded by four oxygen atoms, and the structure is a new tetrahedral network. There is a certain resemblance between the coesite structure and the alumina-silica network in feldspar.

II. The relative energies of rings of tetrahedra.

The structure of coesite was compared with the structures of the other forms of silica. It was noted that

high-pressure coesite has 4-membered loops of tetrahedra, that the normal-pressure quartz, tridymite and cristobalite have 6-membered loops of tetrahedra and that intermediate - pressure keatite has 5-membered loops of tetrahedra in their structures. This observation stimulated a quantitative investigation of the relative energies of isolated neutral tetrahedral rings. These rings were assumed to be composed of tetrahedra whose relative orientations were similar to those of the benitoite and beryl rings. The energies of 2- to 10-membered rings and of an infinite chain were computed. The energies obtained indicate that the 5-membered tetrahedral ring is the most stable, and that 6- and 4-membered rings have the next lowest energies. Using these data the relative energies of silica structures containing regular tetrahedral rings were estimated and found to correspond with their relative stability.

III. Classification of tetrahedral structures.

The old classification of the silicates is no longer sufficient to classify the ever-increasing number of determined ionic tetrahedral structures. More detail is desirable in the classification, and consequently, new classification criteria are necessary to provide larger number of subdivisions. The study of the relative energies of isolated rings of tetrahedra suggests that the size of the tetrahedral loops may be used as one additional criterion. A second criterion is based on the different nature of the corner sharing of tetrahedra. A numerical expression, called the sharing coefficient is derived to cover this criterion. These two criteria are added to the revised geometric system of the customary silicate classification, and consequently, the classification proposed is basically in accordance with the accepted scheme.

A classification table is given, and illustrated with examples. Special attention has been paid to the collection of examples of tetrahedral structures with three-dimensional networks of tetrahedra. These examples include silicates, sulphates, germanates, and other compounds with tetrahedral structures.

IV. Classification of silicates.

A revised classification is presented with a sufficient number of subdivisions, not only for the simpler silicate structures, but also for the more complicated three-dimensional networks. This classification is based on the classification of tetrahedral structures previously presented by the author. A consistent treatment of the different tetrahedrally coordinated cations in the silicates is discussed. It is suggested that all of the tetrahedrally coordinated cations should be considered as part of the tetrahedral frame of a silicate. provided, that their bonding is similar to that of the silicon.

Tetrahedral models were constructed for the illustration of the tetrahedral frames of the silicates with three-dimensional networks of tetrahedra. Photographs of these models are enclosed.

V. Simple technique for the construction of polyhedral structure models.

A simple, inexpensive and efficient technique is described for the construction of polyhedral crystal-structure models. The polyhedra are made of acetate sheets and are assembled by cementing the polyhedra together with acetone and narrow acetate strips. The construction does not require calculations, but can be done with the aid of tracing a good drawing of the structure. The models made by this technique are illustrative and semi-permanent.

Table of contents.

Part I.

Chapter I. The crystal structure of coesite, the dense, high-pressure form of silica

Chapter III. Classification of tetrahedral structures

Part II.

Supplement to Chapter I.

Supplement to Chapter II.

Supplement to Chapter III.

Supplement to Chapter IV.

Supplement to Chapter V.

List of figures and plates.

Part I.

Part II.

Plates.

Photographs of models of the tetrahedral frames of silicates and of the tetrahedral models of silica structures.

List of tables.

Part I.

Part II.

Acknowledgement.

Thanks are due to Professor M.J. Buerger for his patient guidance, his suggestions and constructive criticism of the thesis text. Thanks are also due to Dr. N. W. Thibault and Dr. L. Coes Jr. for the samples of coesite crystals, and to Dr. W. Sly for his assistance in the computations of the various mathematical problems associated with the structure analysis of coesite. Dr. E. Parthe's suggestions in the energy computations of the rings of tetrahedra and Professor W. Dennen's constructive criticism of the classification of silicates are gratefully acknowledged. A special thanks is expressed to Messrs. W. Tupper, B. Wuensch, C. T. Prewitt, C. Burnham and D. Peacor for their help in the correction of the English of the text of this thesis.

The author is especially grateful to his wife, Olga, for her tireless patience and understanding during the course of this study.

Chapter I

The crystal structure of coesite, the dense, high-pressure form of silica

Introduction

About five years ago a new form of silica was discovered by Coes[1] who obtained it at high pressures and high temperatures. Since the form has a density of 3.01 g/cc, which is considerably greater than that of quartz, 2.65 g/cc, this discovery aroused considerable interest. There was some informal speculation about the possibility that, in this form, silicon might have six coordination, although MacDonald[2] pointed out that this would require an even greater density than 3.01 g/cc.

We were gathering intensity data for a complete structure determination of coesite when Ramsdell's paper[3] on the crystallography of coesite appeared. When assured by Ramsdell that he planned to proceed no further than the unit cell and space-group determination, we continued our investigation.

Unit cell and space group

The unit cell and space group of coesite were determined with the aid of precession photographs. Ordinarily, unit cell and space-group determinations are routine, but several points are of more than routine interest in this case. In the first place the cell of coesite is dimensionally hexagonal, and no departure from this dimensional symmetry could be observed. The cell dimensions are as follows:

$\underline{a} = 7.17$ Å

$\underline{b} = 7.17$ Å $\qquad \gamma = 120.0°$.

$\underline{c} = 12.38$ Å

$\underline{V} = 550$ A^3

In spite of this hexagonal dimensional symmetry, the distribution of intensities is distinctly monoclinic. To emphasize the hexagonal dimensional symmetry, the first monoclinic setting is chosen. Because of the hexagonal dimensional symmetry the space group can be described in three ways: *A*2/*a*, *B*2/*b*, and I2/*a*. The relations between these descriptions are shown in Fig. 1-1. Due to the close relation of *B*2/*b* to Ramsdell's setting *C*2/*c*, the description *B*2/*b* was retained by us.

The second unusual feature of the cell is that, assuming that the density determination is correct, the cell contains excess matter in some form, for it appears to have 16.6 formula weights of SiO_2 per cell. The cell mass is

$$\begin{aligned} \text{mass} &= \text{density} \times \text{volume} \\ &= 3.01 \times 350 \times 10^{-24} \\ &= 1656 \times 10^{-24} \text{ grams} \\ &= \frac{1656 \times 10^{-24}}{1.66 \times 10^{-24}} = 996 \text{ chemical mass units} \end{aligned}$$

The mass of 16 SiO_2 is 961. Thus a cell contains an excess mass of 35 chemical mass units. Our material was kindly supplied by the Norton Company, Worcester, Massachusetts, through the courtesy of Dr. N. W. Thibault. It was prepared by heating a charge of dry sodium metasilicate and diammonium phosphate at 700°C. and 40,000 atmospheres for 16 hours.

The hexagonal dimensional symmetry and excess cell density were both observed by Ramsdell[3]. Our cell dimensions agree with his within close limits. Our space-group designations differ by interchange of *b* and *c* axes since Ramsdell chose the traditional second monoclinic setting and we have chosen the first monoclinic setting to emphasize the dimensional hexagonal symmetry.

Fig. 1-1

Space group symbols of coesite.

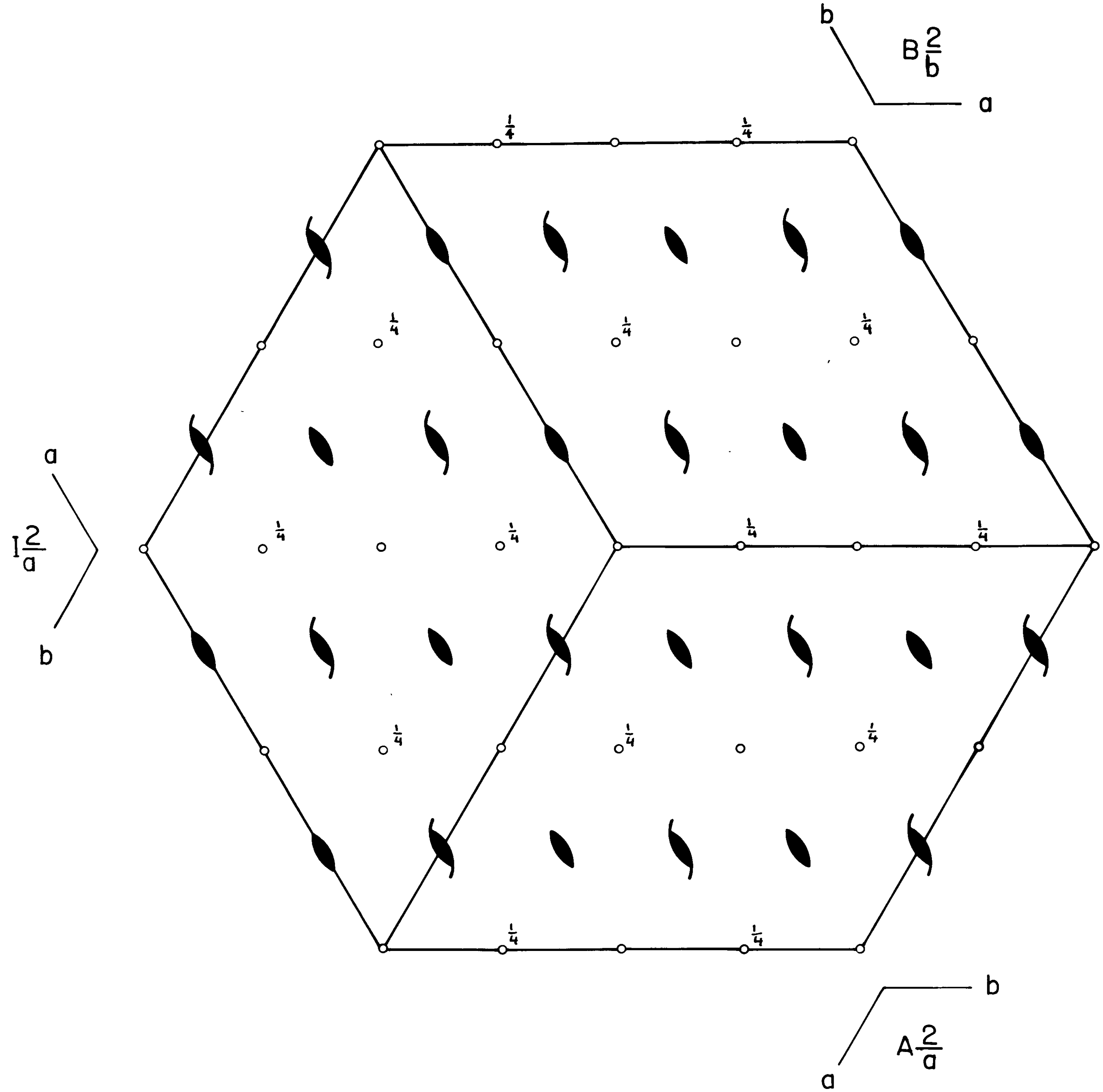
b
B 2/b
a
1/4
a
I 2/a
b
b
A 2/a
a

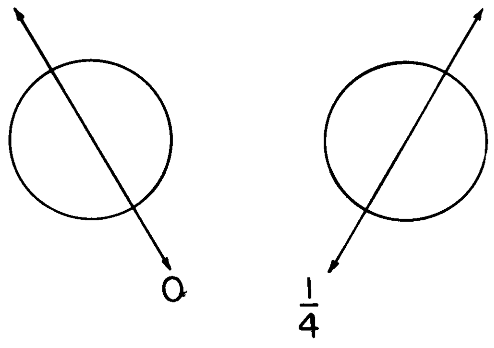
0
1/4

Intensity data

A full set of three-dimensional x-ray diffraction intensities was obtained with a single setting of a crystal, using precession photographs and Mo$K\alpha$ radiation. Some orthographic projections of the crystal used in structure determination are given in Fig. 1-2. The pseudo-hexagonal aspect is evident. The intensities were determined by the M.I.T. modification of the Dawton method[4]. About 900 reflections were measured, some two or three times on different films. All such duplicates were found to correspond to the same F^2 to within 10% error. Although the shape of the crystal was flat (.03 x .10 x .15 mm) the maximum error due to neglect of differential absorption effects when using Mo$K\alpha$ radiation was found to be only about 10%. Accordingly, in transforming intensities to F^2's, absorption was neglected. It was discovered subsequently that extinction was not negligible, however.

Structure analysis

Preliminaries. The structure was solved by solving the three-dimensional Patterson synthesis. This function was computed from our F^2_{hkl} data at the M.I.T. Computation Center using the I.B.M. 704 computer. The program for the Fourier synthesis was prepared by Dr. W. Sly, who also aided us in using it in the computer.

The space group of coesite is $B2/b$. The space group of the corresponding Patterson function is $B2/m$, Fig. 1-3. The asymmetric unit of this space group has a volume of $\frac{1}{8}$ cell. We accordingly computed an asymmetric block of the Patterson synthesis for the range 0-1 along a, 0-$\frac{1}{2}$ along b, and 0-$\frac{1}{4}$ along c. These were synthesized as sections parallel to (001).

Fig. 1-2

Drawing of a well-developed coesite crystal

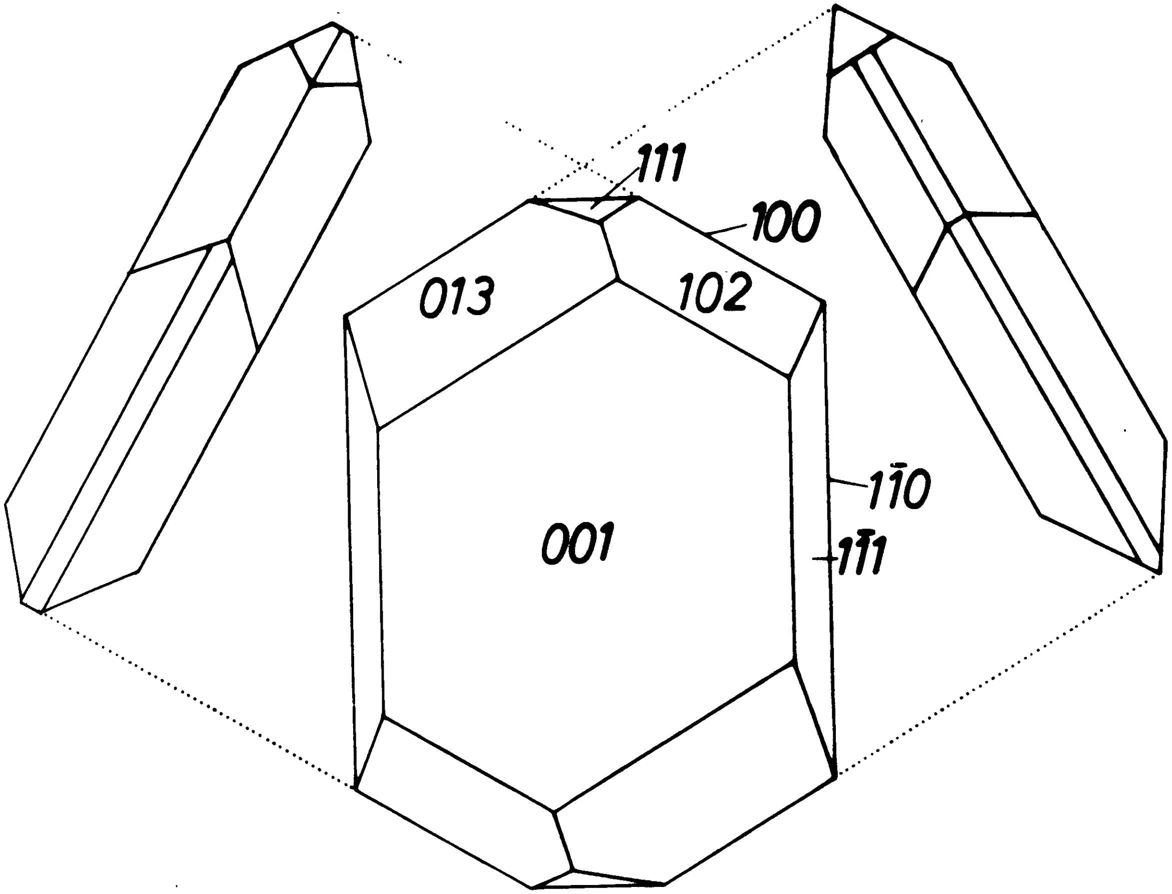
111
100
013
102
001
1$\bar{1}$0
1$\bar{1}$1

Fig. 1-3

Crystal and vector space group of coesite

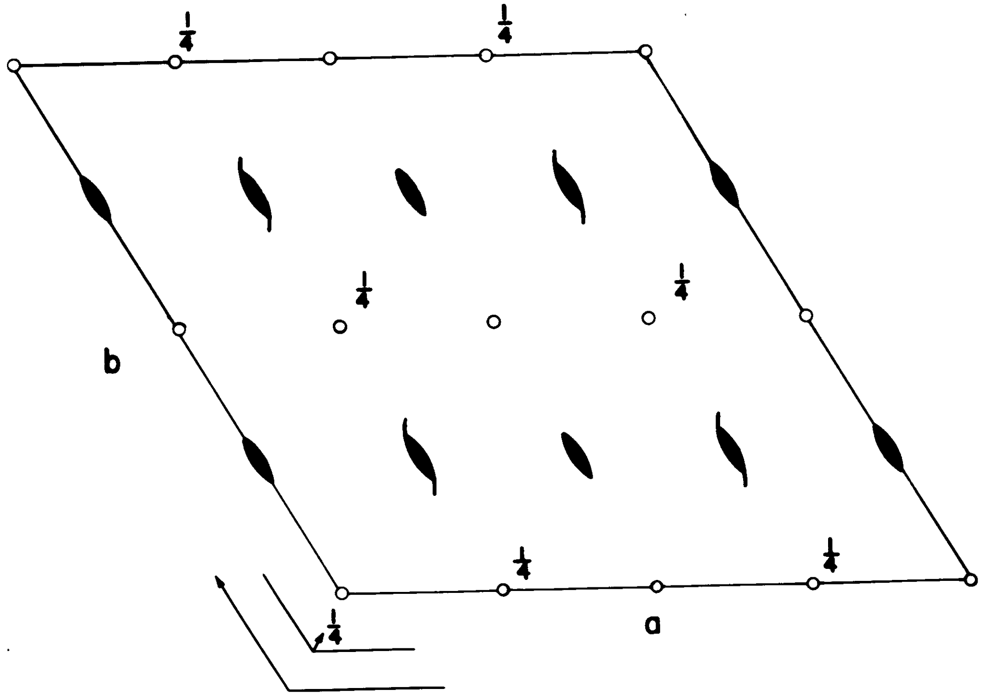

B 2/b

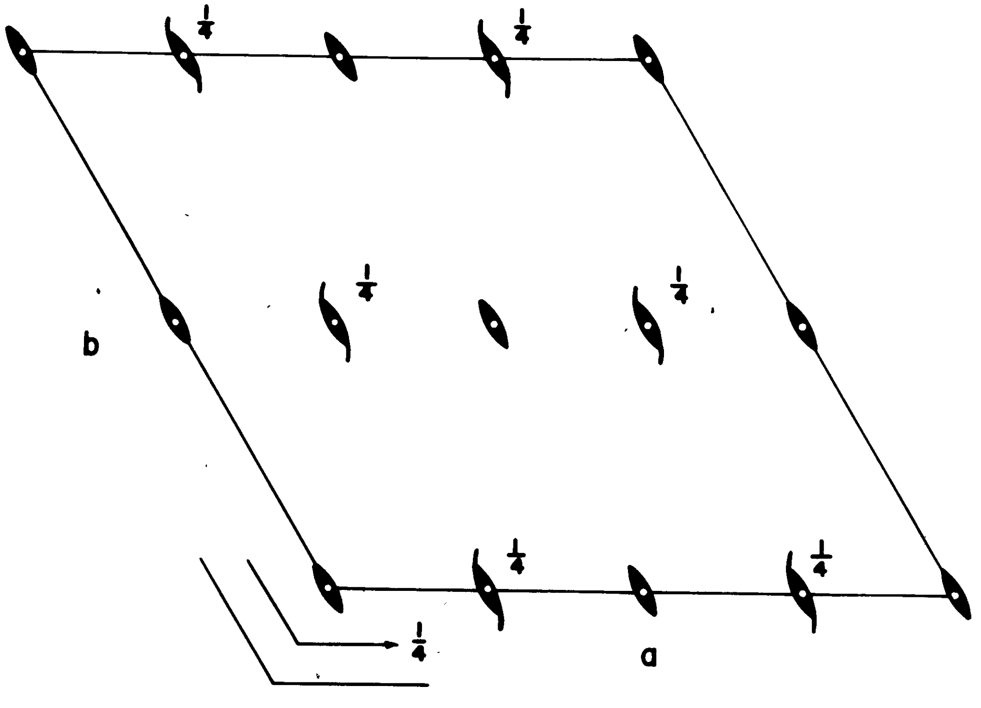

B 2/m

General features of the Patterson function. Accepting 16 SiO_2 per cell, this corresponds to 8 SiO_2 per primitive cell, and 2 SiO_2 per asymmetric unit. The relative weights of the peaks to be expected can be predicted[5]. Assuming silica and oxygen to be half ionized, i.e. Si^{2+}, and O^-, these should have 12 and 9 electrons respectively, and the weights of certain peaks, on an absolute basis, should be

single Si - Si: $12 \times 12 = 144$
single O - O : $9 \times 9 = 81$
double Si - Si: $2 \times 12 \times 12 = 288$
double O - O : $2 \times 9 \times 9 = 162$
double Si - O : $2 \times 12 \times 9 = 216$
origin : $8(12^2 + 9^2) = 2448$

The distribution of the various types of peaks in the Patterson cell is analyzed in Table 1-1.

It is easiest to solve a Patterson synthesis by starting with an inversion peak[5]. The heaviest such peak is that due to Si - Si. According to Table 1, this has a weight of only 144, and there are only two such peaks per asymmetric unit, embedded in a collection of 40 miscellaneous non-origin peaks all but 4 of which have greater weight. Accordingly it is not easy to find the desired inversion peaks without some theoretical help.

Use of the minimum function to find inversion peaks. The theory of finding inversion peaks will be discussed in some detail elsewhere[6]. If the space group contains reflection operations (including glides) as well as inversions, it must contain rotation (possibly screw) operations. The points in vector space due to a pair of points related by an inversion, and those due to a pair of points related by a rotation, comprise images of the same pair, but the images are separated by the glide component of the glide plane, plus an unknown component normal to the glide plane. If a minimum function is formed of two portions of the Patterson function which are separated by the glide plus an unknown parameter (z in this case) normal to the glide plane, the inversion peaks are automatically found.

In space group $B2/b$ there are glide planes at $z = 0$ with glide b, and another set at $z = \frac{1}{4}$ with glide n. In this case, the former were chosen, so that the rotation images at level $z = 0$ were compared with possible inversion images at all levels z by superposing the latter levels on level zero, but with level zero shifted by the amount of the glide, namely $b/2$. An example is shown in Fig. 1-4.

This procedure turned up six candidate inversion peaks. To test these, each was treated as an inversion peak, and an M_2 minimum-function map was prepared for the particular level on which an atom should occur in order to provide that inversion peak. Of the six maps so prepared, four were very similar while two others were different from these four and from each other. The two candidate inversion peaks giving rise to these wild maps were rejected.

Of the four candidate inversion peaks not rejected, two gave rise to strong M_2 maps, the other two to weak M_2 maps. Since there are two Si atoms per asymmetric unit, the strong maps were assumed to be based upon Si inversion peaks. The candidate peaks giving rise to these maps were accordingly treated further to improve the power of the minimum function.

Formation of minimum functions. Each of the two inversion peaks was used as an image point to form a complete set of sections of an $M_2(xyz)$ function. Each such section involves forming the minimum function for two different Patterson levels, the levels differing by the z

Fig. 1-4

Illustration for the location of an inversion peak candidate

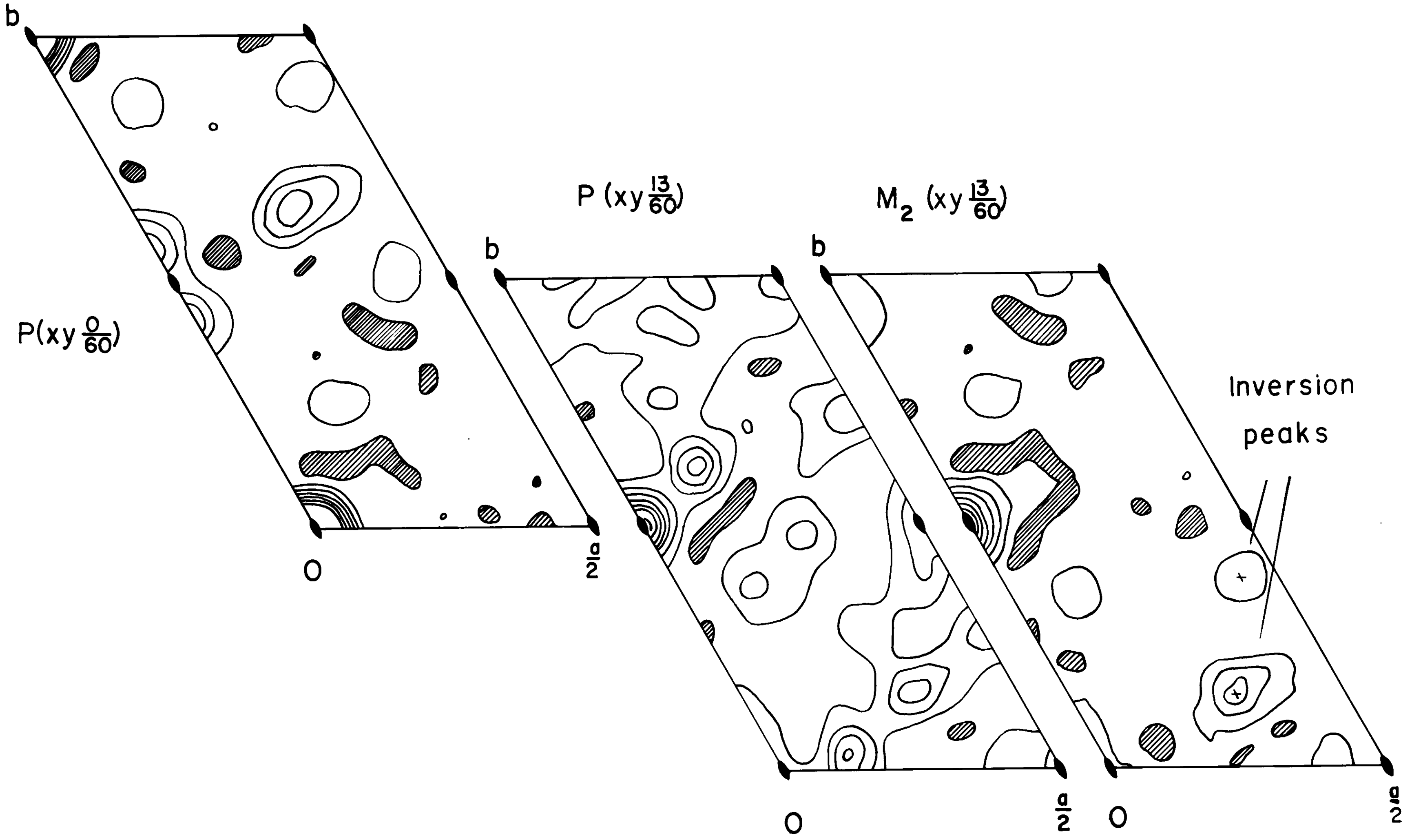
b
P(xy 0/60)
O
a/2
P (xy 13/60)
b
O
a/2
M2 (xy 13/60)
b
O
a/2
Inversion peaks

coordinate of the inversion peak. As a result of this procedure two separate $M_2(\underline{xyz})$ functions became available, each based (presumably) on one centrosymmetrical pair of the two kinds of silicon atoms per asymmetric unit.

Each of the sections of these two M_2 functions conformed approximately to the symmetry of the 2-fold axes of the space group as it intersected the section. Each M_2 section can be combined with itself by making use of this symmetry operation, thus forming an M_4 function of greater power. This was done for all sections of each of the two initial $M_2(\underline{xyz})$ functions. The result was two complete $M_4(\underline{xyz})$ functions.

These two $M_4(\underline{xyz})$ functions were similar in that both outlined similar areas of electron density, except that these were referred to different origins. Each was also of substantially the same weight, a fact further confirming that each was based upon the inversion peak of a different Si atom. Assuming that they are both based upon Si inversion peaks, they can be combined without scaling.[5]

An $M_8(\underline{xyz})$ function was then available. This shows a peak for each of the atoms expected in the asymmetric unit. The projection of these maxima on (001) is shown in Fig. 1-5. The coordinates of the atoms derived from it are shown in Table 1-2. The table also shows the manner in which the coordinates changed as the result of subsequent refinement. This brings out how well the minimum function corresponds to the actual structure.

Refinement

The coordinates, as found from the $M_8(xyz)$ function, were refined along with individual isotropic temperature factors by the least-squares method using the I.B.M. 704 computer. Again we are indebted to Dr. W. Sly for his help

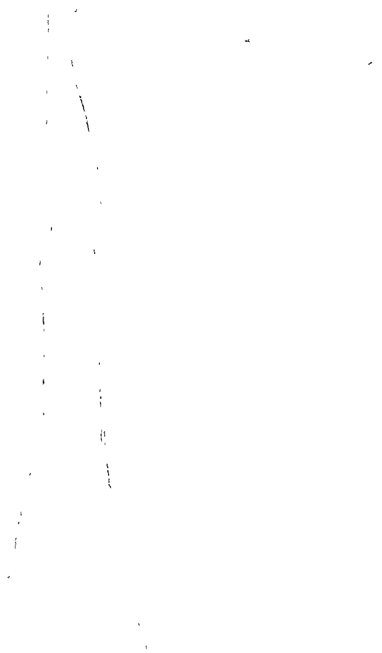

Fig. 1-5

(001) projection of the M_s maps

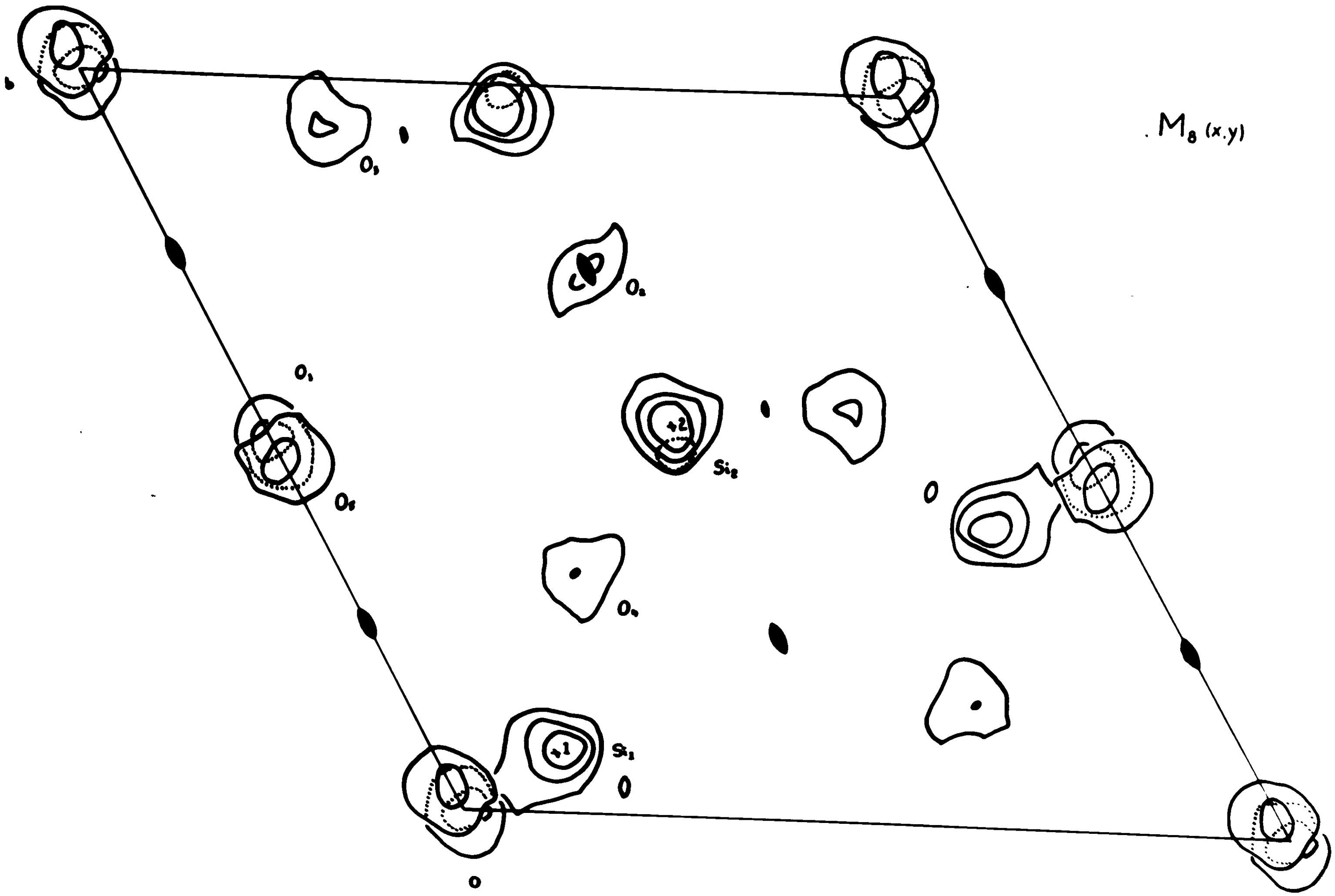

$M_8(x,y)$

in performing the computation.

Using an arbitrary value of $B = 1.0$ for all atoms, the discrepancy factor R for the original coordinates derived from the $M_8(xyz)$ function was found to be 36.1%. Using all reflections, and including unobserved reflections at $F_o = 0$, this discrepancy was reduced by three cycles of refinement to $R = 25.2\%$. On detailed comparison of observed and computed F's, six intense reflections of small sin θ value ($\bar{2}40$, $\bar{2}20$, 220, 020, $\bar{2}12$, and 004) uniformly showed $|F_c| > |F_o|$. This was attributed to extinction. More generally, similar effects could be observed within a sphere in the reciprocal lattice of radius corresponding to $\sin\theta = .095$. Accordingly, five more cycles of refinement were undertaken omitting all 56 possible reflections within this range, and also omitting reflections for which $F_o = 0$. This resulted in a set of coordinates and isotropic temperature factors for which $R = 16.9\%$. These are listed in Table 1-3.

After the refinement was complete, a three-dimensional electron-density function was prepared by Fourier synthesis. The peaks of this function are shown projected on (001) in Fig. 1-6 for comparison with the corresponding minimum function in Fig. 1-5. We would like to point out that in the method of analysis we used, Fourier syntheses are unnecessary, and this one was prepared entirely for the purposes of making the comparison of the minimum function with the final electron density.

The coesite structure

The coordinates of the atoms given in Table 1-3 define a structure in which each silicon atom has as nearest neighbor four oxygen atoms in tetrahedral arrangement. The actual distances between nearest neighbors are systematically listed in Table 1-4. All the Si-O distances in

Fig. 1-6

(001) projection of the electron density maps

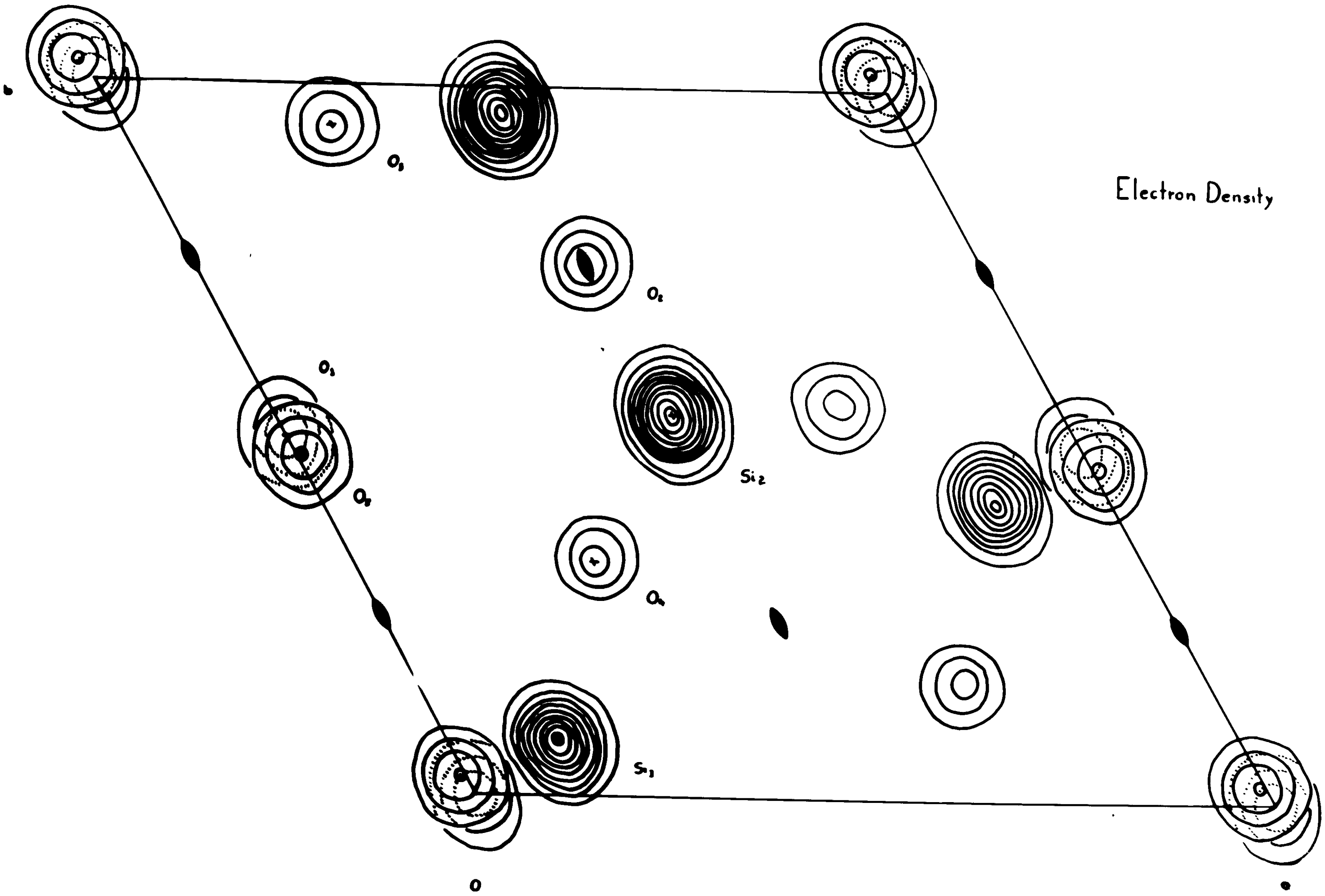

Electron Density

the two kinds of tetrahedra are almost exactly the same (1.60 Å to 1.63 Å), and the eight edges of the two kinds of tetrahedra are closely the same (2.60 Å to 2.67 Å). The tetrahedra are therefore quite regular and substantially equal.

The tetrahedra are joined together in a single network which is a new type. Fig.1-7 illustrates the network by means of a pair of stereoscopic drawings. The nature of the new network can perhaps be best understood by noting that the tetrahedra are required by symmetry to join into two kinds of rings of four tetrahedra. The two-fold axis in the lower middle of Fig. 1-6 causes the tetrahedra to form a ring parallel to the (001) plane, while the symmetry center at $.\frac{1}{4}0\frac{1}{4}.$ requires them to form a ring of four approximately parallel to (010). The whole network may therefore be described as one composed of a network of 4-rings, each ring having eight external connections. Both the feldspar and paracelsian networks also share these characteristics.

The specific nature of the coesite network can be appreciated somewhat by following the connections of the 4-rings. The centrosymmetrical rings are centrosymmetrical about inversion centers at levels $z = \frac{1}{4}$ and $\frac{3}{4}$. Such rings join one another through the oxygen atoms on the other kind of inversion centers on levels $z = 0$ and $\frac{1}{4}$ to form diagonal chains. For example, the ring centering at $.\frac{1}{4}0\frac{1}{4}.$ is approximately parallel to (010) and joins body-centering translation-equivalent rings to form a chain whose direction is 101 , Fig. 1-8. This chain is isolated from other translation-equivalent chains in the same plane. The two-fold rotation axis requires that an equivalent chain occur in the center of the cell, also parallel to (010) but trending in the direction of the other diagonal. 101 .

Fig. 1-7

Stereoscopic drawing of the coesite structure.

THE COESITE STRUCTURE

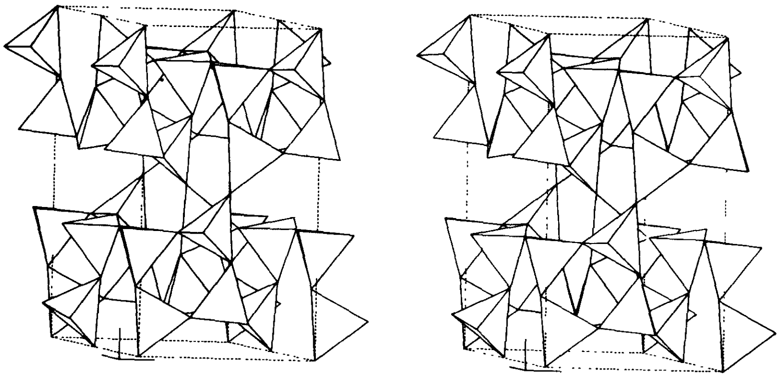

Fig. 1-8

Illustration of the rings of tetrahedra
parallel to(010)

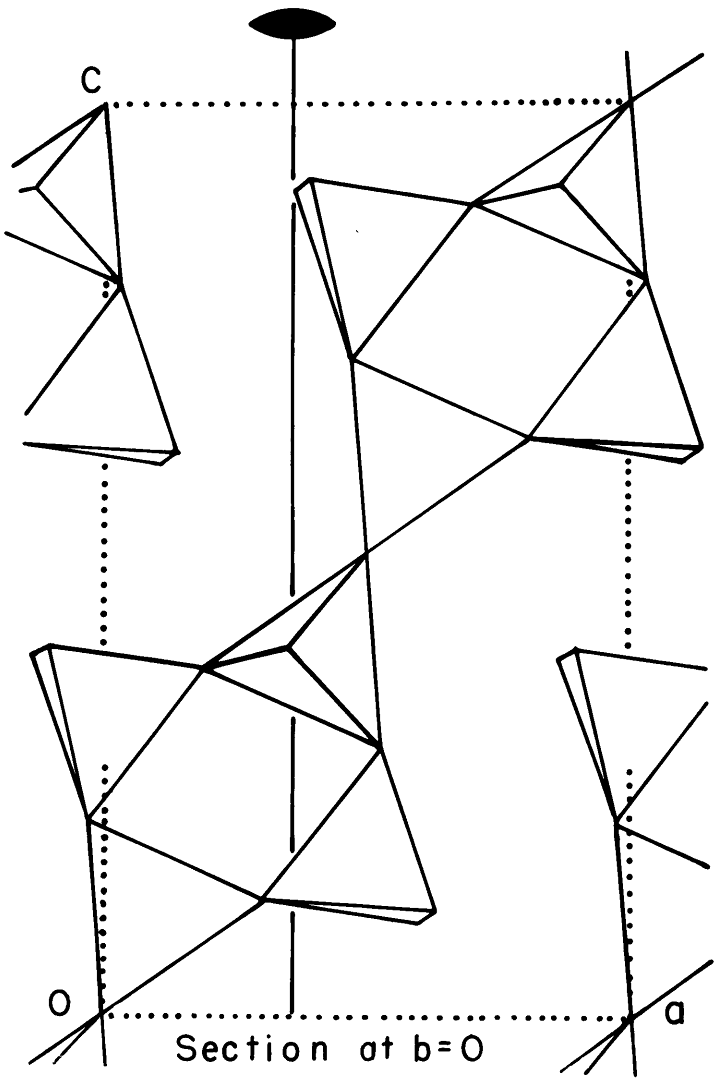

Section at b=0

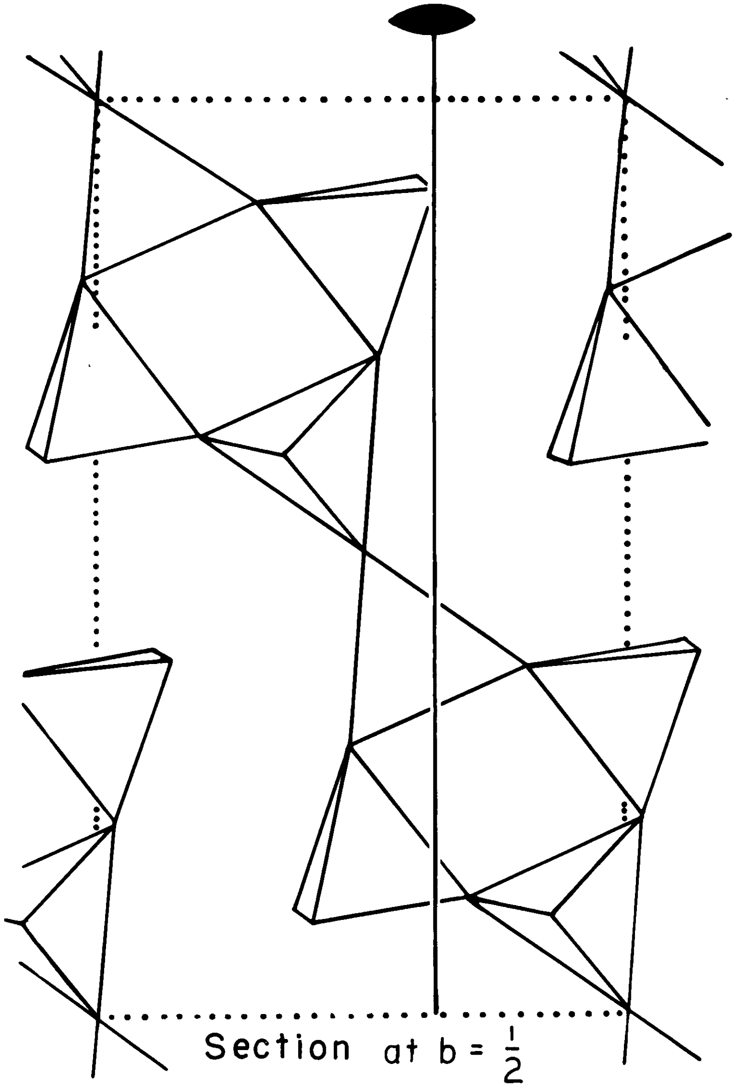

Section at b = $\frac{1}{2}$

This is shown in the right of Fig. 1-8. The coesite structure can be described in terms of these criss-crossed chains, which are connected in a manner which can be seen in Fig. 1-7.

The structure can also be described in terms of the rings symmetrical with respect to the 2-fold axes. These rings are parallel to (001) and form chains parallel to 010 , Fig. 1-9. The chains on the same level are not connected together, but are joined by the rings of glide-equivalent chains in the levels above and below, Fig. 1-9.

Fig. 1-9

Illustration of the rings of tetrahedra
parallel to (001)

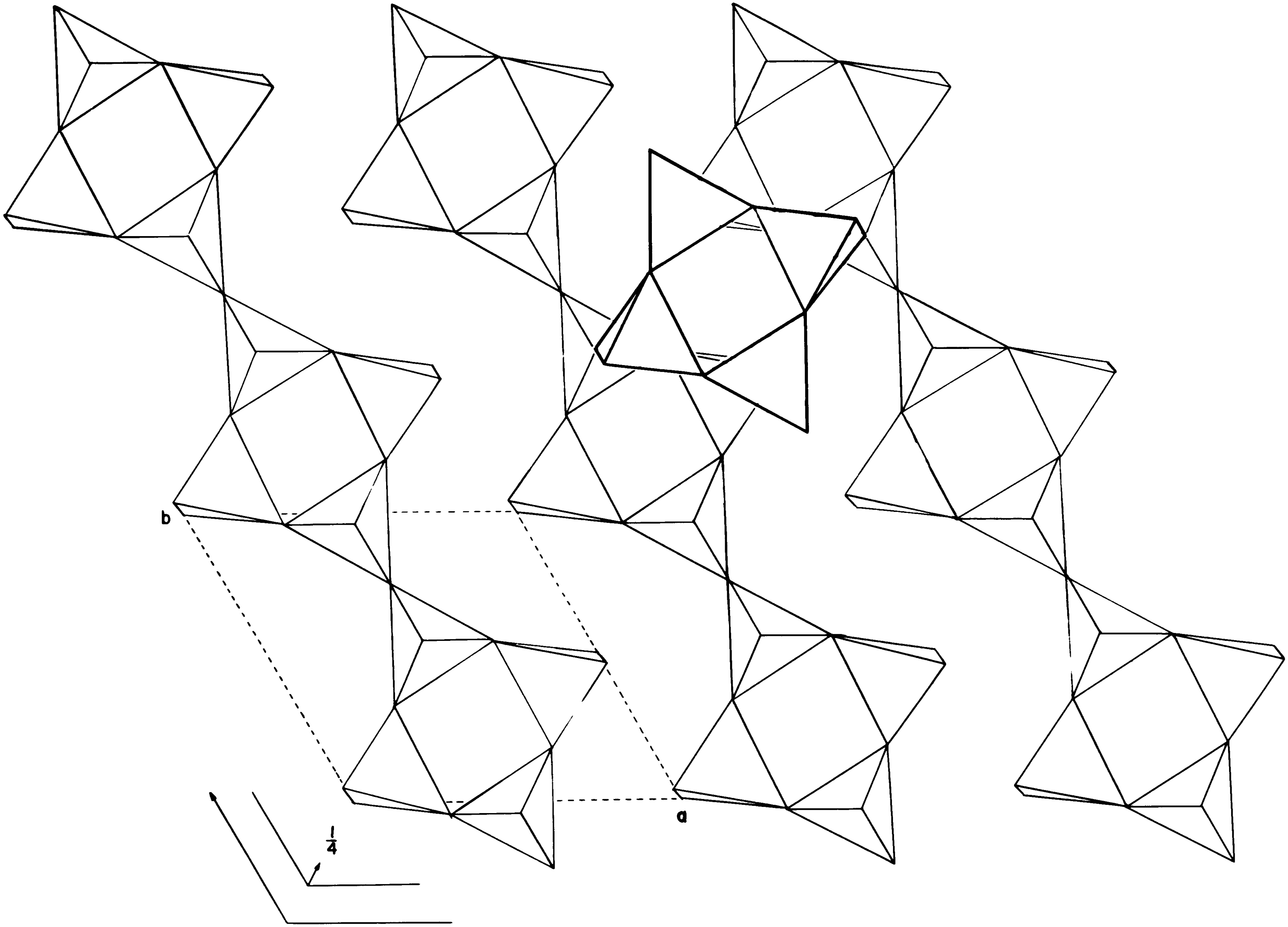
b
a
1/4

Table 1-1.

Enumeration of peak types to be expected in the Patterson synthesis of coesite.

Peak due to atom pair	Symmetry of pair	Number of individual peaks per primitive cell	Number of indistinguishable peaks		Total weight of indistinguishable peaks	Co-ordinate type
			per primitive cell	per asymmetric unit		
Si-Si	identity	8	1(orig.)			000
	inversion	8	8 single	2	144	$x_1, y_1+\frac{1}{2}, z_1$
	rotation	8	4 double	1	288	$x_1, y_1, 0$
	reflection	8	4 double	1	288	$0, \frac{1}{2}, z_1$
	asymmetric	32	16 double	4	288	$x, y, z,$
	(total)	$(8^2 = 64)$				
0-0	identity	16	1(orig.)			000
	inversion	16	16 single	4	81	$x_2, y_2+\frac{1}{2}, z_2$
	rotation	16	8 double	2	162	$x_2, y_2, 0$
	reflection	16	8 double	2	162	$0, \frac{1}{2}, z_2$
	asymmetric	192	96 double	24	162	x, y, z
	(total)	$(16^2 = 256)$				
Si-0	asymmetric	256	128 double	32	216	x, y, z
	(total)	$(24^2 = 576)$		(40)		

Table 1-2.

Coordinates of atoms in coesite, as determined from minimum function maps.

	As obtained from $M_8(xyz)$ (for which R=46.69)			Changes due to refinement (after which R=16.95)		
	x	y	z	Δx	Δy	Δz
Si_1	0.16	0.08	0.11	-0.020	-0.006	-0.002
Si_2	0.51	0.53	0.16	-0.003	0.009	-0.002
O_1	0	0	0	0	0	0
O_2	1/2	3/4	0.11	0	0	0.007
O_3	0.27	0.92	0.13	-0.001	0.021	-0.004
O_4	0.30	0.32	0.11	0.008	0.009	-0.007
O_5	0.01	0.47	0.22	0.002	0.003	-0.008

Table 1-3.

Final coordinates of atoms in coesite and their isotropic temperature factors.

Atom	Coordinates			Temperature coefficient
	x	y	z	B
Si_1	.1403	.0375	.1084	0.813 Å^2
Si_2	.5063	.5388	.1576	0.600
O_1	0	0	0	0.856
O_2	1/2	3/4	.1166	1.197
O_3	.2694	.9405	.1256	1.111
O_4	.3080	.3293	.1030	1.381
O_5	.0123	.4726	.2122	0.656

Table 1-4.

Interatomic distances in tetrahedra of coesite structure.

Si_1 tetrahedron

	O_1	O_3	O_4	O_5
Si_1	1.60	1.63	1.61	1.61 Å
O_1		2.67	2.62	2.64
O_3			2.63	2.61
O_4				2.61

Si_2 tetrahedron

	O_2	O_3	O_4	O_5
Si_2	1.62	1.60	1.62	1.61 Å
O_2		2.63	2.62	2.63
O_3			2.65	2.60
O_4				2.66

References

[1] L. Does, Jr. *A new dense crystalline silica*.
Science 118 (1953) 131 - 132.

[2] G. J. F. MacDonald. *Quartz-coesite stability relations at high temperatures and pressures*.

[3] Lewis S. Ramsdell. *The crystallography of "coesite"*.
Am. Mineral. 40 (1955) 975 - 982.

[4] Ralph H. V. M. Dawton. *The integration of large numbers of x-ray reflections*.
Proc. Phys. Soc. 50 (1938) 919 - 925.

[5] M. J. Buerger. *A new approach to crystal-structure analysis*.
Acta Cryst. 4 (1951) 531 - 544.

[6] M. J. Buerger. *Vector space and its application in crystal-structure investigation*.
(John Wiley and Sons, New York, 1959) Chapter 13.

Chapter II

The relative energies of rings of tetrahedra

When the structure of coesite was solved, its structure was compared with those of the other forms of silica. All these structures, of course, are composed of silica tetrahedra linked into three-dimensional networks. The structures can be described in many ways, but one of their obvious qualitative features is the relative compactness of the structures. Thus, the cristobalite and tridymite structures are comparatively open, the quartz structure is less open, and the coesite structure is compact, displaying little void space. Of course, the compactness of the coesite structure is to be expected because of its relative denseness, and this is consistent with its stability at high pressures[1].

This observation, however, does not explain the structural reason for the compactness. In studying the several silica structures it became evident that the compactness is related to the relative shortness of loops in the silica network. In coesite, stable only at high pressures, two kinds of loops, requiring four tetrahedra to complete them, are distinguishable. In the more open quartz, tridymite and cristobalite structures, stable at ordinary pressures, no loops shorter than six tetrahedra occur. In keatite, stable in a pressure range between quartz and coesite[1], loops of five tetrahedra occur[2].

These structures also have different relative energies. At normal pressures quartz is stable, keatite less stable and coesite most unstable, so that it is tempting to speculate that 6-membered loops are stable, 5-membered loops less stable and 4-membered loops most unstable. But feldspar and paracelsian, also composed of silica and alumina networks, have 4-membered loops like coesite, and are stable at room pressures. In these instances the additional alkali can be regarded as supplying an internal pressure which stabilizes the 4-membered loops.

Loops are not confined to three-dimensional networks, but are also known in two-dimensional networks (sheets), in double chains and in metasilicate rings. Among two-dimensional networks the commonest have 6-membered loops (micas, clays, chlorites), while 5-membered loops (hardystonite) and 4-membered loops (apophyllite) are relatively rare, and 3-membered loops are unknown. Among double chains, 6-membered loops are the most common (amphiboles) but 4-membered loops are also known in high-pressure (sillimanite). Among rings the 6-membered loops occur in the most common minerals (tourmaline, dioptase), 5-membered rings are unknown, 4-membered rings are rare (axinite) and 3-membered rings occur in the rare minerals, benitoite and catapleite.

The common occurrence of 6-membered loops suggests that it is the most stable loop under normal conditions, and that 5-, 4- and 3-membered loops are less stable. Loops with two members share an edge, and so are inherently high-energy loops.

It is interesting to seek a rational explanation for the relative frequency of occurrence of n-membered loops of tetrahedra. The most commonly observed loops have probably the least energies. The solution of this problem calls for computing the relative energies of these loops. Of course, the energy of an n-membered loop depends on many things, including the detailed shape of the loop and the relative orientation of the loop to the other parts of the structure. But the general trend of the relative energies of the various n-membered loops can be examined by computing the energies of free loops.

To make a start on this problem, the energies of the most symmetrically shaped rings, like the beryl, the axinite and the benitoite rings were investigated. In these rings, the plane of the ring is a plane of symmetry; the atoms shared between tetrahedra lie in this plane, and the unshared atoms are mirror images of each other, on each side of the plane, Fig.2-1. The atoms at the centers of the tetrahedra were assumed to have charges of +4 (like silicon if completely ionized) the atoms at the shared corners to have charges of -2 (like oxygen if completely ionized) while the atoms at the unshared corners charges of -1 (like fluorine) in order to make the ring neutral. The tetrahedra were assumed to have the same size in all rings. The energy of a tetrahedral unit due to the rest of the ring was computed. If the chemical composition is regarded as $SiOF_2$ then the energy of this unit was computed, that is, of the atom at the center, the two unshared F atoms and the two half oxygens pertaining to the unit. The energy was computed by summing for these atoms, the energies due to all the other atoms of the ring, by means of the relation (for any two atoms):

$$U = \frac{e_1 \cdot e_2}{r}$$

where e_1 is the charge on atom 1, e_2 the charge on the other and r the distance between them. In this preliminary work r was determined by measuring it on a carefully drawn diagram of the ring. The computation was carried out for rings of 2, 3, 4, 5, 6, 7, 8, 9, 10 and ∞ tetrahedral units.

The relative energies of these rings are plotted in Fig.2-2. It can be seen that the computed energies bear out the original expectations. There is a minimum energy at the 5-membered ring, with the 6-membered ring having a little more energy and 4-, 3- and 2-membered rings having sharply increasing energies. The 7-, 8-, 9- and 10-membered rings have nearly the same energies and the straight chain still higher energy.

Although these conclusions are not strictly applicable to the relative energies of complete tetrahedral structures

Fig. 2-1

4- and 6-membered rings of tetrahedra

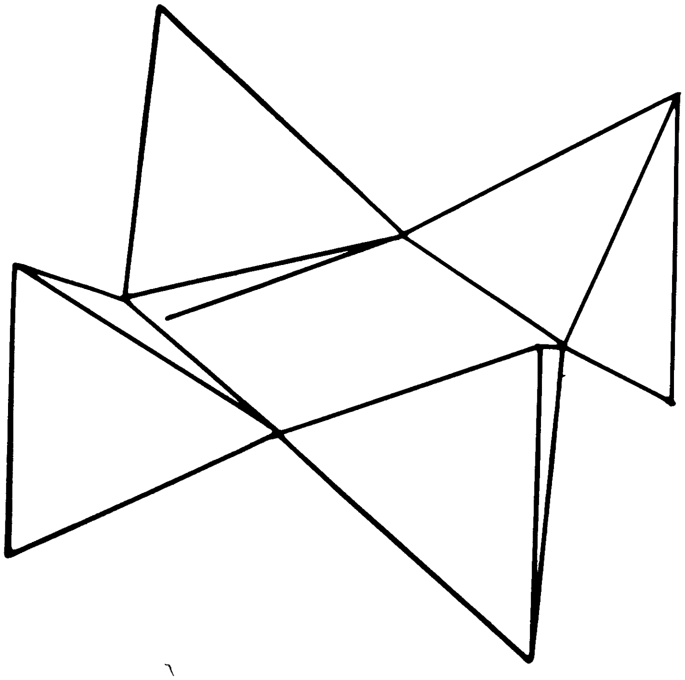

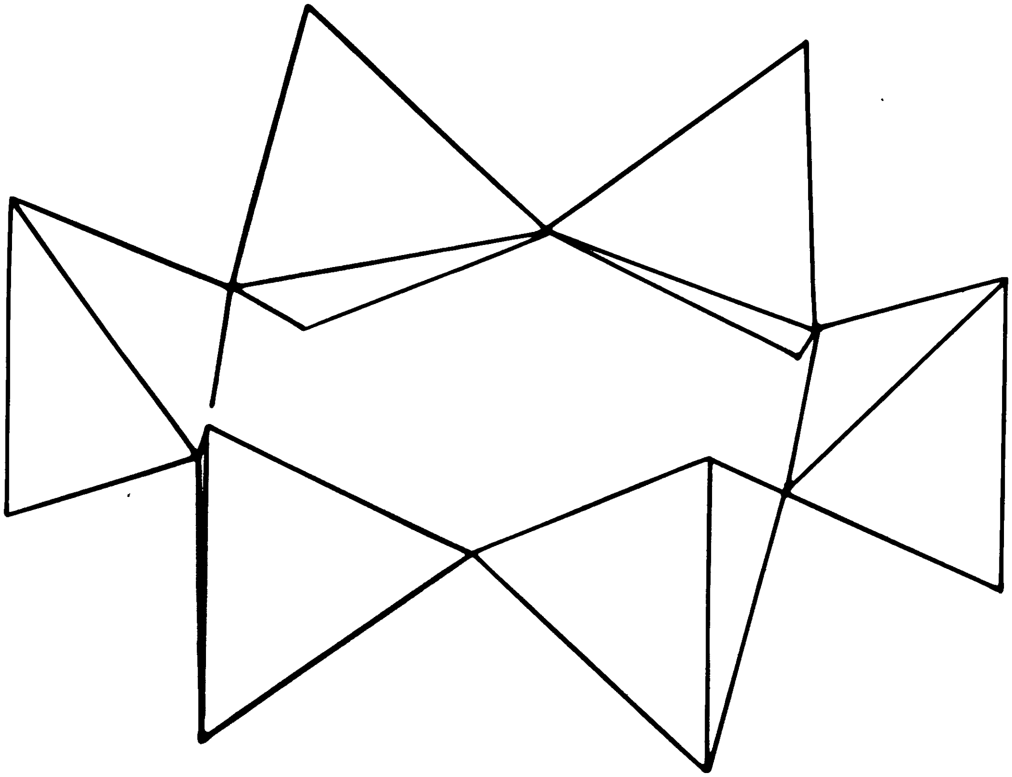

Fig. 2-2

Relative energies of *n*-membered rings of tetrahedra

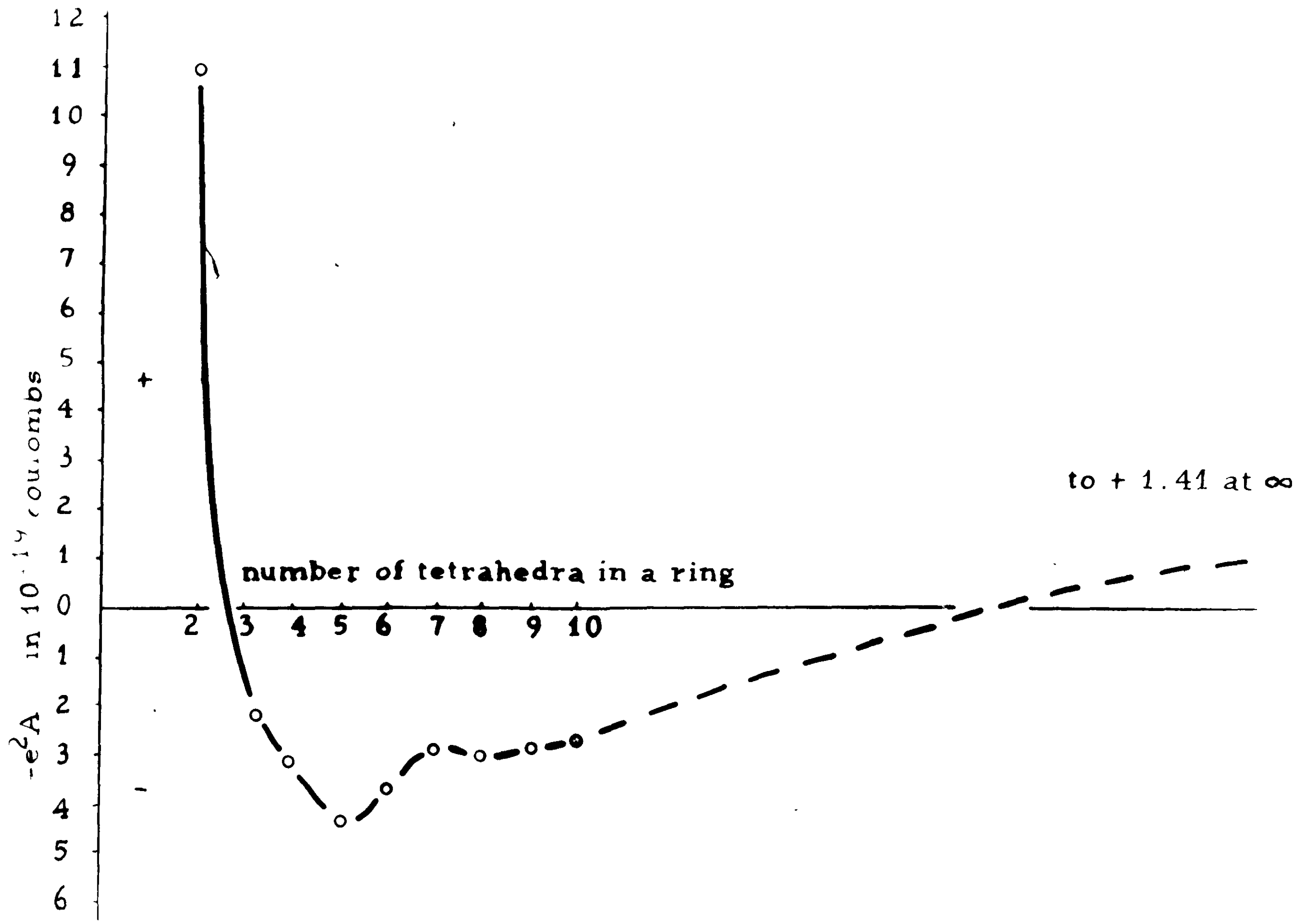
$-e^2A$ in 10^{-19} coulombs
12
11
10
9
8
7
6
5
4
3
2
1
0
1
2
3
4
5
6
+
-
number of tetrahedra in a ring
2
3
4
5
6
7
8
9
10
to + 1.41 at ∞

with *n*-membered rings, it is still reasonable to expect that the energy of the *n*-membered ring will significantly affect the energy of the whole structure. A tetrahedral structure composed only of regular 5-membered rings is expected to have lower energy than a structure composed of 6- or 4-membered rings. The 6-membered rings are, however, the most common, since no two- or three-dimensional network structure can be composed of regular 5-membered rings alone.

Most structures are composed of more than one kind of loop each containing a different number of tetrahedra. The energy of such a structure is expected to be affected by the energy of each kind of loop. The structure of keatite is composed of 5-, 7- and 8-membered rings, while the structures of tridymite and cristobalite are composed only of 6-membered rings. It seems reasonable to expect the combined energy of 5-, 7- and 8-membered rings to be higher than the energy of 6-membered ring, and that the tridymite and cristobalite structures should have lower energies than the structure of keatite.

Because the rings are comparatively regular in these structures, the energies of the tridymite and cristobalite structures can be compared with the energy of the keatite structure by utilizing the relative energies of the *n*-membered rings. A similar comparison, however, can not be made with quartz, since the rings in quartz are collapsed and their energy probably became less than the energy of a corresponding open *n*-membered ring.

References

1
L. Coes, Jr. A new dense crystalline silica.
Science 118 (1953) 131 - 132.

2
P. P. Keat. The transformation of silicic acid to quartz and the synthesis of a new crystalline silica.
Ph.D. Thesis (1956) Rutgers Univ., N.J.

Chapter III

Classification of tetrahedral structures

Introduction

The classification of things of scientific interest is not merely a filing system, but is also a basis for evaluation and comparison of these things. As such, it constitutes an important step in the progress of science and may lead to the better understanding of nature, and to the establishment of new directions of research. Machatschki's classification of the tetrahedral silicate structures[1] was an excellent system for classifying a large number of silicates. It also explained many of the important physical properties of silicates. Consequently, the classification was of considerable importance in the understanding of the silicates and other crystals with similar tetrahedral structures. Since 1928 the number of tetrahedral structures determined has grown so tremendously that Machatschki's classification is no longer adequate for the classification of the tetrahedral structures, especially for structures with a three-dimensional network of tetrahedra. There is a definite need for an improved classification, first, to provide more subdivisions in the system of classification and, second, to point out minor, but important, similarities between different tetrahedral structures.

After the structure of coesite was determined and compared with structures of other silicas, the significance of tetrahedral loops in the tetrahedral structures became apparent. In Machatschki's classification the geometric forms of the tetrahedral structures are related to the cleavage, hardness and the optical properties of the crystals; similarly the size of the tetrahedral loops are related to the energies of the tetrahedral structures. The importance of the size of the tetrahedral loops in a structure and its prospective application as a natural classification criterion stimulated an investigation of tetrahedral structures and the construction of an improved classification.

fication.

Other important features of tetrahedral structures were discovered during the course of this study. Most of them are applied in the proposed classification system. The classification criteria are discussed in detail in their order of application.

The geometrical forms

Machatschki's classification is based on outstanding geometrical forms created by the aggregation of tetrahedra. These forms are referred to as "types" in the literature. They are: isolated tetrahedra, groups, chains, rings, sheets and three-dimensional networks of tetrahedra. These features are important, and are widely accepted. Consequently they are adopted in this classification. Minor revisions, however, are made in order to systematically group these types, and to cover all the possible ionic tetrahedral structures. Some of the types have distinct directions in which the tetrahedral structures extend to infinity. In others the tetrahedral structures are terminated in all directions. Consequently, if the tetrahedral structures are extended to infinity in zero-, one-, two- and three-dimensions, four major types of tetrahedral structures are possible. These four types are:

(1) Isolated groups of tetrahedra.
(2) One-dimensionally non-terminated structures of tetrahedra.
(3) Two-dimensionally non-terminated structures of tetrahedra.
(4) Three-dimensionally non-terminated structures of tetrahedra.

It is theoretically possible that a crystal can be composed of two or more different types of tetrahedral structures. To cover such possibilities a fifth type is established:

(5) Mixed types of tetrahedral structures.

These types, except for the last one, have distinct form structures which are the simplest possible structures defined by the dimensional termination of the types. In the first type, the form structure is a single tetrahedron, in the second type it is an endless chain of tetrahedra, in the third type it is an endless sheet of tetrahedra, and in the fourth type it is an endless three-dimensional network of tetrahedra. Within each type, subtypes can be established. In the first three types the subtypes can be conveniently defined by the number of form structures welded into one unit, and by the presence of one or more such units in the structure of a crystal. In the fourth type the subtypes are defined according to the sharing of tetrahedral corners, or by sharing in addition one or more tetrahedral edges or faces.

In the isolated groups of tetrahedra there is a special form in which several tetrahedra form a closed ring. In order to follow popular practice, this ring structure is separated from the group structures. Instead of an isolated group of tetrahedra it is regarded as an endless chain curved into a ring, and is treated as an extra form structure in the two-dimensionally non-terminated structure type.

The fifth type is merely a collection of the possible combinations of the different types in the structure of a crystal. The subtypes are the descriptions of each type composing the collection of types.

The types and subtypes are listed in the first two columns of Table 3-1.

Corner sharing of the tetrahedral structures

A brief study of the tetrahedral structures revealed that a different number of tetrahedral corners can be shared and still make up the same type, and even the same subtype structure. For example, two single chains can be welded into a double chain if each tetrahedron of the first chain is connected to a tetrahedron of the second chain. Two single chains can also be welded into a double chain if only every second tetrahedra of the first chain is connected to every second tetrahedra of the second chain. In the former case six tetrahedral corners are shared per two tetrahedra and in the latter only five. The geometric form, however, still remains a double chain. A similar situation exists in the sheet structures. A sheet can be constructed if each tetrahedron shares three corners with other tetrahedra. A sheet can also be constructed if certain tetrahedra share only two corners. Once again, the number of tetrahedral corners shared is the only difference between the two sheets. In the three-dimensional network usually all four corners are shared. In some structures a few corners are left unshared, and consequently the number of tetrahedral corners shared becomes less than four.

In these examples it was tacitly assumed that only two tetrahedra can share a tetrahedral corner. This is not always the case. There are several three-dimensional networks of tetrahedra where three or even more tetrahedra share a tetrahedral corner. In order to distinguish between such structures, the number of tetrahedral corners shared is no longer sufficient. It has to be supplemented with the number of tetrahedra participating in the sharing of a corner.

It is possible to derive a single numerical value which can express both the number of tetrahedral corners shared and the number of tetrahedra participating in the sharing, if we make two assumptions:

A. The difference between the smallest and the largest number of tetrahedra participating in the sharing of a tetrahedral corner in a structure can not be more than one.

B. No tetrahedral corners can be shared between more than two tetrahedra and no tetrahedral edges or faces can be shared in structures other than three-dimensionally non-terminated structures of tetrahedra.

Assumption A means, for example, that as long as there are free corners present in a structure, no corners can be shared between more than two tetrahedra; or if some corners are shared between two tetrahedra only, no corners can be shared between more than three tetrahedra. Assumption B states that in groups, chains, rings and sheets of tetrahedra, where the structure is terminated in one or more directions the maximum number of tetrahedra participating in the sharing of a corner is two, and that no edges or faces can be shared.

Under these conditions the average number of tetrahedra participating in the sharing of a tetrahedral corner in a structure also defines the number of corners shared. The average number of tetrahedra participating in the sharing of a corner in a structure is called the sharing coefficient of the structure. Since the sharing coefficient is an average number it can be an integer as well as a fraction. An integer number defines a state in which each corner of each tetrahedra is shared between *n* tetrahedra, where *n* is the integer in question. A fractional number, on the other hand, defines a state in which some corners are shared between *n* tetrahedra and others between *n*+1 tetrahedra, where *n* is the integral part of the sharing coefficient. The fractional part, further, defines the ratio of the number of corners shared between *n* and *n*+1 tetrahedra. A sharing coefficient of $n+\frac{1}{2}$ means, for example, that all the corners are shared between at least *n* tetrahedra and in addition every fourth corner is shared between *n*+1 tetrahedra; or a sharing coefficient of $n+\frac{1}{20}$ means that all the corners are shared between at least *n* tetrahedra and in addition every twentieth corner is shared between *n*+1 tetrahedra.

There is a simple relationship between the sharing coefficient and the cation-anion ratio in the tetrahedral radical of the chemical formula. The relationship is obvious when a tetrahedral corner is shared between two or more tetrahedra. Then the same anion simultaneously belongs to two or more cations. The cation-anion ratio in a single tetrahedron is 1:4 and in a pair of tetrahedra it is 1:3½, and the corresponding sharing coefficients are 1.00 and 1.25 respectively. Consequently the sharing coefficient not only describes a geometric feature, but also defines part of the chemical formula. A list of possible sharing coefficient ranges for the types and subtypes of the tetrahedral structures, and the corresponding cation-anion ratios are tabulated in the third and fourth columns of Table 3-1.

Assumptions *A* and *B* were found, empirically, to be correct for dominantly ionic crystals. These assumptions are generalizations of Pauling's third rule which states, briefly, that the sharing of edges and particularly of faces of ionic polyhedra decreases the stability of the structure. This is because such sharing necessitates the close approach of two cations and thus increases the potential energy of the system. Our assumptions can be supported by similar arguments. When more tetrahedra share a tetrahedral corner, more tetrahedra come in contact, and the high valence cations approach each other, thereby increasing the potential energy of the system. Since a system tends toward the lowest energy state possible the corners should be shared by the least possible number of tetrahedra. Thus no corner is shared by three tetrahedra unless there is no lower energy state available. Similarly no tetrahedral corners will be shared between three tetrahedra in a double chain when a multiple chain or other geometric forms represent lower energy with the corners shared between two tetrahedra only. The same argument restricts the sharing of edges and of faces to structures where it is necessitated by geometry, in extremely dense three-dimensional networks.

Repeat-units and loops of tetrahedra

With the exception of the isolated groups of tetrahedra, the single chains, and the three-dimensional networks with one or more faces shared, all the tetrahedral structures contain loops of tetrahedra. These loops are outstanding features. They are also important in the consideration of the energies of structures. Consequently the tetrahedral loops are simple and non-artificial classification criteria.

Modern investigators of the tetrahedral and other polyhedral structures noticed the significance of these loops, and, in one form or other, they applied the loop concept to the subclassification of certain types of tetrahedral and polyhedral structures. Wells[3] subdivided the polyhedral networks according to the size of the loops formed by polyhedra. Tetrahedral networks are also included in his classification. However, he considered only the highly regular tetrahedral networks with a sharing coefficient of 1.75 and 2.00. Liebau[4] classified the tetrahedral silicate structures on the basis of the number of tetrahedra in the periodic unit of the tetrahedral structure. Liebau's classification subclassifies the simpler tetrahedral structures very conveniently, but fails to give a sufficient number of subdivisions for the three-dimensional networks.

The combination of Wells and Liebau's principles could conveniently be applied to the subclassification of all types of tetrahedral structures. The structures containing no loops of tetrahedra (with the exception of the face-sharing three-dimensional networks) can be subdivided according to the number of tetrahedra in the periodic unit of the tetrahedral structure, and structures containing loops of tetrahedra can be subclassified according to the number of tetrahedra in the loops. The former term is called the repeat-unit of tetrahedra, and the latter the loop of tetrahedra.

The repeat-unit of tetrahedra in the isolated groups of tetrahedra would be simply the number of tetrahedra in the groups. If there are different kinds of groups in the structure, several units will be listed and one number will represent each kind of group.

In an endless single chain the repeat-unit of tetrahedra is the number of tetrahedra in the motif of the chain which is repeated by translation to form the chain . If, for example, all the tetrahedra of the chain are similarly oriented and are translation equivalents, the repeat-unit is one tetrahedron. But if every second tetrahedron is oriented differently from the first one, then only every third tetrahedron is a translation equivalent, and the repeat-unit of the chain is two tetrahedra.

In most of the other types of tetrahedral structures there are loops of tetrahedra and every tetrahedron of the structure is part of one or more loops. These structures can be subclassified either (1) by the size of the smallest loop of the structure, or (2) by the list of the different sizes of loops occurring in the structure, or (3) by the list of all the symmetrically non-equivalent loops, in order of the increasing size of the loops. The first alternative has only five or six subdivisions, which is not sufficient to distinguish between a large number of possible structures, especially in the three-dimensional networks. The second alternative increases the number of subdivisions considerably. The third alternative, however, increases it to such an extent that almost every known structure has a different list of loop sizes.

Although the third alternative offers a greater number of subdivisions than the second, the second has been chosen for this classification for the following reasons: because the determination of the symmetrically non-equivalent loops is difficult and in complicated structures might become confusing; secondly because the number of subdivisions offered by the much simpler second alternative seems to be sufficient since only very similar structures have the same loop sizes.

The loop sizes can be determined either by simple observation or by a more systematic approach offered by the symmetry of the structure: all the possible loops of the structure must include the tetrahedra of the tetrahedral motif of the structure. The number of tetrahedra in a motif is usually less than five. Unfortunately in complicated structures there might be a very long list of loop sizes, especially for the larger loops. In order to avoid an unnecessarily long list, the loop sizes can be limited arbitrarily. It seems to be satisfactory to limit the number of loop sizes of a structure to four, and the size of the largest loop to twelve.

As the sharing coefficient increases above 4.00, tetrahedral edges are shared, and in addition to the loops incomplate polyhedral openings are present. When the sharing coefficient approaches 8.00 certain openings become complate polyhedra, but when the sharing coefficient reaches 8.00, all the edges are shared and all the openings are polyhedral. For example, the openings in the fluorite structure are octahedral. In structures with a sharing coefficient higher than 3.00, the polyhedral openings start to disappear, making room for solid bodies of tetrahedra. With a sharing coefficient at and above 3.00 there are no more loops of tetrahedra. Instead of units and loops these structures can be subdivided according to the shape of their polyhedral openings.

Structure families

After the tetrahedral structures are classified according to types, subtypes, sharing coefficients, and repeat-units or loops of tetrahedra, there remains only very similar structures in each category of the classification. They are in most cases isomorphic, isotypic, or derivative structures. It is theoretically possible, however, that two structures can be so similar that they have the same tetrahedral loops, yet their tetrahedral linkages are different; these should not be left in the same final group. Two such structures are apophyllite and gillepsite. They are similar in every respect, except in the linkage of tetrahedra. In both structures the tetrahedra are oriented so that they form triangular pyramids with their bases in the plane of the sheet of the sheet structure. In apophyllite the three basal corners of the pyramids are shared, but in gillepsite the two basal corners and the apices of the pyramids are shared. Such structures should be separated as two different families, so that in the final column of the families there are only closely related structures.

Table 3-1.

Sharing coefficients and cation-anion ratios of the types and subtypes of tetrahedral structures.

Types	Subtypes	Sharing coefficients	Cation-anion ratios
1. Isolated groups of tetrahedra	a. single tetrahedron	1.00	1:4
	b. pair of tetrahedra	1.25	$1:3\frac{1}{2}$
	c. large groups	1.25-1.50-(1.75)*	$1:3\frac{1}{2}$ - 1:3 - $(1.2\frac{1}{2})$
	d. mixed groups	1.25-1.50-(1.75)	$1:3\frac{1}{2}$ - 1:3 - $(1:2\frac{1}{2})$
2. One-dimensionally non-terminated structures of tetrahedra	a. single chains	1.50	1:3
	b. single rings	1.50	1:3
	c. double chains	1.50-1.75	1:3 - $1:2\frac{1}{2}$
	d. double rings	1.50-1.75	1:3 - $1:2\frac{1}{2}$
	e. multiple chains	(1.50)-1.75-2.00	(1:3) - $1:2\frac{1}{2}$ - 1:2
	f. multiple rings	(1.50)-1.75-2.00	(1:3) - $1:2\frac{1}{2}$ - 1:2
	g. mixed chains and rings	(1.50)-1.75-2.00	(1:3) - $1:2\frac{1}{2}$ - 1:2
3. Two-dimensionally non-terminated structures of tetrahedra	a. single sheets	1.50-1.75	
	b. double sheets	(1.50)-1.75-2.00	(1:3) - $1:2\frac{1}{2}$ - 1:2
	c. multiple sheets	(1.50)-1.75-2.00	(1:3) - $1:2\frac{1}{2}$ - 1:2
	d. mixed sheets	(1.50)-1.75-2.00	(1:3) - $1:2\frac{1}{2}$ - 1:2
4. Three-dimensionally non-terminated structures of tetrahedra	a. networks with corners shared	1.75-4.00	$1:2\frac{1}{2}$ - 1:1
	b. networks with one or more edges shared	4.00-8.00	1:1 - $1:\frac{1}{2}$
	c. networks with one or more faces shared	8.00-	$1:\frac{1}{2}$
5. Mixed types			

* Sharing coefficients in parentheses indicate theoretically possible but practically improbable ranges.

Table 3-2.

Classification of tetrahedral structures.

Types	Subtypes	Sharing coefficients	Repeat-units and loops of tetrahedra	Families	Members
1. Isolated groups of tetrahedra	a. single tetrahedron	1.00			Olivine, garnet, sphene, gypsum etc.
	b. pair of tetrahedra	1.25			Ilvaite, tilleyite, ZrPO4 etc.
	c. large groups	1.40	5		Zunyite
	d. mixed groups	1.11	1-2		Vesuvianite, allanite
2. Two-dimensionally non-terminated structures of tetrahedra	a. single chains	1.50	2	Pyroxenes	Enstatite etc.
		1.50	3	Wollastonite	
		1.50	5	Rhodonite	
	b. single rings	1.50	3	Benitoite	Catapleite, wadeite
		1.50	4	Axinite	
		1.50	6	Tourmaline	Dioptase, caledonite
	c. double chains	1.62	8	Xenotlite	
		1.67	6	Amphiboles	Anthophyllite etc.
		1.75	4	Sillimanite	
	d. double rings				
	e. multiple chains				
	f. multiple rings				
	g. mixed chains and rings				
3. Two-dimensionally non-terminated structures of tetrahedra	a. single sheets	1.75	4-8	Apophylite	Datolite
		1.75	4-8	Gillepsite	
		1.75	6	Mica	Clay etc.
		1.75	6	Sepiolite	Beryllonite, V_2O_5
		1.78	5	Hardystonite	Melilite, gehlenite, akermanite

Table 3-2. (continued)

Types	Subtypes	Sharing coefficients	Repeat-units and loops of tetrahedra	Families	Members
	b. double sheets	2.00	4-6	α Celsian	
	c. multiple sheets				
	d. mixed sheets				
4. Three-dimensionally non-terminated structures of tetrahedra	a. networks with corners shared	1.75	10	P_2O_5	
		1.82	8-10	$12CaO.7Al_2O_3$	
		2.00	3-6	GeS_2	
		2.00	4-5-8	Scapolites	Marialite etc.
		2.00	4-6	Sodalite	Ultramarine, helvite, danalite, hauynite
		2.00	4-6-8	Paracelsian	Danburite, hurlbutite
		2.00	4-6-8	Analcite	Pollucite, leucite
		2.00	4-6-8-9	Coesite	BeF_2 (?)
		2.00	4-6-8-10	Feldspars	Sanidine etc.
		2.00	4-6-8-12	Chabazite	
		2.00	4-6-8-12	Gmelinite	
		2.00	4-6-9	Beryl	Cordierite
		2.00	4-6-9	Milarite	Osumilite
		2.00	4-6-12	Faujasite	
		2.00	4-6-12	Cancrinite	
		2.00	4-8	Edingtonite	Natrolite, thomsonite
		2.00	5-6	Petalite	
		2.00	5-6-8	Heulandite	Philippsite
		2.00	5-7-8	Keatite	
		2.00	6	Cristobalite	Carnegieite, cuprite, BPO_4, $BaSO_4$, $K_2Fe_2O_4$ $K_2Al_2O_4$, $BaAsO_4$, Na_2CaSiO_4, $4H_2O.Zn(OH)$
		2.00	6	Tridymite	Nepheline, $LiKSO_4$

Table 3-2. (continued)

Types	Subtypes	Sharing coefficients	Repeat-units and loops of tetrahedra	Families	Members
		2.00	6-8	Quartz	Berlinite, $AlAsO_4$, H-Eucryptite, GeO_2 $BAsO_4$
		2.75	3-4-6	Bertrandite	
		2.75	3-4-6-8	Hemimorphite	
		2.75	3-4-7	B_2O_3	
		3.00	3-4-5	Phenacite	Willemite
		3.00	3-4-6	Ag_2HgI_4	
		4.00	3-4	Wurzite	BeS, BeTe
		4.00	3-4	Sphalerite	BeO, MgTe
	b. networks with one or more edges shared	4.00	3-5	Cubanite	
		4.00	4	Cooperite	
		6.00	3-6	Bi_2O_3	Zn_3P_2
		8.00	octahedron	Fluorite	Antifluorite, Na_2O, K_2O, ZrO_2, Li_2O
	c. networks with one or more faces shared				
5. Mixed types					

References

1
F. Machatschki. Zur Frage der Struktur und Konstitution der Feldspate.
Zbl. Min. Geol. Palaent. A (1928) 97 - 104.

2
R. C. Evans. An introduction to crystal chemistry.
Caledon Press (1952).

3
A. F. Wells. The geometrical basis of crystal chemistry. Part 1 - 6.
Acta Cryst. 7 (1954) 535 - 554, 842 - 853, 8 (1955) 32 - 36, 9 (1956) 23 - 27.

4
F. Liebau. Bemerkungen zur Systematik der Kristallstrukturen von Silikaten mit hochkondensierten Anionen.
Zeit. Phys. Chem. 206 (1956) 73 - 92.

5
M. J. Buerger. Derivative crystal structures.
J. Chem. 15 (1947) 1 - 16.

6
M. J. Buerger. The stuffed derivatives of the silica structures.
Contr. from E. Washken Lab., Cambridge, Mass.
(1953) 600 - 614.

References for structure data

7
Strukturbericht, Band I - VIII.
Zeit. Krist. (1913 - 1939).

8
Structure Reports, Vol. 8 - 15.
Intern. Union Cryst. (1940 - 1951).

9
S. V. Berger. Crystal structure of B_2O_3.
Acta Cryst. 5 (1952) 388 - 389.

10
G. Berghoff, W. H. Baur, W. Nowacki. *Uber die Kristallstruktur des Faujasites*.
Neues Jb. Min. Mh. 9 (1958) 193 - 200.

11
K. Brauner, A. Preisinger. *Struktur und Enstahung des Sepioliths*.
Tschermaks Min. Petr. Mitt. 6 (1956) 120 - 140.

12
L. S. Dent, J. V. Smith. *Crystal structure of Chabazite, a molecular sieve*.
Nature 181 (1958) 1794 - 1796.

13
H. G. Heide. *Die Struktur des Dioptas*.
Die Naturwiss, 41 (1954) 402 - 403.

14
D. E. Henshaw. *The structure of wadeite*.
Min. Mag. 227 (1955) 585 - 595.

15
T. Ito, H. Mori. *The crystal structure of datolite*.
Acta Cryst. 6 (1953) 24 - 32.

16
T. Ito, Y. Takeuchi. *The crystal structure of axinite*.
Acta Cryst. 5 (1952) 202 - 208.

17
A. Miyashiro. *Osumilite, a new silicate mineral and its crystal structure*.
Amer. Miner. 41 (1956) 104 - 116.

18
B. Nagy, W. F. Bradley. *The structural scheme of sepiolite*.
Amer. Miner. 40 (1955) 885 - 892.

19
J. V. Smith. *The crystal structure of paracelsian*.
Acta Cryst. 6 (1953) 613 - 620.

20
H. Strunz. Die Zeolithe Gmelinite, Chabasit, Levyn.
Neues Jb. Min. Mh. 7 (1956) 250 - 259.

21
U. Ventriglia. La struttura della heulandite.
Period. Min. 24 (1955) 49 - 83.

22
A. Zemann-Hedlik, J. Semann. Die Kristallstruktur von Petalite.
Acta Cryst. 8 (1955) 781 - 787.

23
B. B. Zviagin. Determination of the structure of caledonite by electron diffraction.
Russ. Phys. Cryst. Vol. 2 (1957) No.3. 388 - 394.

Chapter IV

Classification of silicates

There is a complication in the structures of the silicates which makes their classification difficult. This complication gives rise to an inconsistency in the treatment of various silicates by different authors and can be illustrated in three points.

(1) It is generally accepted that Al can replace Si and when it does the Al tetrahedra still remain part of the tetrahedral framework. In some cases, however, the Al tetrahedra are not so regarded. For example, cordierite is usually regarded as a collection of isolated rings of six Si tetrahedra, but Al tetrahedra connect these rings into a continuous three-dimensional network.

(2) In other cases, other cations occur in tetrahedra and they are sometimes accepted as part of the frame and sometimes not. For example, B in danburite is accepted as part of the frame, and danburite is classified as a silicate with a three-dimensional tetrahedral network. Ca occurs in tetrahedral coordination in Na_2CaSiO_4 and is accepted as part of the framework, so that the crystal is a derivative of the cristobalite structure. But tetrahedrally coordinated Be is not accepted in beryl, phenacite or bertrandite, nor Zn in willemite, hemimorphite or hardystonite.

(3) Almost every author treats this matter differently[1-6]. Most authors exclude cations other than Si or Al from the frame, and some authors include a few. Strunz[5] accepts most tetrahedrally coordinated cations as part of the frame, and even treats beryl and cordierite as three-dimensional networks. Nobody, however, has given this problem a systematic treatment, as yet.

Geometrically there are several cations which can substitute for silicon in a tetrahedron without changing significantly the size of the tetrahedron. Table 4-1 is a list of some cations which can be found tetrahedrally coordinated in silicate structures and some which might conceivably be present in tetrahedral coordination. They are listed in order of increasing cation-oxygen radius ratio. The minimum radius ratio geometrically required for a tetrahedron is .225, so that any one of the cations listed from B to Ca in Table 4-1 can fit into an oxygen tetrahedron. Due to its large size, however, Ca distorts the tetrahedron considerably. It is interesting to note that most of these cations have similar electro-negativity, so that their substitution for silicon would not significantly change the nature of the chemical bond.

The list of the observed cation-oxygen distances indicates that the variation in the size of the tetrahedron is not great. Except in the case of the B and Ca tetrahedra, the different cation-anion distances are almost equal to the cation-anion distances in the Si or in the Al tetrahedra.

There is only one important criterion which can lead to discarding a tetrahedron from consideration as part of the tetrahedral frame, namely the nature of its bonding. The silicates are considered to be mesodesmic structures; strictly speaking, however, only the pure silicas are really mesodesmic. In the aluminosilicates the oxygen bond to Al cease to be mesodesmic, since the charge of the oxygen is not halved exactly between two cations. The frame, however, remains a unit, since in each tetrahedron more than half of the cation's bond strength is expended holding the tetrahedral frame together, and less than half is connecting the cation to the rest of the structure. In conclusion, not only the silicon tetrahedra should be considered as constituents of the tetrahedral frame of a silicate but also tetrahedra of other cations, provided that half or more of the cation's bond strength is distributed within the tetrahedral frame. If less than half of the bond strength is distributed within the frame, the tetrahedra belong to the rest of the structure rather than to the frame. A good example is offered by axinite. Here the four membered rings of Si tetrahedra are connected by Al tetrahedra, but the Al's contribute less than half of their bonding strength to connect the Si tetrahedra and more than half to connect the Fe octahedra and B triangles.

Of course, it is expected that in a silicate a large number of tetrahedra are Si tetrahedra in order to classify the crystal chemically as a silicate. If the replacement of Si by another cation goes as far as the complete replacement of all the Si, the compound should not be called a silicate, chemically, although structurally it still might be included in the silicates. An example is yttro-garnet in which practically all the Si is replaced by Al.

By including several cations in the tetrahedral frame of the silicates, some major and minor changes have to be made in the classification of a few silicates. The most striking of these changes concern the classification of beryl, cordierite, hemimorphite, phenacite, willemite, bertrandite, hardystonite and melilite. Beryl and cordierite are three-dimensional networks instead of single rings, and hemimorphite, phenacite and willemite are three-dimensional networks instead of pairs of tetrahedra. Bertrandite is also a three-dimensional network instead of a complex of chains and groups of tetrahedra. In hardystonite and melilite the pairs of tetrahedra become sheets of tetrahedra.

In hemimorphite, phenacite, willemite and bertrandite, all of the cations are tetrahedrally coordinated. These tetrahedra build up a neutral network, somewhat similar to that of the pure silicas. The cation-anion ratio in these minerals is higher than in SiO_2, and consequently the sharing of one oxygen by two cations would no longer give a neutral structure. In order to obtain neutrality, the oxygens in these minerals are shared by up to three cations and some of the O^{--} is replaced by $(OH)^{-}$.

In Table 4-2 the silicates are classified according to the classification of the tetrahedral structures, presented by the author, and according to the suggested evaluation of the tetrahedrally coordinated cations. In the preparation of this table, special attention was paid to the silicates with three-dimensional networks of tetrahedra. Photographs of the models representing the tetrahedral frames of the three-dimensional silicate networks are shown in the plates. The technique by which these models were constructed is described elsewhere.

Table 4-1.

Some important tetrahedrally coordinated cations in silicates.

Cation	Radius ratio (calculated)	Observed M-O distance	Electro-negativity	Examples
B^{3+}	.25	1.50 ±.05 A	2.0	Danburite, datolite,homolite
Be^{2+}	.28	1.60	1.5	Beryl,phenacite
As^{5+}	.30	-	2.0	--
P^{5+}	.34	-	2.1	Stillwellite
Si^{4+}	.38	1.60	1.8	Silicas,silicates
Li^{+}	.39	-	1.0	
Al^{3+}	.41	1.78	1.5	Aluminosilicates
Ge^{4+}	.43	1.80	1.8	Many silicates
Ga^{3+}	.46	-	1.5	Many silicates
Mg^{2+}	.47	1.80	1.2	Melilite, akermanite
Fe^{2+3+}	.48-.50	1.80	1.5 -2.0	Staurolite, cordierite
Zn^{2+}	.50	1.82	1.8	Hemimorphite, hardystonite
Ti^{4+}	.55	1.82	1.6	Schlorlomite, astrophyllite
Ca^{2+}	.67	1.90	1.0	Na_2CaSiO_4

Data from Pauling[8], Hori[9], Smith[10].

Table 4-2.

Classification of silicates.

Types	Subtypes	Sharing coefficients	Repeat-units and loops of tetrahedra	Families	Members
1. Isolated groups of tetrahedra	a. single tetrahedron	1.00			Olivine, garnet, zircon etc.
	b. pairs of tetrahedra	1.25			Ilvaite, tilleyite, thorveitite
	c. large groups	1.40	5		Zunyite
	d. mixed groups	1.11	1-2		Vesuvianite, allanite
2. Two-dimensionally non-terminated structures of tetrahedra	a. single chains	1.50	2	Pyroxenes	Enstatite etc.
		1.50	3	Wollastonite	
		1.50	5	Rhodonite	
	b. single rings	1.50	3	Benitoite	Catapleite, wadeite
		1.50	4	Axinite	
		1.50	6	Tourmaline	Dioptase, caledonite
	c. double chains	1.62	8	Xenotlite	
		1.67	6	Amphiboles	Anthophyllite etc.
		1.75	4	Sillimanite	
	d. double rings				
	e. multiple chains				
	f. multiple rings				
	g. mixed chains and rings				
3. Two-dimensionally non-terminated structures of tetrahedra	a. single sheets	1.75	4-8	Apophylite	Datolite
		1.75	4-8	Gillepsite	
		1.75	6	Mica	Clay etc.
		1.75	6	Sepiolite	
		1.78	5	Melilites	Hardystonite etc.
	b. double sheets	2.00	4-6	α Celsian	
	c. multiple sheets				
	d. mixed sheets				

Table 4-2. (continued)

Types	Subtypes	Sharing coefficients	Repeat-units and loops of tetrahedra	Families	Members
4. Three-dimensionally non-terminated structures of tetrahedra	a. networks with corners shared	2.00	4-5-6-8	Scapolites	Marialite etc.
		2.00	4-6	Sodalite	Ultramarine, hauynite, danalite, helvite
		2.00	4-6-8	Paracelsian	Danburite, hurlbutite
		2.00	4-6-8	Analcite	Pollucite, leucite
		2.00	4-6-8-9	Coesite	
		2.00	4-6-8-10	Feldspar	Sanidine etc.
		2.00	4-6-8-12	Chabazite	
		2.00	4-6-8-12	Gmelinite	
		2.00	4-6-9	Beryl	Cordierite
		2.00	4-6-9	Milarite	Osumilite
		2.00	4-6-12	Faujasite	
		2.00	4-6-12	Cancrinite	
		2.00	4-8	Edingtonite	Natrolite, thomsonite
		2.00	5-6	Petalite	
		2.00	5-6-8	Heulandite	Philippsite
		2.00	5-7-8	Keatite	
		2.00	6	Cristobalite	Carnegieite, Na_2CaSiO_4
		2.00	6	Tridymite	Nepheline
		2.00	6-8	Quartz	Hi-Eucryptite
		2.75	3-4-6	Bertrandite	
		2.75	3-4-6-8	Hemimorphite	
		3.00	3-4-5	Phenacite	Willemite
	b. networks with one or more edges shared				
	c. networks with one or more faces shared				
5. Mixed types					

References

1
W. L. Bragg. The structure of silicates.
Z. Krist. 74 (1930) 237 - 305.

2
W. L. Bragg. Atomic structure of minerals.
Cornell Univ. Press (1937).

3
H. Berman. Constitution and classification of the natural silicates.
Amer. Miner. 22 (1937) 342 - 408.

4
J. W. Gruner. Structure of some silicates.
Amer. Miner. 16 (1931) 437 - 454.

5
H. Strunz. Systematik und Struktur der Silikate.
Zeit. Krist. 98 (1937) 60 - 83.

6
Ch. Swartz. Classification of the natural silicates.
Amer. Miner. 22 (1937) 1073 - 1087, 1161 - 1174.

7
F. Liebau. Bemerkungen zur Systematik der Kristallstrukturen von Silikaten mit hochkondensierten Anionen.
Zeit. Phys. Chem. 206 (1956) 73 - 92.

8
L. Pauling. The nature of chemical bond.
Cornell Univ. Press (1940).

9
F. Hori. On the diadochic substitution in silicates.
Miner. Jour. 1 (1954) 109 - 125.

10
J. V. Smith. A review of the Al-O, Si-O distances.
Acta Cryst. 7 (1954) 585 - 595.

11
Strukturbericht, Band I - VII
Zeit. Krist. (1913 - 1939).

12
Structure Reports, Vol. 8 - 15
Intern. Union Cryst. (1940 - 1951).

The following plates are photographs of models of the tetrahedral frames of silicates, and of the tetrahedral models of silica structures.

Plate 1.

Scapolite Sodalite

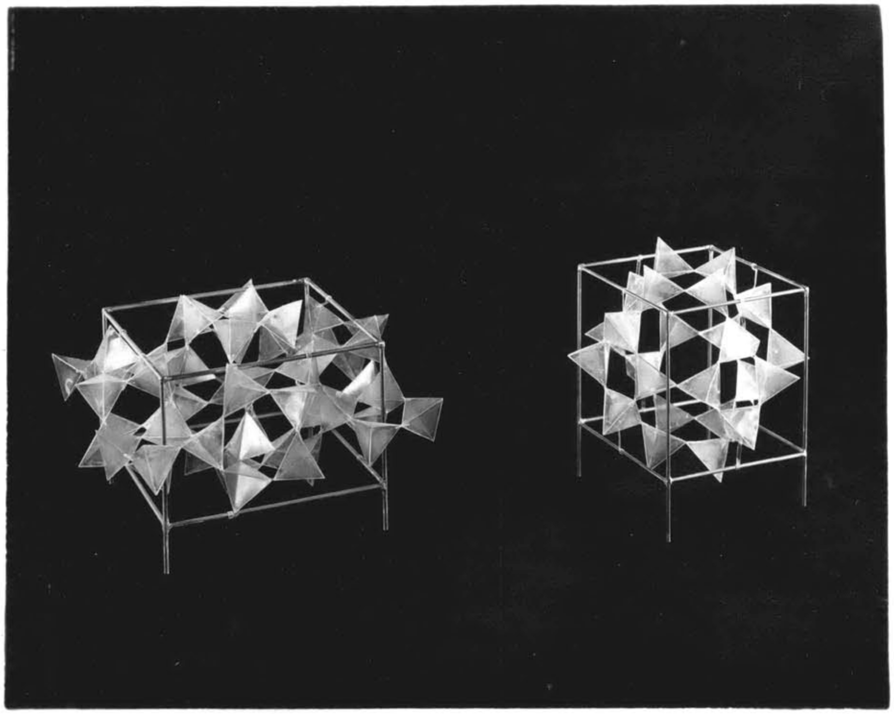

Plate 2.

Paracelsian Analcite

Plate 3.

Coesite Sanidine

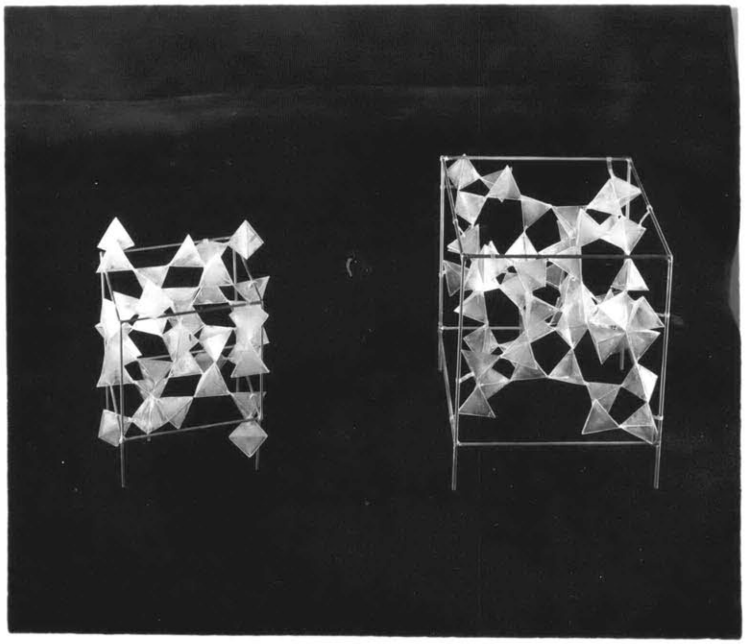

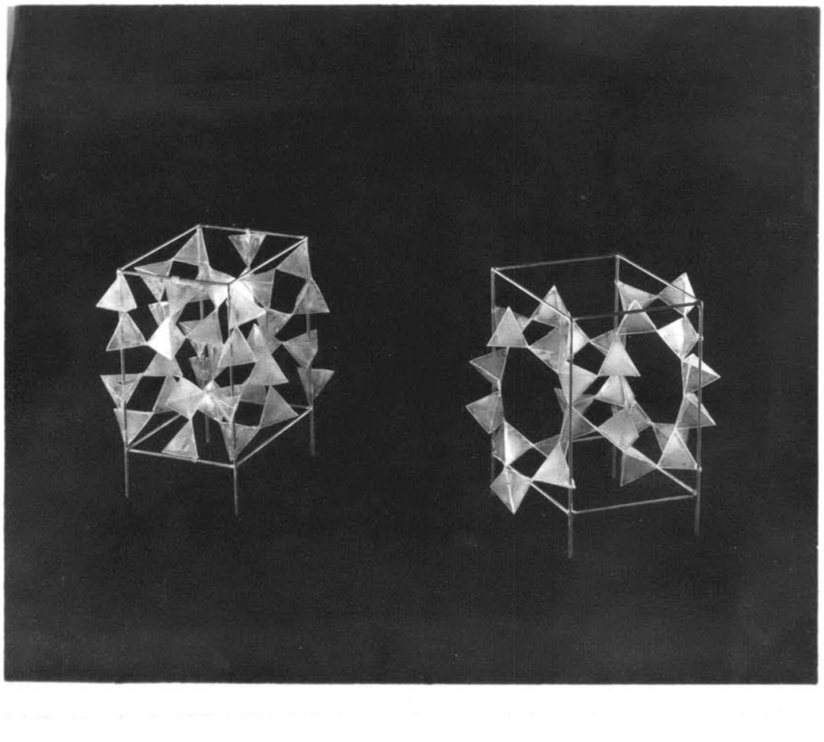

Plate 4.

Chabazite Gmelinite

Plate 5.

Beryl Milarite

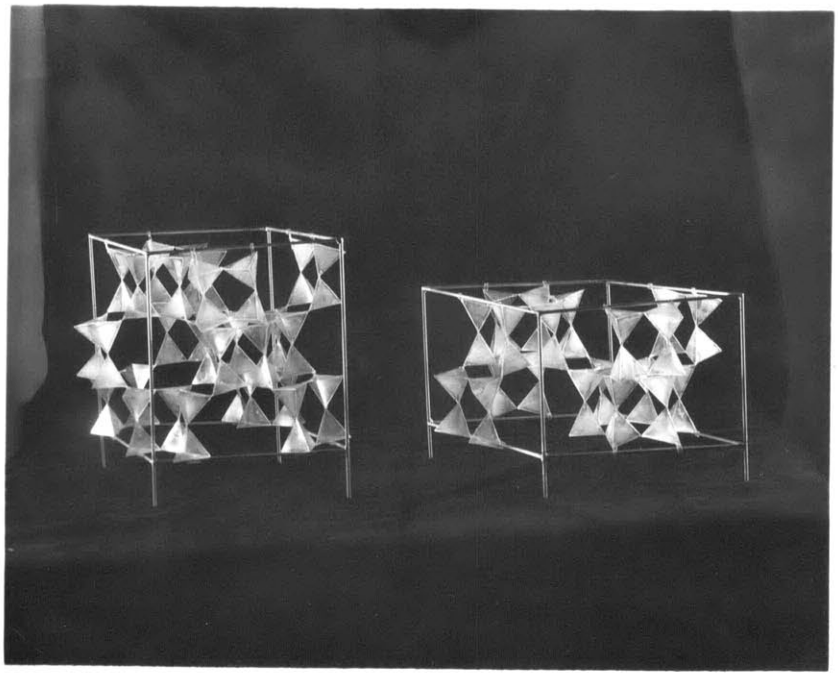

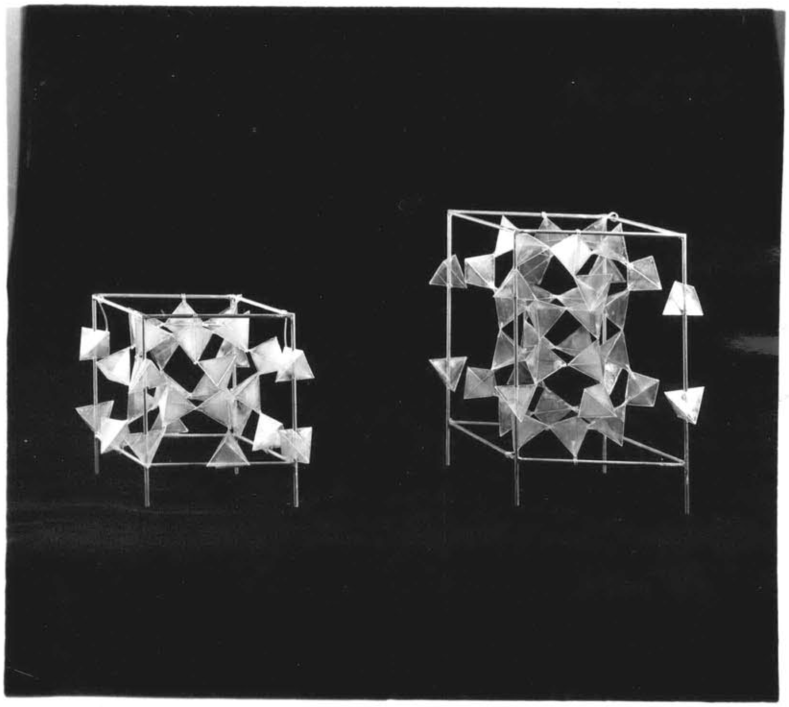

Plate 6.

Faujasite **Canorinite** **Edingtonite**

Plate 7.

Petalite **Heulandite** **Keatite**

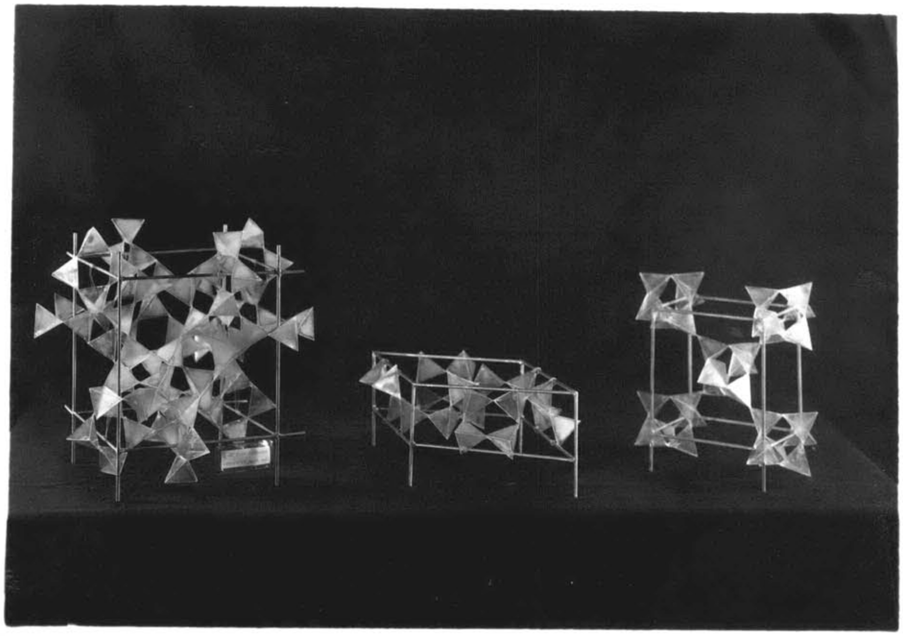

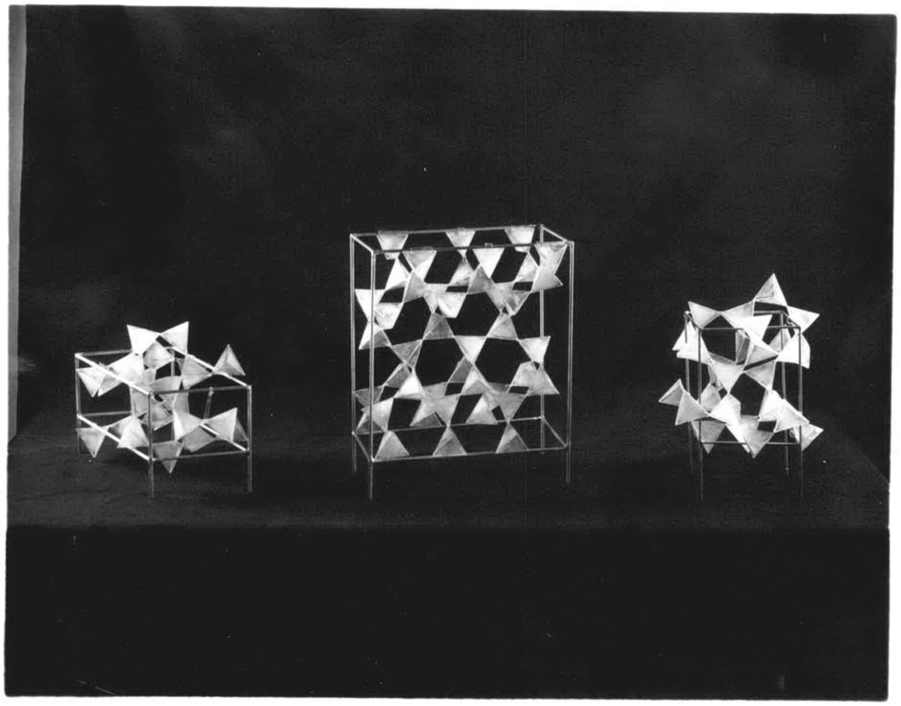

Plate 8.

Hi-Cristobalite Hi-Tridymite Hi-Quartz

Plate 9.

Bertrandite Hemimorphite Phenacite

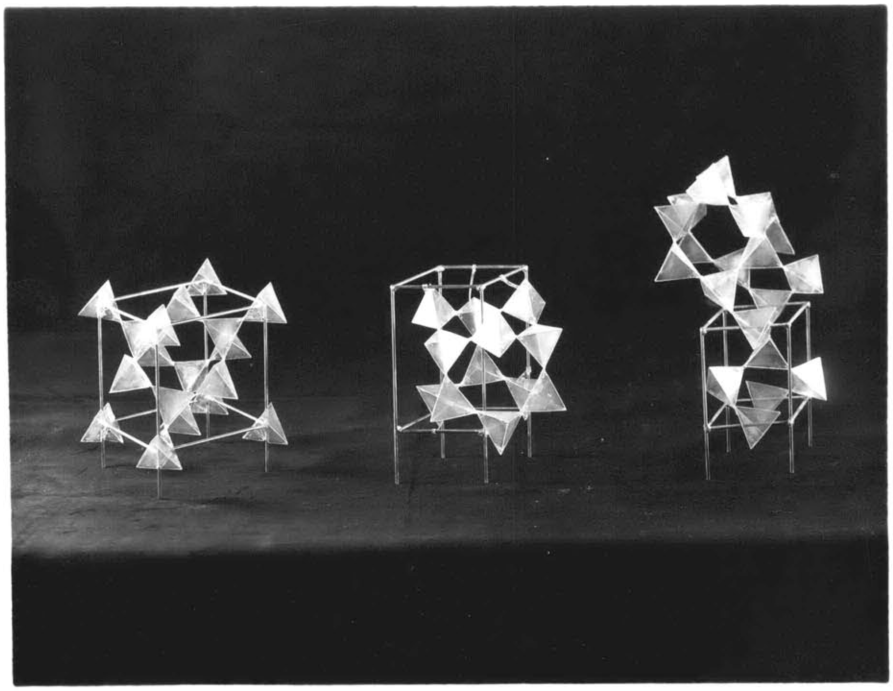

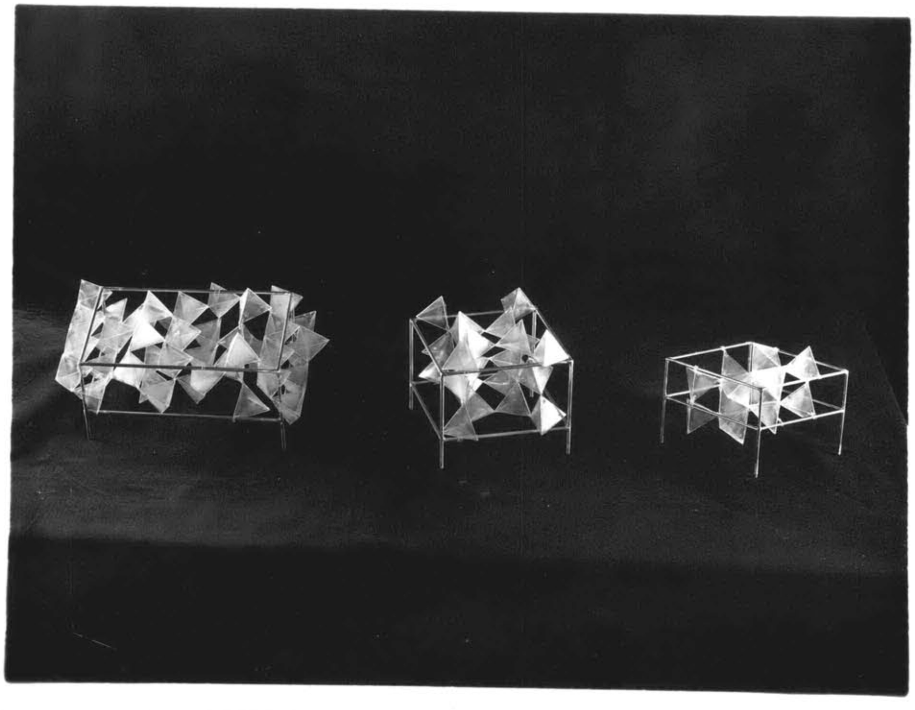

Chapter V.

A simple technique for the construction of polyhedral models.

When complex crytal structures are studied the visualization of the structures requires good structure models. The standard ball models help this visualization, but they are often either too expensive to purchasse or too time-consuming to construct. Most structures, however, can be illustrated by polyhedral models, where the polyhedra represent the coordination polyhedra of the cations. These polyhedral models not only illustrate the linkage of the polyhedra and the whole structure, in many cases better than a ball model, but also offer possibilities for simpler and inexpensive model construction techniques.

The use of polyhedral models is not unknown among crystallographers. Most of the published models are made of cardboard paper and some are made of wooden blocks or plaster of paris. The first technique is simple and time-saving, but the models are primitive and temporary only. In studying tetrahedral structures the author sought a simple and fast technique to make over 40 structure models. An efficient and inexpensive technique was found which permits making well-constructed and sturdy models in a matter of a few hours.

(1) The tetrahedra of the model are made of acetate sheets. Acetate sheets of 15 mils thickness were found to be the most satisfactory for the construction of models with a scale of 1 inch to 2 Angstroms. The acetate sheets are first dulled with steel-wool. This fogging provides the necessary opacity of the tetrahedra and helps to hide the minor imperfections in the model. Equilateral triangles are then cut out. This cutting can be

achieved by a simple paper cutter, but if a large number of models is anticipated, it pays to have a die made for mechanical cutting. The acetate triangles are then glued into tetrahedral form with acetone, which is a solvent of the acetate and dries very quickly. This process can be accelerated if a mold, such as shown in Fig. 5-1. is used for the assemblage of the tetrahedron.

(2) The tetrahedra are attached to each other by means of narrow acetate strips (1 mm. by 8 mm.). These strips are set at the approximate linkage angle and fastened to the corresponding corners of the tetrahedra with acetone. The two softened acetate surfaces stick immediately and the joint hardens in a matter of a few seconds. This approximate angle is later changed to the correct engle by softening the acetate strips with a drop of acetone. The model is assembled by following a good drawing of the structure, or by constructing the motif of tetrahedra of the structure and repeating it according to the symmetry of the space group.

(3) Before attaching the last few tetrahedra to the model, the model is placed in a 1/8 inch brass wire frame. The frame might represent a unit cell or any multiple or fraction of the unit cell. The last tetrahedra are then added to the model to complete it. In some cases the brass wire has to be embedded in a tetrahedron. This can be done easily by cutting and partially opening the tetrahedron, and removing a circular area of acetate where the wire is to penetrate through

Fig. 5-1.

Photograph of a mold to aid the assemblage of a tetrahedron.

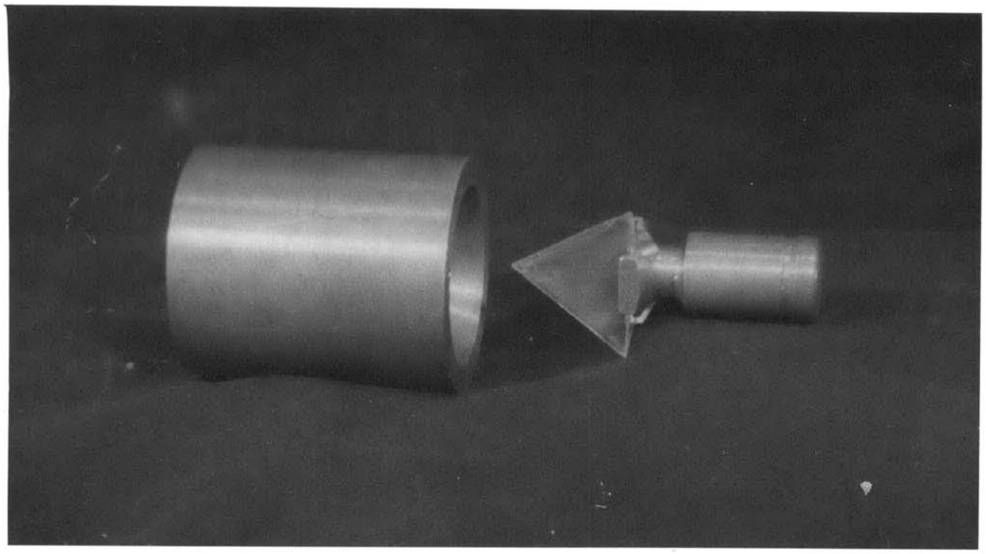

the face. The tetrahedron is then glued together again after it is placed on the frame. In order to fix the position of the model in the wire frame a few narrow strips of acetate can be glued to peripherially located tetrahedra and the frame. Transparent strips of acetate can be used for this purpose in order to prevent their interference in the appearance of the model. When the model is ready and all the linkage angles are set correctly and extra acetate strip can be added to each connected corner to assure firm connections. The model with the frame can then be fixed to a base, if desired.

A model of high-quartz constructed by this technique is shown in Fig. 5-2. In this model the structure is extended beyond a unit cell in order to illustrate the 6- and 8- membered loops of tetrahedra. All the silica and silicate models can be constructed similarly and plastic balls can be added to illustrate the location of the non-tetrahedrally coordinated cations of the silicates. Mica and clay models can be constructed by the combination of tetrahedral and octahedral sheets.

This technique is believed to be satisfactory for the construction of any polyhedral model. If so desired the polyhedra of the different cations can be painted in different colors. These models are impressive and fairly permanent. Unfortunately, the acetate becomes brittle after a few years and the model may fall apart if they are handled constantly. It is, therefore advisable to keep them in closed display cases as much as possible.

Fig. 5-2.

Photograph of a high-quartz model constructed by this technique.

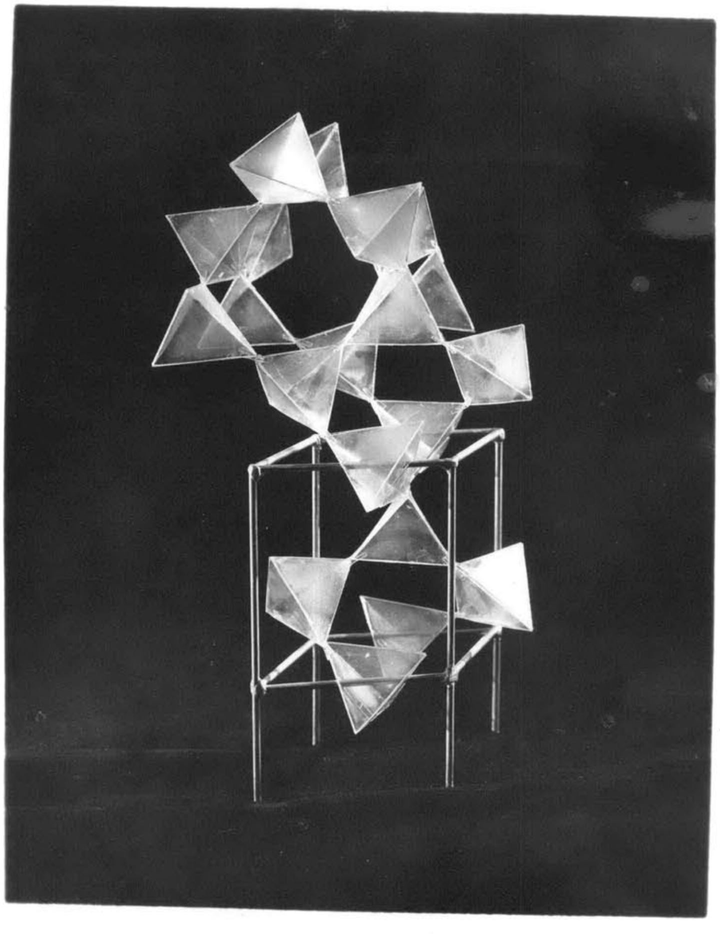

PART II.

Supplement to Chapter I.

The crystal structure of coesite, the dense, high-pressure form of silica.

Introduction and historical notes.

Coesite was first made by L. Coes Jr. He discovered this new form of silica, performing high-pressure experiments in 1952. In his paper[1] announcing this discovery he listed some of the physical and chemical properties of coesite. The most important of them are:

Composition: pure SiO_2,

Density: 3.01 gm/cc.,

Hardness: in the hardness range of spinel,

Refractive indices: $n_o=1.599$, $n_e=1.604$,

Chemical innertness: coesite can not be dissolved in hot hydrofluoric acid,

Stability: coesite can be made at a pressure of 35,000 atmospheres and at a temperature of 500-800°C. Below and above this pressure quartz is produced.

Inversion: Above 1,700°C. coesite transforms to silica glass and cristobalite.

This discovery aroused considerable interest in mineralogical and geological as well as in chemical and thermodynamical circles. The mineralogists were obvicusely interested in the new member of the silica family, while the geologists anticipated coesite to be a possible mineral in deep seated rocks. Eclogites, kimberlites and peridotites were treated with hydrofluoric acid in order to obtain coesite. The results were unsuccessful. This failure, however, does not exclude the possibility of natural occurance of coesite in other deep seated rocks,or even in these ultramafic rocks, in a small amount. Some geologists expected to find coesite in meteorites, which may represent the composition of the mantle of the earth. These tries were also unsuccessful. The chemists and the thermodynamists, obviousely, had great interest in coesite, one of the first fruits of extensive high-pressure experiments.

Crystallographers also looked at coesite with a special interest. It offered a new silica structure which might not only give a new structure but could be expected to illustrate the behaviour of the silica structure at higher pressures. Professor M. J. Buerger expected to find a basic silica structure in coesite for some silicate derivatives. Feldspar appeared to be a possible derivative structure of coesite, due to the close similarity between the cells of the two compounds.

Morphology of coesite.

We were presented a small sample of coesite crystals by Dr. N. W. Thibault, Assistant Director of Research and Development, Norton Company. The crystals were made at 40,000 atmospheres pressure, at 700°C. temperature and were cured for 15 hours. Some of the crystals measured up to 100 microns and offered good material for x-ray investigation. Approximately 10% of the sample was composed of single crystals and the remaining 90% of twins. Ramsdell's[3] description of the crystals applied to our sample, except that almost all of our sample was euhedral. The twins were mostly twinned on the (012) plane resulting in perfect tetrahedral prisms. The single crystals were flat, and as Ramsdell describes them, they resemble small gypsum crystals.

Many of the well developed single crystals were examined with an optical goniometer. All the single crystals appeared to have developed the same faces. The best crystal is shown in Fig. 1-2. The calculated interfacial angles, axial ratios and gnomonic projection standards are listed in Table 1-5. The observed interfacial angles were found to correspond to the calculated angles within ± 30', and they were found to correspond to the data recorded by Ramsdell.

Preliminary x-ray investigation.

A perfect single crystal of coesite, similar to the one shown in Fig. 1-2., was mounted on a precession camera and diffraction photographs were obtained with MoK_{α} radiation. Good photographs were obtained and the following cell dimensions were measured:

$$a = b = 7.17\ \text{Å}. \quad c = 12.38\ \text{Å}. \quad \text{and} \quad \gamma = 120^{\circ}.$$

These measurements are slightly lower than the measurements recorded by Ramsdell. No significance is attached to this discrepancy, since, first, the two samples came from different charges and may have had different cell dimensions and, second, neither of the two investigators used precision instruments.

The precession photographs showed regular extinctions as follows:

(hkl) type, h+l= 2n

(hk0) type, k= 2n

These extinctions indicate a B-centered cell and a b glide. The possible space groups are, consequently, B2/b and Bb. Since the morphological investigation indicated a center of symmetry, B2/b was expected to be the more probable space group.

The number of formula weight of SiO_2 per cell was calculated. It was found that the coesite cell contains an excess mass of 35 chemical mass units. The nature of this excess mass has not been investigated, but it appears probable that it represents impurities in the structure. Through private communications (F. Dachille, V. Walkenberg) we learned that coesite with a density of 2.94 was also made. With this density the number of SiO_2 per unit cell of coesite would be just slightly above 16 (i.e. 16.22). This indicates that man-made coesite contains considerable amount of impurities, and probably our sample contained more than some others.

X-ray powder pattern.

A few crystals of coesite were powdered and mounted in a 114.6 mm. diameter Debye-Scherrer camera. CuKα radiation at 40 kv. and 20 ma. was used. Relatively good powder patterns were obtained. The d values were calculated from the diffraction lines and were compared with the d values recorded by Coes[1]. The correspondance was found to be very satisfactory.

Since a large number of diffraction lines were obtained and the lines were relatively sharp, an attempt was made to index them. Since coesite has a monoclinic cell the indexing could not be achieved by the aid of charts. A modification of Ito's method for the indexing of powder photographs, was selected: the $\frac{1}{d^2}$'s of the diffraction lines were computed and compared with the $\frac{1}{d^2}$'s calculated from the unit cell dimensions obtained previousely. According to the correspondance of the calculated and observed $\frac{1}{d^2}$'s the diffraction lines were indexed. Most of the lines, especially the stronger lines, were indexed with no difficulty. Some weaker lines, however, could be indexed but with a larger discrepancy between the calculated and observed $\frac{1}{d^2}$'s. The correspondance between the calculated and observed $\frac{1}{d^2}$'s ranged between ± .005 and ± .01. Considering that the camera used is a standard non-focusing camera and that the radiation wavelength is relatively short, this correspondance can be regarded satisfactory. The calculated and observed d's and the $\frac{1}{d^2}$'s with the corresponding indices are listed in Table 1-6.

(The observed intensities were later checked with the structure factors and were found to be reasonable.)

Collection of three-dimensional intensity data.

The symmetry of space group B2/b defines that one quarter of the limiting sphere contains all the diffraction spots with non-equal intensities. Consequently, it is sufficient to obtain one quarter of the limitng sphere. The following quarter has been selected:

along a axis	from -a to +a,
along b axis	from 0 to +b
along c axis	from 0 to +c

The precession camera was used to obtain the intensity data. Due to the mechanical limitation of the camera and to the blank area in the center of the photographs of higher levels, different settings of the dial axis was necessary to obtain data for the full quarter. Four settings were found to be necessary:

Settings:		dial readins:
	A	0°00'
	B	90°00'
	C (a),(b)	49°12', 229°12'
	D	30°05'

These four settings are illustrated in Fig. 1-10.

Several levels were recorded with each setting. With setting A the levels from 0 to 6, with B from 0 to 3, with C

(a) and (b) from 0 to 5 and with D from 0 to 4 were recorded. Settings C (a) and C (b) do not require two different photographs, since with either setting the data of both are recorded, one on the top and other on the bottom half of the same film.

The intensities were measured by the M.I.T. modification of the Dawton method:

The x-ray films were not developed in the usual x-ray developer, but in a specially prepared Kodak D-76 developer, to which 2 cc of 1.0% KI and 20 cc. KBr were added per gallon. These films were then printed on Kodak commercial ortho film, so the dark diffraction spots of the first film became transparent spots on the print. The light transmission of these spots was then measured by means of a photoelectric cell, whose light aperture was kept constant during the whole procedure. After measuring the light transmission of the spots, the transmission of the background was measured on the white radiation streak, adjacent to the spot. The difference of these two readings gave the relative integrated intensity of the diffraction spot. The weaker spots could not be measured by the photoelectric cell, consequently, the intensities of these spots were estimated by eye. Invisible diffraction spots, which were not absent due to extinctions, were assigned a minimum intensity.

The relative intensities obtained were then multiplied by the reciprocal value of the Lorentz and polarization factor. The Lorentz and polarization factor was read from the Waser-Grenville-Abrahams charts available in the crystallographic laboratory.

Fig. 1-10.

Dial settings of the precession camera.

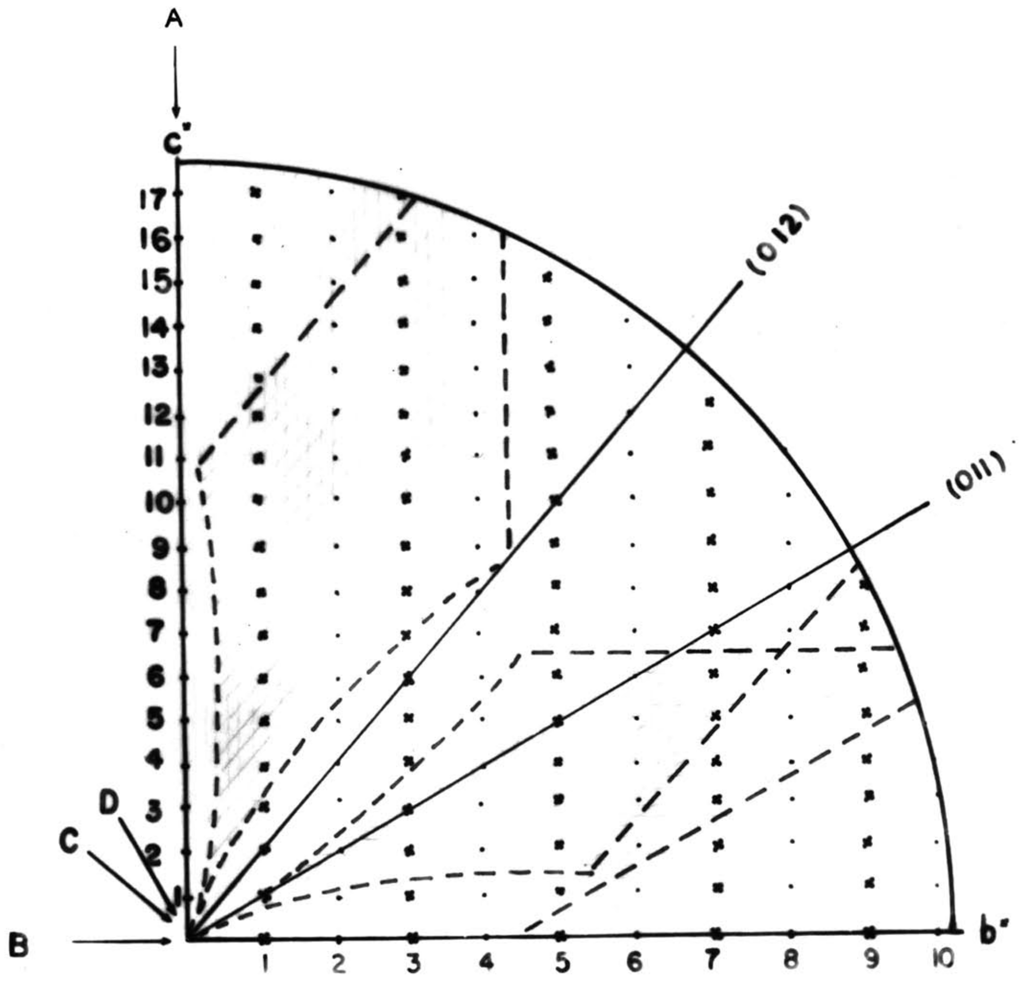
A
c*
B
C
D
(012)
(011)
b*
17
16
15
14
13
12
11
10
9
8
7
6
5
4
3
2
1
1
2
3
4
5
6
7
8
9
10

The linear absorption coefficient for SiO_2 has been calculated using the mass absorption data in the Internationale Tabellen zur Bestimmung von Kristallstrukturen:

$$\mu_l = \left(\frac{W_{Si}}{100} \times \mu/\rho_{Si} + \frac{W_O}{100} \times \mu/\rho_O \right) \times \quad =$$

$$= \left(\frac{W_{Si}}{100} \times 6.70 + \frac{W_O}{100} \times 1.50 \right) \times 3.01 =$$

$$= (.467 \times 6.70 + .533 \times 1.50) \times 3.01 =$$

$$= 11.8 \text{ cm}^{-1} \qquad = 1.18 \text{ mm}^{-1}$$

where $\underline{W}$ is the weight percent of the element in the formula, $\underline{\mu/\rho}$ is the mass absorption coefficient and $\underline{\rho}$ is the density of the compound.

The dimensions of the crystal used are .10 x .03 x .15 mm. and the crystal was mounted with the largest dimension perpendicular to the direction of the x-ray beam. Consequently, the largest mean distance the x-ray beam had to travel in the crystal is in the order of .12 mm. and the shortest mean distance is .03 mm. So the x-ray beam effected by the most and by the least absorption is:

$$I = I_o e^{-.142} = .868$$

$$I = I_o e^{-.0354} = .965$$

This means that the maximum variation in the effect of the absorption on the intensity of the diffraction, due to different orientations of the crystal, is less than 10% of the intensity. This is small enough to be neglected.

Preparation of the Patterson maps.

From the adjusted intensity data the three-dimensional Patterson function was computed at the M.I.T. Computation Center. The three-dimensional Fourier program was prepared by Dr. W.Sly. The Patterson function was evaluated at 1/60-th intervals for 1/8-th of the reciprocal cell. These functions were plotted on reciprocal cell maps and were contoured.

Since it was decided that the minimum function method would be applied, a set of maps was prepared for $1\frac{1}{2}$ by $1\frac{1}{2}$ unit cell in tha plane of the a and b axes and for each 1/60-th level along the c axis. The contours on these maps were coloured according to the magnitude of the peaks, and depressions were shaded.

Location of inversion peaks.

The possible types of Patterson peaks, their number, relative weight and relationships with each other are illustrated in Table 1-1. This table shows that there are 24 inversion peaks in the primitive cell of coesite, 8 of them are Si-Si and 16 O-O inversion peaks. In order to solve the Patterson function by the minimum function method one or more of these inversion peaks have to be located[5]. There is a convenient relationship between inversion, rotation and reflection peaks which is

Fig. 1-11.

Illustration of the relationship between inversion, rotation and reflection peaks.

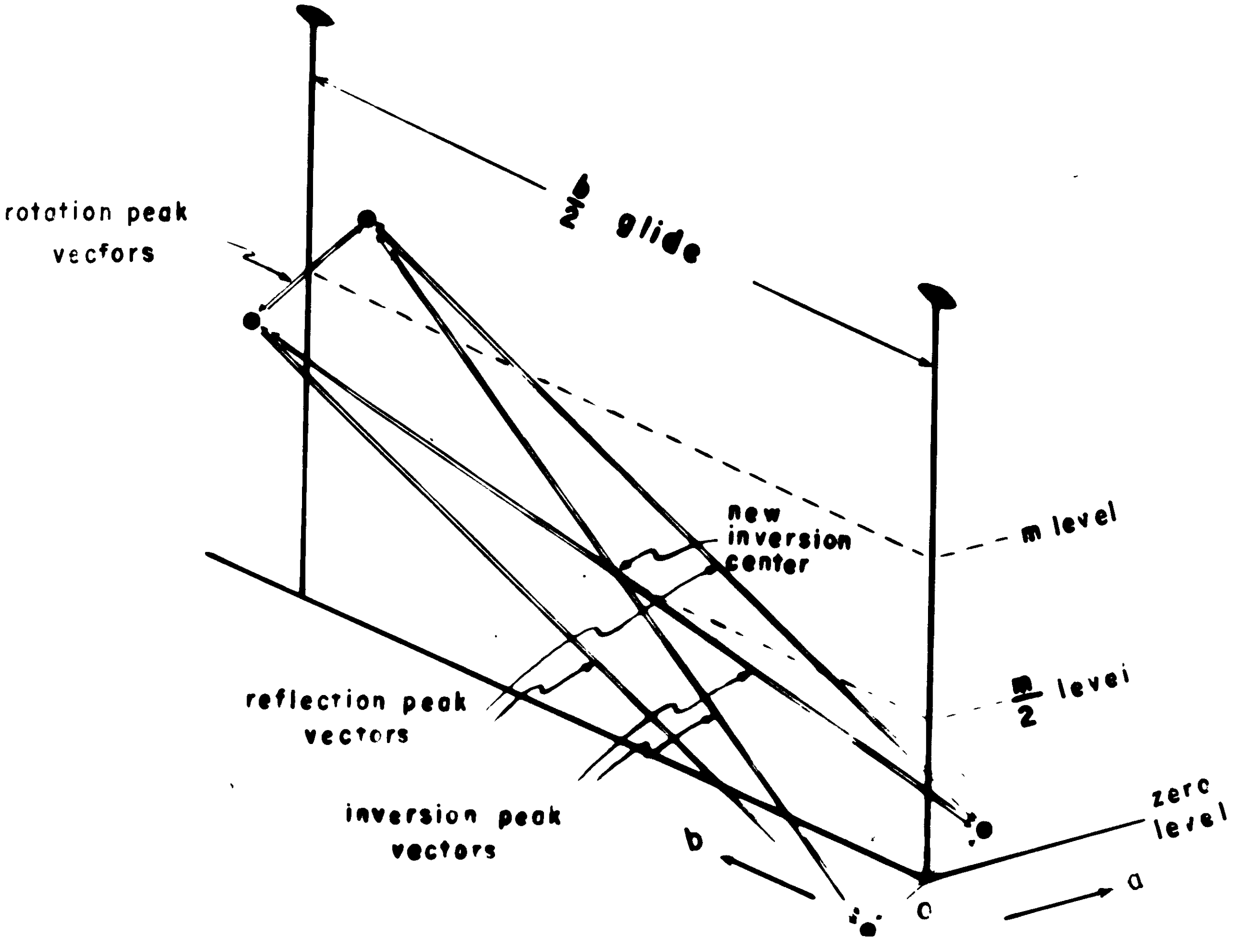
rotation peak vectors
$\frac{b}{2}$ glide
new inversion center
m level
$\frac{m}{2}$ level
reflection peak vectors
inversion peak vectors
zero level
b
o
a

illustrated in Fig.1-11., for the space group of coesite. 24 inversion peak candidates have been located in the primitive cell by the procedure which has been described previousely and is illustrated in Fig. 1-4.

A large number of these inversion peak candidates, however, were expected to be false. Half of them, right away, were known to be false, since half of the candidate peaks are only symmetry repetitions of the others. An inversion peak candidate below the reflection plane at $\underline{c}/4$ has a symmetry equivalent above the reflection plane and they both fulfill the inversion-rotation-reflection peak relationship. But only one of the two represents the inversion vector. Only 1/4 of the primitive cell is the assymmetric unit. In order to cover both sides of the reflection plane, however, 1/2 of the primitive cell had to be considered in the search for inversion peaks. Consequently, there were only 12 possible inversion peaks in the 1/2 primitive cell considered. The location of these peaks are listed in Table 1-7. The symmetrically equivalent peaks from which only one can be a true inversion peak, are recorded side-by-side as ($\underline{a}$) and ($\underline{b}$).

There is no other way to distinguish between true and false inversion peaks but to carry out the construction of one or more $\underline{M}_2$ maps for each of these peaks. The same level $\underline{M}_2$ map has been constructed by the aid of each one of the candidates. Four out of the 12 gave essentially the same pattern while the other eight had different wild patterns. It was concluded that the four inversion peak candidates yielding similar $\underline{M}_2$ maps were true inversion peaks and the others were false. The true inversion peaks in Table 1-7. are 1(a), 2(a), 3(a) and 4(b). The relative magnitude of the peaks in the $^1M_2$ and $^2M_2$ maps were almost the same, and the relative magnitude of the peaks in the other two M_2 maps were also similar but different from that of the first two maps. It was decided to use number 1 and 2 inversion peaks for the construction of complete sets of minimum function maps.

Construction of the minimum function maps.

A set of M_2 maps was prepared for both number 1 and 2 inversion peaks. This is accomplished by superimposing two Patterson maps, with a z coordinate difference between them, which z coordinate corresponds to the z coordinate of the inversion peak. The origin of the higher level map is placed at the x,y coordinates of the inversion peak on the lower level map. The origin of the M_2 map is then taken at the new center of inversion which is half way between the origins of the two Patterson maps. In Table 1-8. the corresponding pairs of Patterson maps are listed for both of the inversion peaks, with the new z coordinates of the M_2 maps. All the coordinates are given in 1/60-th units.

The M_2 maps were combined into M_4 maps by tracing the minimum function of the two rotation-equivalent halves of the M_2 maps, Fig. 1-12. The two sets of M_4 maps were, in turn, combined into one set of M_8 maps by tracing the minimum function of the corresponding $\underline{M}_4$ maps of each set. It was found that these two sets of $\underline{M}_4$ maps had two different centers of inversion at their origins. The origin of the ${}^1\underline{M}_4$ maps was accepted and the origin of the ${}^2\underline{M}_4$ maps was shifted to the center of inversion corresponding to the origin of the ${}^1\underline{M}_4$ maps. Fig.1-13. illustrates this procedure.

The resulting ${}^{1-2}\underline{M}_8$ maps revealed the structure of coesite. There are only two small and insignificant peaks in the $\underline{M}_8$ maps which do not represent an actual atom location.

Refinement.

The atomic coordinates of the $\underline{M}_8$ maps were then refined by eight cycles of refinement. This has been described in detail previousely. Table 1-9.shows in detail the coordinates of each cycle of refinement and the R, R', B and scale factors. After the third cycle of refinement six diffractions, and after the sixth cycle of refinement all the diffractions with sinθ less than .095 were removed, since it is believed that these diffractions were too much effected by primary extinction. The list of the indices of these diffractions are given in Table 1-10.

The refinement program simultaneousely calculated the structure factors and printed them along with the observed intensities. The latters were scaled down by the computer to the scale of the computed structure factors. The correspondance

Fig. 1-12.

Combination of $\underline{M}_2$ maps into $\underline{M}_4$ maps.

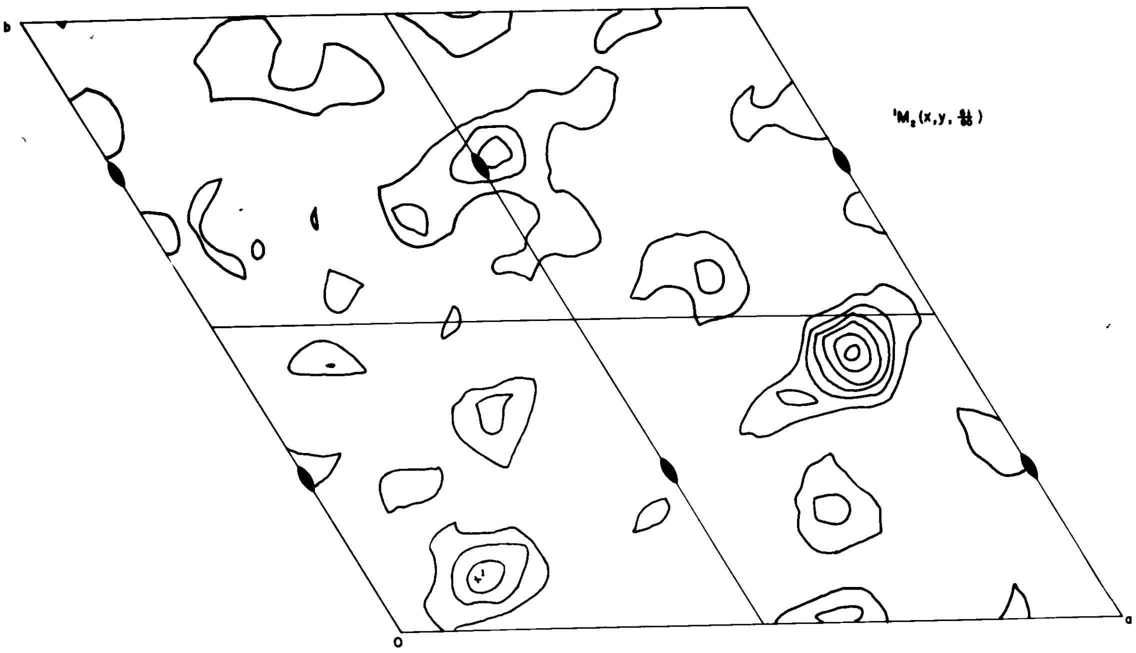
b
$^1M_2(x, y, \frac{31}{60})$
+1
o
a

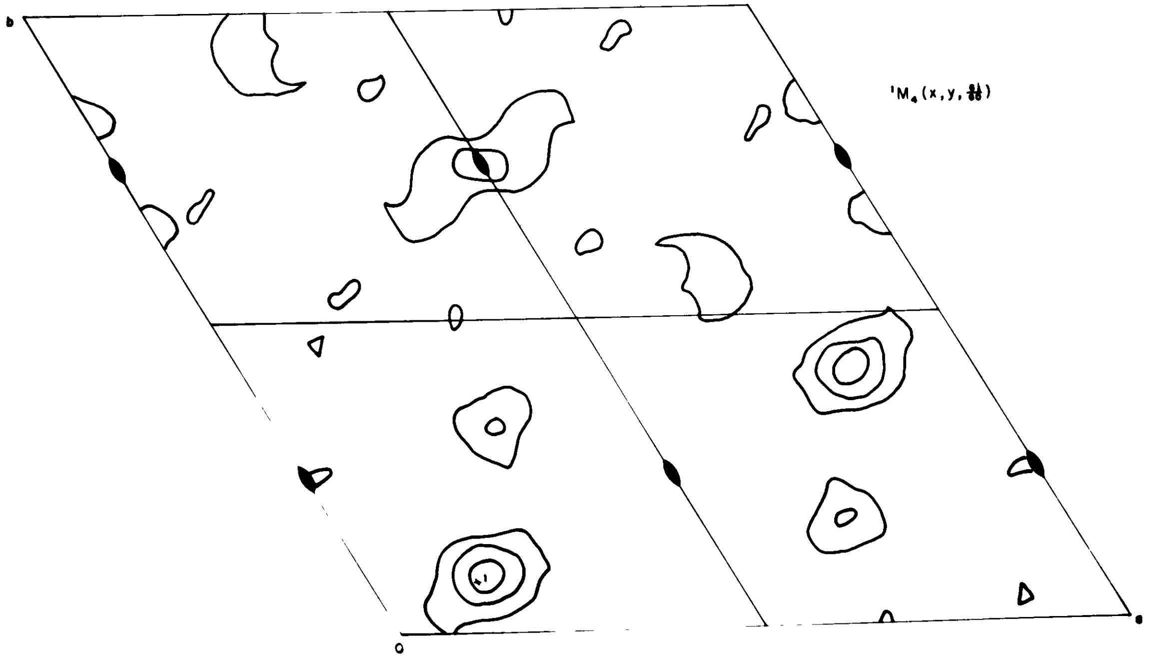
b
$^1M_4(x, y, \frac{31}{60})$
+1
o
a

Fig. 1-13.

Combination of two $\underline{M}_4$ maps into one $\underline{M}_8$ map.

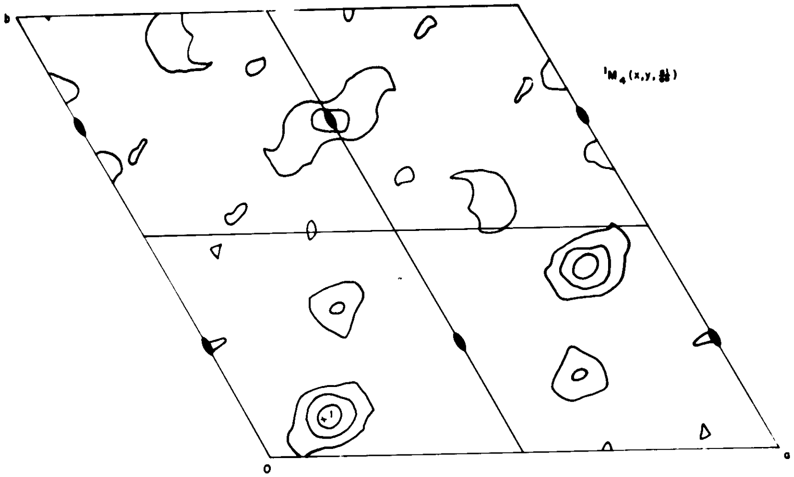

b
$^{1}M_{4}(x,y,[illegible])$
+1
0
a

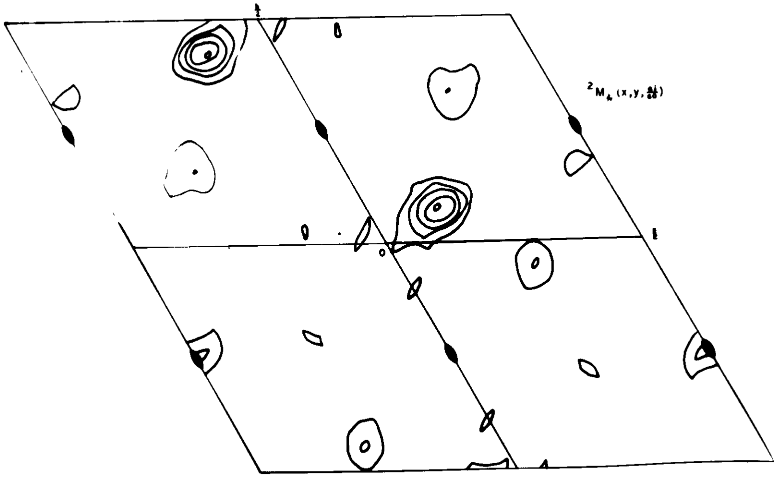

½
$^{2}M_{4}(x,y,[illegible])$
0
½

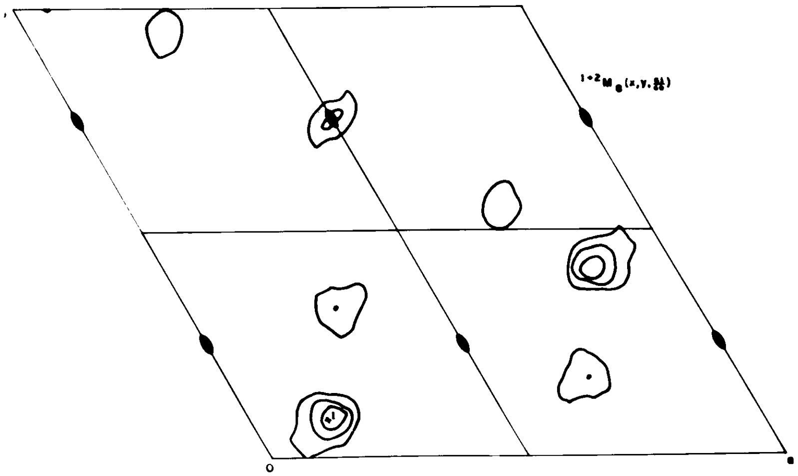

$^{1+2}M_{8}(x,y,[illegible])$
+1
0
a

between the observed and computed values was satisfactory. In order to save considerable typing, the structure factors and the comparative intensities as printed by the computer have been deposited in Professor M. J. Buerger's files.

The difference between the coordinates as obtained from the $\underline{M}_8$ maps and the final coordinates after eight cycles of refinement are listed in Table 1-3. The final coordinates for all the atoms in a full unit cell are listed in Table 1-11.

The coesite structure.

The structure of coesite has been described previousely and is illustrated in Fig.'s 1-7, 1-8 and 1-9. It is a new three-dimensional silica network, but it shows striking similarities with the tetrahedral network of the feldspar structure. Both structures can be described as a composition of 4-membered loops of tetrahedra. There are two symmetrically non-equivalent 4-membered loops in each of these two structures, and the whole structure can be built up by the repetition of either one of these two rings. One of the 4-membered loops has a center of symmetry and the other is perpendicular to a 2-fold rotation axis. Both these 4-membered loops are shown in Fig.1-14., in both the coesite and the sanidine (feldspar) structures. The diagram illustrates that the rings in the two structures differ only in the orientation of the free corners of the tetrahedra.

These 4-membered rings are also present, in the paracelsian, analcite and scapolite structures. But the orientation

Fig. 1-14.

The two non-equivalent 4-membered loops of tetrahedra in coesite and in sanidine.

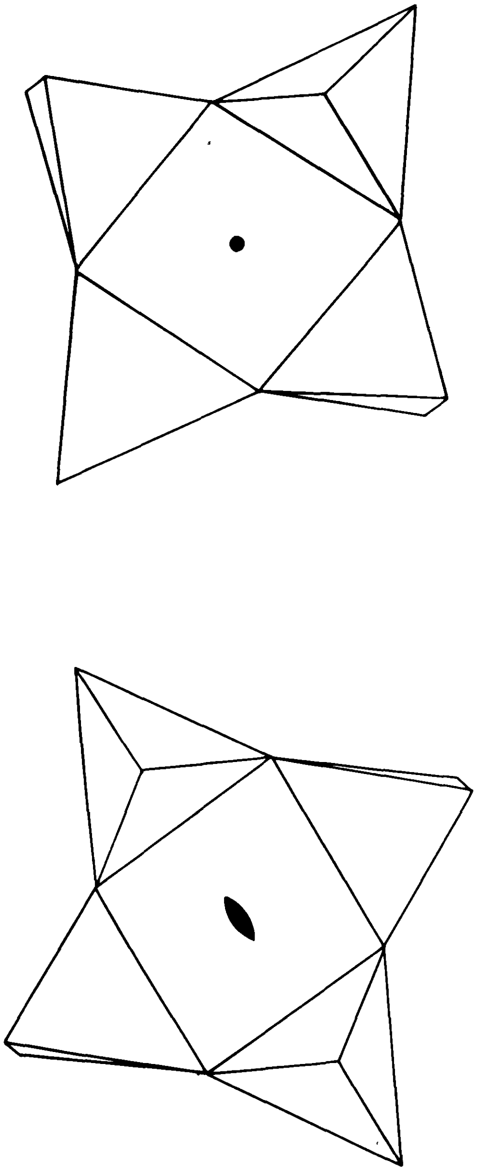

Coesite

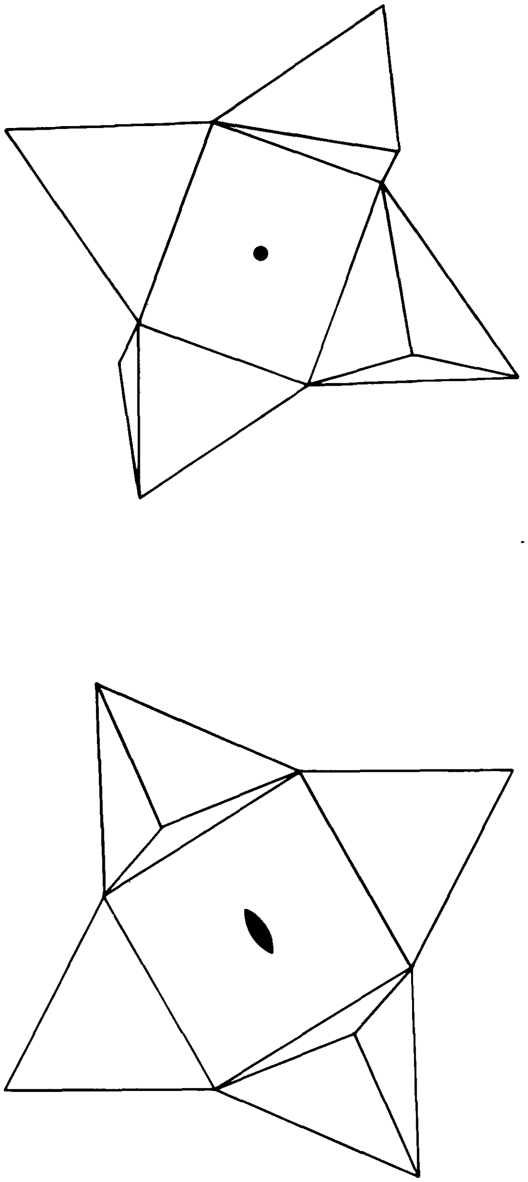

Sanidine

of the tetrahedra in the rings of these structures differ considerably from the orientation of tetrahedra in the coesite and feldspar rings. It can be concluded that the coesite structure is a new structure, but its basic characteristics are similar to the structures of several silicates.

Table 1-5.

Crystal morphologic data
of coesite.

a= 7.17 Å
b= 7.17 Å
c= 12.38 Å
γ = 120°00'
a:b:c:=.5791:.5791:1

$p_0:q_0:r_0$ = 1:.501:1
$r_2:p_2:q_2$ = 1.944:1.944:1
$p_0':q_0':x_0'$ = 1.1547:.5791:.5773
μ = 60°00'

Forms*	ϕ	ρ	ϕ_2	ρ_2=C	B	A
c 010	90°00'	30°00'	60°00'	90°00'	-	60°00'
b 001	0 00	90 00	-	0 00	90°00'	90 00
g 103	33 40	90 00	0 00	33 40	73 55	56 20
x 012	26 30	52 19	60 00	44 55	45 05	69 19
d 110	-90 00	30 00	120 00	90 00	60 00	120 00
v 111	71 31	61 18	30 00	73 50	33 43	33 43
p 111	-44 55	39 17	120 00	63 22	63 27	116 33

* L.S. Ramsdell[3] observed additional ((101)) and ((01$\bar{1}$)) forms

Table 1-6.

X-ray powder data of coesite.

No.	Intensity	Observed		Calculated		Indices
		d	$\frac{1}{d^2}$	$\frac{1}{d^2}$	d	
1	vw	6.23	.0258	.0258	6.23	(002)
2	vw	5.69	.0308	.0320	5.57	(101) $(1\bar{1}1)$
3	s	3.42	.0851	.0844	3.34	(103) (111)
4	vs	3.09	.1040	.1034	3.10	(020) $(2\bar{2}0)$ (252) $(2\bar{1}2)$
5	m	2.77	.1298	.1294	2.78	(022)
6	m	2.70	.1369	.1360	2.71	(113) $(1\bar{2}3)$
7	m	2.29	.1894	.1885	2.30	(105) (121) $(3\bar{1}1)$ $(3\bar{2}1)$ $(1\bar{1}5)$
8	m	2.19	.2076	.2076	2.19	(024) (220) $(2\bar{2}4)$ (212) $(2\bar{3}2)$
9	m	2.04	.2402	.2402	2.04	(301) $(3\bar{3}1)$ (123) (115) $(1\bar{3}3)$ $(3\bar{2}3)$
10	m	1.85	.2927	.2922	1.85	(303) $(3\bar{3}3)$ $(1\bar{2}7)$
11	m	1.80	.3089	.3100	1.80	(220)
12	m	1.71	.3415	.3448	1.70	(107) (311) $(3\bar{4}1)$ (125) $(3\bar{2}5)$ (135)
13	m	1.66	.3620	.3620	1.66	$(4\bar{1}2)$ $(4\bar{3}2)$
14	m	1.59	.3953	.3953	1.59	(305) (133) (313) $(3\bar{4}3)$ (305) $(3\bar{3}5)$
15	m	1.55	.4166	.4166	1.55	(008) (040) (216) $(4\bar{4}0)$ $(2\bar{3}6)$
16	vw	1.50	.4444	.4402	1.51	$(4\bar{1}4)$ $(4\bar{4}2)$ $(3\bar{5}3)$ (042)
17	w	1.46	.4670	.4670	1.46	(036)
18	vw	1.41	.5013	.5013	1.41	$(5\bar{5}3)$ $(5\bar{2}1)$ $(3\bar{5}1)$ $(3\bar{4}5)$ (223) (135)

Table 1-6. (continued)

No.	Intensity	Observed		Calculated		Indices
		d	$\frac{1}{d^2}$	$\frac{1}{d^2}$	d	
19	m	1.347	.5515	.5498	1.438	(323) $(5\bar{4}1)$ (109) $(2\bar{4}6)$ (323) (226)
20	vw	1.323	.5716	.5704	1.324	$(1\bar{1}6)$ $(4\bar{3}6)$ (452)
21	m	1.288	.6031	.6014	1.289	(143) $(5\bar{1}3)$ (234) $(2\bar{5}4)$ $(1\bar{4}7)$ (218)
22	w	1.235	.6557	.6538	1.237	(325) (551) (501) (355) $(5\bar{2}5)$ (535)
23	m	1.188	.7090	.7048	1.191	(503) (331) $(3\bar{6}1)$ (145) $(5\bar{1}5)$ (129)
24	vw	1.170	.7324	.7239	1.175	$(6\bar{3}2)$ (240) $(2\bar{5}6)$ (228) $(2\bar{4}8)$ (428)
25	vw	1.071	.8699	.8598	1.078	(513) (335) $(1\bar{5}7)$ (319) (139) (149)
26	w	1.040	.9242	.9306	1.037	(060) $(6\bar{3}6)$ (519)
27	m	1.025	.9519	.9566	1.012	(062) (346) (418)
28	m	1.015	.9709	.9824	1.009	(432) $(1\bar{6}5)$ (515) (1,2,11) $(3,\bar{1},11)$
29	w	.997	1.005	1.016	.992	$(3\bar{6}7)$ (329) $(5\bar{3}9)$ $(5\bar{2}9)$
30	vw	.986	1.028	1.034	.983	(260) (604) (343) $(3\bar{7}3)$
31	w	.973	1.057	1.061	.971	(434) $(7\bar{2}3)$ (523) $(0\bar{5}8)$
32	w	.960	1.085	1.080	.962	(345) (149) (735) $(6\bar{3}8)$ $(1\bar{5}9)$
33	w	.941	1.130	1.132	.940	$(2\bar{7}4)$ $(3\bar{7}5)$ (157) (517) (1,3,11)
34	vw	.936	1.141	1.137	.938	(612) (248) $(2\bar{6}8)$ (428) $(6\bar{2}8)$
35	w	.921	1.179	1.170	.924	$(1\bar{7}3)$ $(7\bar{1}3)$ (525) $(7\bar{2}5)$ (606) (509)
36	w	.903	1.226	1.225	.903	(353) $(6\bar{1}8)$ (339)
37	w	.886	1.274	1.273	.886	(351) (440) (531) (165) (701) (163)

Table 1-6, (continued)

No.	Intensity	Observed		Calculated		Indices
		d	$\frac{1}{d^2}$	$\frac{1}{d^2}$	d	
38	w	.886	1.286	1.293	.882	(072) (1,2,13) (3,2,11) $(3,\bar{2},13)$
39	w	.867	1.332	1.332	.866	(701) $(3\bar{8}3)$ (527) (159) $(1\bar{6}9)$
40	vw	.860	1.351	1.347	.862	(616) (608) (4,0,12)$(2,\bar{1},14)$
41	vw	.855	1.369	1.369	.855	$(8\bar{2}2)$ (074) (262) (622) (438)
42	w	.850	1.377	1.347	.853	(2,4,10) $(6,\bar{2},10)$ $(2,\bar{2},14)$
43	w	.835	1.434	1.429	.836	(355) (705) (535) $(7\bar{1}7)$ (167) $(1\bar{7}7)$
44	w	.826	1.460	1.475	.823	(446) $(6,\bar{1},10)$ (2,1,14)
45	w	.817	1.499	1.499	.817	$(8\bar{1}2)$ (315) (076) $(8\bar{3}6)$ (349)
46	w	.801	1.557	1.542	.805	$(1,\bar{2},15)$ (1,1,15)
47	w	.791	1.598	1.585	.794	(357) (626) (707) (6,0,10)
48	w	.780	1.642	1.638	.782	(175) $(1\bar{8}5)$ $(7\bar{1}9)$
49	w	.776	1.660	1.654	.777	(800)

Notes:

vw = very weak

w = weak

m = medium

s = strong

vs = very strong

Table 1-7.

List of inversion peak candidates.

Peak No.	Location and magnitude of peaks	Inversion peak candidates		Rotation peaks	Reflection peaks
		a	b		
1	x	18	12	18	0
	y	9	9	39	30
	z	13	17	0	13
	Magnitude	342	342	740	750
2	x	0	30	0	0
	y	4	4	34	30
	z	19	11	0	19
	Magnitude	360	360	738	530
3	x	27	3	$26\frac{1}{2}$	0
	y	24	24	$53\frac{1}{2}$	30
	z	13	17	0	13
	Magnitude	300	300	320	750
4	x	0	30	0	0
	y	4	4	34	30
	z	4	26	0	26
	Magnitude	300	300	738	530
5	x	8	22	8	0
	y	22	22	52	30
	z	13	17	0	13
	Magnitude	238	238	348	750
6	x	$9\frac{1}{2}$	$20\frac{1}{2}$	$9\frac{1}{2}$	0
	y	45	45	15	30
	z	13	17	0	13
	Magnitude	232	232	381	750

Note: The denominator of 60 has been omitted in the coordinates of the Patterson maps.

Table 1-8.

Superposition data for the construction of M_2 maps.

Inversion peak No.	Place the origin of map No.	at the inversion peak location of map No.	to give M_2 map level
1	7	54 Or (6)	1/2
	8	55 (5)	1 1/2
	9	56 (4)	2 1/2
	10	57 (3)	3 1/2
	11	58 (2)	4 1/2
	12	59 (1)	5 1/2
	13	0	6 1/2
	14	1	7 1/2
	15	2	8 1/2
	16 or (14+a/2)	3	9 1/2
	17 (13+a/2)	4	10 1/2
	18 (12+a/2)	5	11 1/2
	19 (11+a/2)	6	12 1/2
	20 (10+a/2)	7	13 1/2
	21 (9+a/2)	8	14 1/2
2	10	51 or (9)	1/2
	11	52 (8)	1 1/2
	12	53 (7)	2 1/2
	13	54 (6)	3 1/2
	14	55 (5)	4 1/2
	15	56 (4)	5 1/2
	16 or (14+a/2)	57 (3)	6 1/2
	17 (13+a/2)	58 (2)	7 1/2
	18 (12+a/2)	59 (1)	8 1/2

Table 1-8. (continued)

Inversion peak No.	Place the origin of map No.	at the inversion peak location of map No.	to give M_2 map level
2 (cont.)	19 (11+a/2)	0	9 1/2
	20 (10+a/2)	1	10 1/2
	21 (9+a/2)	2	11 1/2
	22 (8+a/2)	3	12 1/2
	23 (7+a/2)	4	13 1/2
	24 (6+a/2)	5	14 1/2

Note: The denominator of 60 has been omitted in the coordinates of the Patterson maps.

Table 1-9.

Atomic coordinates and other data of each cycle of refinement.

Description	Cycles of refinement								
	0	1st	2nd	3rd	4th	5th	6th	7th	8th
Scale factor	.5652	.5431	.5423	.5444	.5406	.5427	.5378	.5374	.5363
R	46.69	36.11	27.55	25.26	18.35	18.00	16.94	17.03	16.95
R'	36.39	10.37	5.94	5.19	2.58	2.43	1.96	1.93	1.92
Si_1 x	.1600	.1501	.1448	.1443	.1416	.1408	.1406	.1404	.1403
y	.0800	.0803	.0788	.0763	.0749	.0741	.0738	.0738	.0735
z	.1100	.1082	.1083	.1086	.1084	.1084	.1084	.1084	.1084
B	1.000	1.110	1.085	1.027	.903	.875	.817	.817	.813
Si_2 x	.5100	.5052	.5054	.5058	.5060	.5060	.5063	.5063	.5063
y	.5300	.5373	.5383	.5386	.5383	.5384	.5385	.5386	.5388
z	.1600	.1581	.1577	.1577	.1574	.1575	.1576	.1577	.1576
B	1.000	.790	.724	.689	.632	.639	.589	.599	.600
O_1 x	.0000	.0000	.0000	.0000	.0000	.0000	.0000	.0000	.0000
y	.0000	.0000	.0000	.0000	.0000	.0000	.0000	.0000	.0000
z	.0000	.0000	.0000	.0000	.0000	.0000	.0000	.0000	.0000
B	1.000	..984	.967	1.009	.828	.858	.817	.839	.856
O_2 x	.5000	.5000	.5000	.5000	.5000	.5000	.5000	.5000	.5000
y	.7500	.7500	.7500	.7500	.7500	.7500	.7500	.7500	.7500
z	.1100	.1124	.1136	.1134	.1154	.1149	.1168	.1164	.1166
B	1.000	1.194	1.146	1.041	.997	1.032	1.102	1.180	1.197
O_3 x	.2700	.2635	.2621	.2648	.2676	.2680	.2686	.2693	.2694
y	.9200	.9302	.9359	.9372	.9376	.9382	.9394	.9397	.9405
z	.1300	.1287	.1277	.1274	.1272	.1270	.1259	.1257	.1256
B	1.000	.878	.903	.923	.908	.975	1.006	1.070	1.111

Table 1-9. (continued)

Description		Cycles of refinement								
		0	1st	2nd	3rd	4th	5th	6th	7th	8th
O_4	x	.3000	.3038	.3031	.3051	.3061	.3076	.3079	.3081	.3080
	y	.3200	.3205	.3235	.3243	.3278	.3285	.3290	.3293	.3293
	z	.1100	.1062	.1038	.1028	.1043	.1040	.1030	.1031	.1030
	B	1.000	1.009	1.193	1.281	1.269	1.231	1.311	1.367	1.381
O_5	x	.0100	.0123	.0135	.0131	.0114	.0135	.0130	.0129	.0123
	y	.4700	.4706	.4701	.4711	.4751	.4740	.4735	.4729	.4726
	z	.2200	.2155	.2133	.2129	.2135	.2121	.2123	.2121	.2122
	B	1.000	.607	.579	.585	.526	.561	.573	.625	.656

Table 1-10.

Indices of diffraction with $\sin\theta \leqslant .095$.

$(\bar{2}40)$
$(\bar{2}20)$
(020)
(220)
$(\bar{2}00)$
(200)
$(\bar{1}41)$
$(\bar{3}31)$
$(\bar{1}31)$
(131)
$(\bar{3}21)$
$(\bar{1}21)$
(121)
$(\bar{3}11)$
(111)
(311)
$(\bar{3}01)$
(301)
$(\bar{4}32)$
$(\bar{2}32)$
(032)
$(\bar{2}22)$
(022)
$(\bar{2}12)$
$(\bar{2}02)$
(002)
(202)
$(\bar{1}33)$
$(\bar{3}23)$
$(\bar{1}23)$
(123)
$(\bar{1}13)$
(113)
$(\bar{1}03)$
(103)
$(\bar{2}24)$
(024)
$(\bar{2}14)$
(014)
(004)
$(\bar{2}04)$
(204)
$(\bar{1}15)$
(115)
$(\bar{1}05)$
(105)
$(\bar{2}06)$
(206)

Table 1-11.

Atomic coordinates in a full unit cell of coesite.

(1) xyz

	x	y	z
Si_1	.1403	.0735	.1084
Si_2	.5063	.5388	.1576
O_1	0	0	0
O_2	1/2	3/4	.1166
O_3	.2694	.9405	.1256
O_4	.3080	.3293	.1030
O_5	.0123	.4726	.2122

(2) $\bar{x}\,\bar{y}\,\bar{z}$

	x	y	z
Si_1	.8597	.9265	.8916
Si_2	.4937	.4612	.8424
O_1	0	0	0
O_2	1/2	1/4	.8834
O_3	.7306	.0595	.8744
O_4	.6920	.6707	.8970
O_5	.9877	.5274	.7878

Table 1-11. (continued)

(3) $\bar{x}, \frac{1}{2}-y, z$

	x	y	z
Si_1	.8597	.4265	.1084
Si_2	.4937	.9612	.1576
O_1	0	1/2	0
O_2	1/2	3/4	.1166
O_3	.7306	.5595	.1256
O_4	.6029	.1707	.1030
O_5	.9877	.0274	.2122

(4) $x, \frac{1}{2}+y, \bar{z}$

	x	y	z
Si_1	.1403	.5735	.8916
Si_2	.5063	.0388	.8424
O_1	0	1/2	0
O_2	1/2	1/4	.8834
O_3	.3694	.4405	.8744
O_4	.3080	.8293	.8970
O_5	.0123	.9726	.7878

Table 1-11.(continued)

(5) $x\ y\ z + \frac{1}{2}\ 0\ \frac{1}{2}$

	x	y	z
Si$_1$	.6403	.0735	.6084
Si$_2$	.0063	.5388	.6576
O$_1$	1/2	0	1/2
O$_2$	0	3/4	.6166
O$_3$	.7694	.9405	.6256
O$_4$	.8080	.3293	.6030
O$_5$	.5123	.4726	.7122

(6) $\bar{x}\ \bar{y}\ \bar{z} + \frac{1}{2}\ 0\ \frac{1}{2}$

	x	y	z
Si$_1$	.3597	.9265	.3916
Si$_2$	.9937	.4612	.3424
O$_1$	1/2	0	1/2
O$_2$	0	1/2	.3834
O$_3$	.2306	.0595	.3744
O$_4$	.1920	.6707	.3970
O$_5$	.4877	.5274	.2878

Table 1-11. (continued)

(7) $\bar{x}, \frac{1}{2}-y, z + \frac{1}{2}\ 0\frac{1}{2}$

	x	y	z
Si_1	.3597	.4265	.6084
Si_2	.9937	.9612	.6576
O_1	1/2	1/2	1/2
O_2	0	3/4	.6166
O_3	.2306	.5595	.6256
O_4	.1920	.1707	.6030
O_5	.4877	.0274	.7122

(8) $x, \frac{1}{2}+y, \bar{z} + \frac{1}{2}\ 0\ \frac{1}{2}$

	x	y	z
Si_1	.6403	.5735	.3916
Si_2	.0063	.0388	.3424
O_1	1/2	1/2	1/2
O_2	0	1/4	.3834
O_3	.7694	.4405	.3744
O_4	.8080	.8293	.3970
O_5	.5123	.9726	.2878

Supplement to Chapter II.

The relative energies of rings of tetrahedra.

Computation of the energies of n-membered rings and an endless chain of tetrahedra.

Projections of n-membered rings of tetrahedra were carefully drawn to a scale of one inch to one unit length. The values for n were 2 to 10. The tetrahedra in these rings were oriented as described before, and consequently, in the drawings the two shared corners and the center of the tetrahedron are in the same plane, while the unshared corners are equal distances above and below this plane. The corners of the tetrahedra were lettered, and the centers were assigned a number, as it is shown in Fig. 2-3. The interatomic distances were carefully measured to three significant figures on the drawings. The multiplicity of each type of interatomic distance was determined by the symmetry of the rings. The interatomic distances, their multiplicity factors and the pruducts of the involved atoms were tabulated and the calculation of the energies was carried out in the tables, as it is shown in Table 2-1.

A similar calculation for an endless chain of tetrahedra was also undertaken, with certain approximations. A chain of 30 tetrahedra, oriented similarly to the tetrahedra of the rings , was drawn to a scale of one inch to two unit lengths. The lettering of the elements of the tetrahedra are shown in Fig. 2-4. It was found that beyond a certain number of tetrahedra some types of interatomic distances differ only by less than the error of measurement, and consequently, they can be regarded equal. These interatomic distances were grouped beyond this critical point and the same interatomic distance was assigned to them. The different types of interatomic distances, and the limits beyond which some of them are assigned the same interatomic distances are shown in Table 2-2,(a). This table also includes other data necessary for the computation of energies, such as the product of the charges of atoms corresponding to the interatomic distances, and the multiplicity factors.

All these essential data are repeated in Table 2-2,(b), and the calculation of energies is carried out in this tabulated form, similarly to that of the n-membered rings of tetrahedra. This calculation is, however, limited to only 20 tetrahedra in the chain. Beyond the 20-th tetrahedron there are only two different interatomic distances, one is between repulsive atoms and the other between attractive atoms. Both have the same products of charges, and multiplicity factors. The repulsive energy is slightly higher than the attractive, consequently, this difference was calculated to a limit beyond which it becomes negligible. This calculation is shown in Table 2-2, (c). The total approximate energy of the endless chain of tetrahedra was obtained by the summation of the final energies of Table 2-2,(b) and Table 2-2,(c).

Fig. 2-3.

Illustration of symbols used in the computation of energies of n-membered rings of tetrahedra.

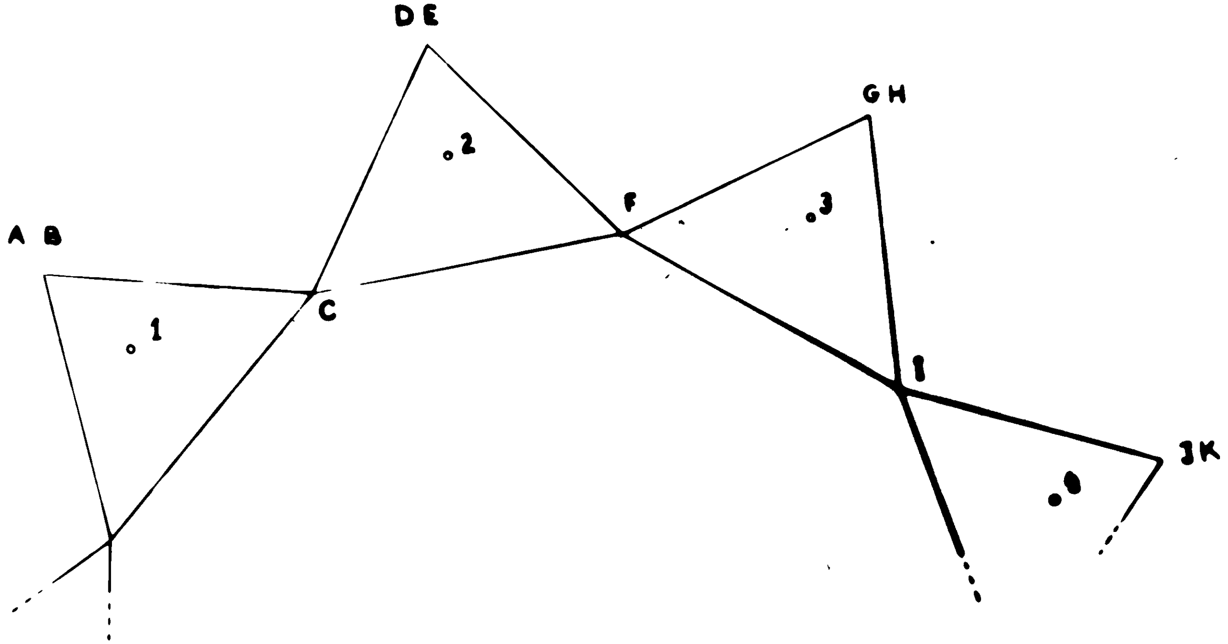

A B
DE
GH
C
F
I
JK
1
2
3
4

Fig. 2-4.

Illustration of symbols used in the computation of energy of an endless chain of tetrahedra.

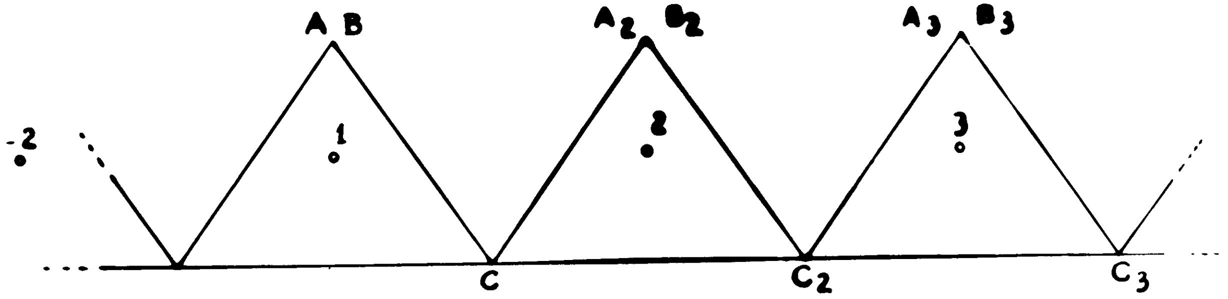
-2
A B
1
C
A2 B2
2
C2
A3 B3
3
C3

Table 2-1.

Energy computation data of n-membered rings of tetrahedra.

n	Type	Charge	Distance	1/Dist.	Potential	Multipl.	Attract^{n}.	Repuls^{n}.
2	1-D	4	1.95	.513	2.052	2	4.104	
	1-2	16	1.14	.877	14.032	1		14.032
	A-2	4	1.95	.513	2.052	2	4.104	
	A-D	1	2.30	.435	.435	2		.870
	A-E	1	2.83	.353	.353	2		.706
	C-2	8	1.00	1.000	8.000	1	8.000	
	C-D	2	1.63	.613	1.226	2		2.452
	C-F	4	1.63	.613	2.452	1		2.452
							16.208	20.512
		Repulsion = 4.304,			$-e^2A = +11.047$			
3	1-D	4	2.47	.405	1.620	4	6.480	
	1-F	8	2.00	.500	4.000	1	4.000	
	1-2	16	1.83	.546	8.736	2		17.472
	A-2	4	2.47	.405	1.620	4	6.480	
	A-D	1	2.81	.356	.356	4		1.424
	A-E	1	3.25	.308	.308	4		1.232
	A-F	2	2.69	.372	.744	2		1.488
	C-2	8	1.00	1.000	8.000	1	8.000	
	C-3	8	2.00	.500	4.000	1	4.000	
	C-D	2	1.63	.613	1.226	2		2.452
	C-F	4	1.63	.613	2.452	1		2.452
	C-G	2	2.69	.372	.744	2		1.488
							28.960	28.008

Attraction = .952, $-e^2A = -2.443$

Table 2-1. (continued)

n	Type	Charge	Distance	1/Dist.	Potential	Multipl.	Attract^{n}.	Repuls^{n}.
4	1-D	4	2.54	.394	1.576	4	6.304	
	1-F	8	2.36	.424	3.392	2	6.784	
	1-G	4	3.46	.289	1.156	2	2.312	
	1-2	16	1.97	.508	8.128	2		16.256
	1-3	16	2.79	.358	5.728	1		5.728
	A-2	4	2.54	.394	1.576	4	6.304	
	A-3	4	3.46	.289	1.156	2	2.312	
	A-D	1	2.79	.358	.358	4		1.432
	A-E	1	3.23	.310	.310	4		1.240
	A-F	2	3.01	.332	.644	4		2.656
	A-G	1	3.93	.254	.254	2		.508
	A-H	1	4.24	.236	.236	2		.472
	C-2	8	1.00	1.000	8.000	1	8.000	
	C-3	8	2.36	.424	3.392	2	6.784	
	C-D	2	1.63	.613	1.226	2		2.452
	C-F	4	1.63	.613	2.452	1		2.452
	C-G	2	3.01	.332	.664	4		2.656
	C-I	4	2.30	.435	1.740	1		1.740
							38.800	37.592

Attraction = 1.208, $\underline{-e^{2}A = -3.104}$

5	1-D	4	2.51	.398	1.592	4	6.368	
	1-F	8	2.50	.400	3.200	2	6.400	
	1-G	4	3.85	.260	1.040	4	4.160	
	1-I	8	3.09	.324	2.592	1	2.592	
	1-2	16	2.06	.485	7.760	2		15.520

Table 2-1. (continued)

n	Type	Charge	Distance	1/Dist.	Potential	Multipl.	Attract^{n}.	Repuls^{n}.
	1-3	16	3.23	.310	4.960	2		9.920
	A-2	4	2.51	.398	1.592	4	6.368	
	A-3	4	3.85	.260	1.040	4	4.160	
	A-D	1	2.66	.376	.376	4		1.504
	A-E	1	3.12	.321	.321	4		1.284
	A-F	2	3.10	.322	.644	4		2.576
	A-G	1	4.30	.233	.233	4		.932
	A-H	1	4.60	.217	.217	4		.868
	A-I	2	3.70	.270	.540	2		1.080
	C-2	8	1.00	1.000	8.000	1	8.000	
	C-3	8	2.50	.400	3.200	2	6.400	
	C-4	8	3.09	.324	2.592	1	2.592	
	C-D	2	1.63	.613	1.226	2		2.452
	C-F	4	1.63	.613	2.542	1		2.542
	C-G	2	3.10	.322	.644	4		2.576
	C-I	4	2.63	.380	1.520	2		3.040
	C-J	2	3.70	.270	.540	2		1.080
							47.040	45.284
			Attraction = 1.756,		$-e^2A = -4.507$			
6	1-D	4	2.45	.408	1.632	4	6.528	
	1-F	8	2.57	.389	3.112	2	6.224	
	1-G	4	4.01	.249	.996	4	3.984	
	1-I	8	3.48	.387	2.296	2	4.592	
	1-J	4	4.57	.219	.876	2	1.752	
	1-2	16	2.00	.500	8.000	2		16.000
	1-3	16	3.44	.291	4.656	2		9.312

Table 2-1. (continued)

n	Type	Charge	Distance	1/Dist.	Potential	Multipl.	Attractn.	Repulsion
	1-4	16	3.99	.251	4.016	1		4.016
	A-2	4	2.45	.408	1.632	4	6.528	
	A-3	4	4.01	.249	.996	4	3.984	
	A-4	4	4.57	.219	.876	2	1.752	
	A-D	1	2.54	.394	.394	4		1.576
	A-E	1	3.01	.332	.332	4		1.328
	A-F	2	3.14	.318	.636	4		2.544
	A-G	1.	4.40	.227	.227	4		.908
	A-H	1	4.68	.214	.214	4		.856
	A-I	2	4.12	.243	.486	4		1.944
	A-J	1	5.14	.195	.195	2		.390
	A-K	1	5.40	.185	.185	2		.370
	C-2	8	1.00	1.000	8.000	1	8.000	
	C-3	8	2.57	.389	3.112	2	6.224	
	C-4	8	3.48	.287	2.296	2	4.592	
	C-D	2	1.63	.613	1.226	2		2.452
	C-F	4	1.63	.613	2.452	1		2.452
	C-G	2	3.14	.318	.636	4		2.544
	C-I	4	2.81	.356	1.424	2		2.848
	C-J	2	4.12	.243	.486	4		1.944
	C-L	4	3.26	.307	1.228	1		1.228
							54.160	52.712

Attraction = 1.448, $\underline{-e^2A = -3.716}$

n	Type	Charge	Distance	1/Dist.	Potential	Multipl.	Attractn.	Repulsion
7	1-D	4	2.42	.413	1.652	4	6.608	
	1-F	8	2.60	.385	3.080	2	6.160	
	1-G	4	4.10	.244	.976	4	3.904	

Table 2-1. (continued)

n	Type	Charge	Distance	1/Dist.	Potential	Multipl.	Attract.^{n}	Repuls.^{n}
	1-I	8	3.73	.268	2.144	2	4.288	
	1-J	4	5.05	.198	.792	4	3.168	
	1-L	8	4.14	.242	1.936	1	1.936	
	1-2	16	1.97	.508	8.128	2		16.256
	1-3	16	3.55	.282	4.512	2		9.024
	1-4	16	4.41	.227	3.632	2		7.264
	A-2	4	2.42	.413	1.652	4	6.608	
	A-3	4	4.10	.244	.976	4	3.904	
	A-4	4	5.05	.198	.792	4	3.168	
	A-D	1	2.46	.406	.406	4		1.624
	A-E	1	2.95	.339	.339	4		1.356
	A-F	2	3.12	.321	.642	4		2.568
	A-G	1	4.44	.225	.225	4		.900
	A-H	1	4.72	.212	.212	4		.848
	A-I	2	4.33	.231	.462	4		1.848
	A-J	1	5.51	.181	.181	4		.724
	A-K	1	5.75	.174	.174	4		.696
	A-L	2	4.76	.210	.420	2		.840
	C-2	8	1.00	1.000	8.000	1	8.000	
	C-3	8	2.60	.385	3.080	2	6.160	
	C-4	8	3.73	.268	2.144	2	4.288	
	C-5	8	4.14	.242	1.936	1	1.936	
	C-D	2	1.63	.613	1.226	2		2.452
	C-F	4	1.63	.613	2.452	1		2.542
	C-G	2	3.12	.321	.642	4		2.568
	C-I	4	2.93	.341	1.364	2		2.728
	C-J	2	4.33	.231	.462	4		1.848

Table 2-1. (continued)

n	Type	Charge	Distance	1/Dist.	Potential	Multipl.	Attract^n.	Repuls^n.
	C-L	4	3.65	.274	1.096	2		2.192
	C-M	2	4.76	.210	.420	2		.840
							60.128	59.028

Attraction = 1.100, $-e^2A = -2.823$

n	Type	Charge	Distance	1/Dist.	Potential	Multipl.	Attract^n.	Repuls^n.
8	1-D	4	2.37	.422	1.688	4	6.752	
	1-F	8	2.59	.386	3.088	2	6.176	
	1-G	4	4.07	.246	.984	4	3.936	
	1-I	8	3.88	.258	2.064	2	4.128	
	1-J	4	5.25	.190	.760	4	3.040	
	1-L	8	4.56	.219	1.752	2	3.504	
	1-M	4	5.68	.176	.704	2	1.408	
	1-2	16	1.94	.515	8.240	2		16.480
	1-3	16	3.58	.279	4.464	2		8.928
	1-4	16	4.68	.214	3.424	2		6.848
	1-5	16	5.07	.197	3.152	1		3.152
	A-2	4	2.37	.422	1.688	4	6.752	
	A-3	4	4.07	.246	.984	4	3.936	
	A-4	4	5.25	.190	.760	4	3.040	
	A-5	4	5.68	.176	.704	2	1.408	
	A-D	1	2.38	.420	.420	4		1.680
	A-E	1	2.88	.347	.347	4		1.388
	A-F	2	3.12	.321	.642	4		2.568
	A-G	1	4.38	.228	.228	4		.912
	A-H	1	4.66	.215	.215	4		.860
	A-I	2	4.44	.225	.450	4		1.800
	A-J	1	5.72	.175	.175	4		.700

Table 2-1. (continued)

n	Type	Charge	Distance	1/Dist.	Potential	Multipl.	Attractn	Repulsn
	A-K	1	5.94	.168	.168	4		.672
	A-L	2	5.12	.195	.390	4		1.560
	A-M	1	6.17	.162	.162	2		.324
	A-N	1	6.37	.157	2.157	2		.314
	C-2	8	1.00	1.000	8.000	1	8.000	
	C-3	8	2.59	.386	3.088	2	6.176	
	C-4	8	3.88	.258	2.064	2	4.128	
	C-5	8	4.56	.219	1.752	2	3.504	
	C-D	2	1.63	.613	1.226	2		2.452
	C-F	4	1.63	.613	2.542	1		2.452
	C-G	2	3.12	.321	.642	4		2.568
	C-I	4	2.99	.334	1.336	2		2.672
	C-J	2	4.44	.225	.450	4		1.800
	C-L	4	3.91	.256	1.024	2		2.048
	C-M	2	5.12	.195	.390	4		1.560
	C-O	4	4.22	.237	.948	1		.948
							65.888	64.690

Attraction = 1.198 $\underline{-e^2A = -3.074}$

9	1-D	4	2.34	.427	1.708	4	6.832	
	1-F	8	2.63	.380	3.040	2	6.080	
	1-G	4	4.07	.246	.984	4	3.936	
	1-I	8	4.00	.250	2.000	2	4.000	
	1-J	4	5.46	.183	.732	4	2.928	
	1-L	8	4.92	.203	1.624	2	3.248	
	1-M	4	6.14	.163	.652	4	2.608	
	1-O	8	5.28	.189	1.512	1	1.512	

Table 2-1. (continued)

n	Type	Charge	Distance	1/Dist.	Potential	Multipl.	Attract.[a]	Repuls.[a]
	1-2	16	1.92	.521	8.336	2		16.672
	1-3	16	3.61	.277	4.432	2		8.864
	1-4	16	4.90	.204	3.264	2		6.528
	1-5	16	5.57	.180	2.880	2		5.760
	A-2	4	2.34	.427	1.708	4	6.832	
	A-3	4	4.07	.246	.984	4	3.936	
	A-4	4	5.46	.183	.732	4	2.928	
	A-5	4	6.14	.163	.652	4	2.608	
	A-D	1	2.33	.429	.429	4		1.716
	A-E	1	2.85	.351	.351	4		1.404
	A-F	2	3.14	.318	.636	4		2.544
	A-G	1	4.36	.229	.229	4		.916
	A-H	1	4.68	.214	.214	4		.856
	A-I	2	4.57	.219	.438	4		1.752
	A-J	1	5.90	.169	.169	4		.676
	A-K	1	6.14	.163	.163	4		.652
	A-L	2	5.52	.181	.362	4		1.448
	A-M	1	6.72	.149	.149	4		.596
	A-N	1	6.94	.144	.144	4		.576
	A-O	2	5.78	.173	.173	2		.692
	C-2	8	1.00	1.000	8.000	1	8.000	
	C-3	8	2.63	.380	3.040	2	6.080	
	C-4	8	4.00	.250	2.000	2	4.000	
	C-5	8	4.92	.203	1.624	2	3.248	
	C-6	8	5.28	.189	1.512	1	1.512	
	C-D	2	1.63	.613	1.226	2		2.452

Table 2-1. (continued)

n	Type	Charge	Distance	1/Dist.	Potential	Multipl.	Attract'n	Repuls'n
	C-F	4	1.63	.613	2.452	1		2.452
	C-G	2	3.14	.318	.636	4		2.544
	C-I	4	3.08	.325	1.300	2		2.600
	C-J	2	4.57	.219	.438	4		1.752
	C-L	4	4.16	.240	.960	2		1.920
	C-M	2	5.52	.181	.362	4		1.448
	C-O	4	4.72	.212	.848	2		1.696
	C-P	2	5.87	.170	.340	2		.680
							70.288	69.196

Attraction = 1.092, $-e^2A = -2.803$

n	Type	Charge	Distance	1/Dist.	Potential	Multipl.	Attract'n	Repuls'n
10	1-D	4	2.30	.435	1.740	4	6.960	
	1-F	8	2.63	.380	3.040	2	6.080	
	1-G	4	4.07	.246	.984	4	3.936	
	1-I	8	4.04	.248	1.984	2	3.968	
	1-J	4	5.53	.181	.724	4	2.896	
	1-L	8	5.07	.197	1.576	2	3.152	
	1-M	4	6.46	.155	.620	4	2.480	
	1-O	8	5.63	.178	1.424	2	2.848	
	1-P	4	6.78	.147	.588	2	1.176	
	1-2	16	1.91	.524	8.384	2		16.768
	1-3	16	3.63	.275	4.400	2		8.800
	1-4	16	4.95	.202	3.232	2		6.464
	1-5	16	5.84	.171	2.736	2		5.472
	1-6	16	6.15	.163	2.608	1		2.608
	A-2	4	2.30	.435	1.740	4	6.960	
	A-3	4	4.07	.246	.984	4	3.936	

Tagle 2-1. (continued)

n	Type	Charge	Distance	1/Dist.	Potential	Multipl.	Attract^n.	Repuls^n.
	A-4	4	5.53	.181	.724	4	2.896	
	A-5	4	6.46	.155	.620	4	2.480	
	A-6	4	6.78	.147	.588	2	1.176	
	A-D	1	2.26	.442	.442	4		1.768
	A-E	1	2.78	.360	.360	4		1.440
	A-F	2	3.10	.323	.646	4		2.584
	A-G	1	4.30	.233	.233	4		.932
	A-H	1	4.60	.217	.217	4		.868
	A-I	2	4.57	.219	.438	4		1.752
	A-J	1	5.89	.170	.170	4		.680
	A-K	1	6.12	.163	.163	4		.652
	A-L	2	5.66	.177	.354	4		1.416
	A-M	1	6.93	.144	.144	4		.576
	A-N	1	7.12	.140	.140	4		.560
	A-O	2	6.25	.160	.320	4		1.280
	A-P	1	7.30	.137	.137	2		.274
	A-R	1	7.60	.132	.132	2		.264
	C-2	8	1.00	1.000	8.000	1	8.000	
	C-3	8	2.63	.380	3.040	2	6.080	
	C-4	8	4.04	.248	1.984	2	3.968	
	C-5	8	5.08	.197	1.576	2	3.152	
	C-6	8	5.63	.178	1.424	2	2.848	
	C-D	2	1.63	.613	1.226	2		2.452
	C-F	4	1.63	.613	2.452	1		2.452
	C-G	2	3.10	.323	...646	4		2.584
	C-I	4	3.09	.324	1.296	2		2.592

Table 2-1. (continued)

n	Type	Charge	Distance	1/Dist.	Potential	Multipl.	Attract^{n}.	Repuls^{n}.
	C-J	2	4.57	.219	.438	4		1.752
	C-L	4	4.25	.235	.940	2		1.880
	C-M	2	5.66	.177	.354	4		1.416
	C-O	4	5.00	.200	.800	2		1.600
	C-P	2	6.25	.160	.320	4		1.280
	C-S	4	5.26	.190	.760	1		.760
							74.992	73.953

Attraction = 1.039, $\underline{-e^2A = -2.667}$

Table 2-2. (a).

Energy computation data of an endless chain of tetrahedra.

Type	1-2	$A-A_2$	$C-C_2$	$1-A_2$	A-2	$A-B_2$	$1-C_2$	C-2	$A-C_2$	$C-A_2$
Charge	16	1	4	4	4	1	8	8	2	2
Attrac^{n} or Repulsion	R	R	R	A	A	R	A	A	R	R
Multipl.	2	4	1	4	4	4	2	1	4	2
Dis-								1.00		1.63
tan-	1.63	=	=	1.91	=	2.33	2.51	=	2.85	=
ces	3.26	=	=	3.42	=	3.66	4.12	=	4.34	=
	4.89	=	=	5.00	=	5.16	5.75	=	5.90	=
	6.52	=	=	6.62	=	6.72	7.39	=	7.50	=
	8.15	=	=	8.24	=	8.34	9.00	=	9.11	=
	9.78	=	=	9.36	=	9.90	10.63	=	10.73	=
	11.41	=	=	11.49	=	11.52	12.27	=	12.35	=
	13.04	=	=	13.10	=	13.15	13.90	=	13.97	=
	14.67	=	=	14.71	=	14.80	15.52	=	15.58	=
	16.30	=	=	16.34	=	16.40	17.16	=	17.20	=
	17.93	=	=	17.95	=	18.02	18.78	=	18.82	=
	19.56	=	=	19.58	=	19.65	20.42	=	20.45	=
	21.19	=	=	21.20	=	21.25	22.04	=	22.08	=
	22.82	=	=	22.83	=	22.90	23.68	=	23.70	=
	24.45	=	=	=	=	24.50	25.30	=	=	=
	26.08	=	=	=	=	26.12	26.92	=	=	=
	27.71	=	=	=	=	27.74	28.56	=	=	=
	29.34	=	=	=	=	29.38	30.18	=	=	=
	30.97	=	=	=	=	30.97	31.78	=	=	=
	1-21	=	=	=	=	=	$1-C_{21}$	=	=	=
Charge x multipl.	------------- 12 R -------------						--------- 12 A -------			

Note: = sign indicates that distance is equal to the one left of it.

Table 2-2. (b).

Type	Charge x multipl.	Distance	1/Dist.	Attraction	Repulsion
1-2	40	1.63	.613		24.520
1-3	40	3.26	.307		12.280
1-4	40	4.89	.204		8.160
1-5	40	6.52	.153		6.120
1-6	40	8.15	.123		4.920
1-7	40	9.78	.101		4.040
1-8	40	11.41	.0876		3.520
1-9	40	13.04	.0767		3.080
1-10	40	14.67	.0682		2.728
1-11	40	16.30	.0613		2.452
1-12	40	17.93	.0558		2.232
1-13	40	19.56	.0511		2.044
1-14	40	21.19	.0472		1.888
1-15	40	22.82	.0438		1.752
1-16	8	24.45	.0409		.327
1-17	8	26.08	.0383		.306
1-18	8	27.71	.0361		.289
1-19	8	29.34	.0341		.273
1-20	8	30.97	.0323		.258
1-A_2	32	1.91	.524	17.344	
1-A_3	32	3.42	.292	9.344	
1-A_4	32	5.00	.200	6.400	
1-A_5	32	6.62	.151	4.832	
1-A_6	32	8.24	.121	3.832	
1-A_7	32	9.86	.101	3.232	
1-A_8	32	11.49	.0870	2.784	

Table 2-2.(b).

(continued)

Type	Charge x multipl.	Distance	1/Dist.	Attraction	Repulsion
1-A_{9}	32	13.10	.0763	2.442	
1-A_{10}	32	14.71	.0680	2.176	
1-A_{11}	32	16.34	.0612	1.958	
1-A_{12}	32	17.95	.0557	1.782	
1-A_{13}	32	19.58	.0511	1.635	
1-A_{14}	32	21.20	.0472	1.510	
1-A_{15}	32	22.83	.0438	1.402	
A-B_{2}	4	2.33	.429		1.716
A-B_{3}	4	3.66	.273		1.092
A-B_{4}	4	5.16	.194		.776
A-B_{5}	4	6.73	.149		.596
A-B_{6}	4	8.34	.120		.480
A-B_{7}	4	9.90	.101		.404
A-B_{8}	4	11.52	.0868		.347
A-B_{9}	4	13.15	.0760		.304
A-B_{10}	4	14.80	.0676		.270
A-B_{11}	4	16.40	.0610		.244
A-B_{12}	4	18.02	.0555		.222
A-B_{13}	4	19.65	.0509		.204
A-B_{14}	4	21.25	.0471		.188
A-B_{15}	4	22.90	.0437		.175
A-B_{16}	4	24.50	.0408		.163
A-B_{17}	4	26.12	.0383		.153
A-B_{18}	4	27.74	.0360		.144
A-B_{19}	4	29.30	.0341		.136

Table 2-2. (b).

(continued)

Type	Charge x multipl.	Distance	1/Dist.	Attraction	Repulsion
$A-B_{20}$	4	30.98	.0323		.129
$1-C_2$	24	2.51	.398	9.552	
$1-C_3$	24	4.12	.243	5.832	
$1-C_4$	24	5.75	.174	4.176	
$1-C_5$	24	7.39	.135	3.240	
$1-C_6$	24	9.00	.111	2.664	
$1-C_7$	24	10.63	.0941	2.258	
$1-C_8$	24	12.27	.0815	1.956	
$1-C_9$	24	13.90	.0719	1.726	
$1-C_{10}$	24	15.52	.0644	1.546	
$1-C_{11}$	24	17.16	.0583	1.399	
$1-C_{12}$	24	18.78	.0532	1.277	
$1-C_{13}$	24	20.42	.0490	1.176	
$1-C_{14}$	24	22.04	.0454	1.090	
$1-C_{15}$	24	23.68	.0422	1.013	
$1-C_{16}$	12	25.30	.0395	.474	
$1-C_{17}$	12	26.92	.0371	.445	
$1-C_{18}$	12	28.56	.0350	.420	
$1-C_{19}$	12	30.18	.0331	.397	
$1-C_{20}$	12	31.78	.0315	.378	
C-2	8	1.00	1.0000	8.000	
$A-C_2$	12	2.85	.351		4.212
$A-C_3$	12	4.34	.230		2.760
$A-C_4$	12	5.90	.169		2.028
$A-C_5$	12	7.50	.133		1.596

Table 2-2. (b).

(continued)

Type	Charge x multipl.	Distance	1/Dist.	Attraction	Repulsion
A-C_6	12	9.11	.110		1.320
A-C_7	12	10.73	.0932		1.118
A-C_8	12	12.35	.0810		.972
A-C_9	12	13.97	.0716		.859
A-C_{10}	12	15.58	.0642		.770
A-C_{11}	12	17.20	.0581		.697
A-C_{12}	12	18.82	.0531		.637
A-C_{13}	12	20.45	.0490		.588
A-C_{14}	12	22.08	.0453		.544
A-C_{15}	12	23.70	.0422		.506
C-A_2	4	1.63	.613		2.542
				109.692	110.081

Repulsion = .389, $\underline{-e^2A = + .998}$

Table 2-2. (c).

No. of tetrahedra	n^{th} average tetrahedron	Multipl. factor	Difference in distance	Total difference	x charge
20					
	25	10	.00052	.0052	.0624
30					
	40	20	.00020	.0040	.0480
50					
	75	50	.000054	.0027	.0324
100					
	150	100	.0000038	.0004	.0048
200					
	400	400	.0000020	.0008	.0096
600					
	5,300	9,400	.00000011	.0001	.0012
10,000					
				.0132	.1584

Additional repulsion = .158

Additional $-e^2A = + .406$

Total energy of endless chain = + .998

+ .406

+ 1.404 = + 1.41 ± .01

Supplement to Chapter III.

Classification of tetrahedral structures.

History of the classification of tetrahedral structures.

Since silicates form an important group of tetrahedral structures and since they represent important minerals in the crust of the earth, they received much attention. Other ionic tetrahedral structures were described and classified according to their analogy with the tetrahedral structures of silicates. Consequently, the history of the classification of tetrahedral structures began with the classification of silicates.

(1) In the early stages of mineralogy several attempts were made to classify the silicates. Most of these classifications were based on chemical and geological principles, and many of them persisted. The history of these classifications is difficult to trace in the literature. Many of them are constantly used, like the distinction between different silicates according to their cleavages, colors and weathering resistance; or the grouping of the silicates according to mineral assemblages, or to their occurance in similar rocks.

(2) The first crystallographic classification was presented by Machatschki[1] in 1928. With this he opened a new era of more rational classification. He recognized three major types:

I. Orthotype: separate tetrahedra of SiO_4

II. Metatype: chains of tetrahedra

III. Feldspar type: networks of tetrahedra.

(3) Machatschki's classification was improved two years later by W. L. Bragg[24] who added two more types. Bragg's classification has the following types:

I. Separate tetrahedra
II. Self-contained groups of tetrahedra
    (a) pairs of tetrahedra
    (b) rings of tetrahedra
III. Chains of tetrahedra
    (a) single chains
    (b) double chains
IV. Sheets of tetrahedra
V. Three-dimensional networks of tetrahedra.

(4) In the same year St. v. Náray-Szabó[25] added subdivisions to Bragg's classification. These subdivisions are based on the presence of accessory cations and anions in the tetrahedral structure of silicates. These subdivisions are:

1. Titano-silicates
2. Boro-silicates
3. Carbonato-silicates
4. Vanado-silicates
5. Sulphato-silicates
6. Sulfo-silicates
7. Silicates with several anions

(5) In 1932 Machatschki[26] enlarged his own classification by the recognition of the sheet structures. The new scheme of his classification is as follows:

I. Orthotypes. (separate tetrahedra, pairs, groups and rings of tetrahedra)
II. Metatypes. (chains of tetrahedra)
III. Mica types. (sheets of tetrahedra)
IV. Feldspar types. (three-dimensional networks of tetrahedra)

(6) In 1936 C. Hermann, O. Lohrmann and H. Philipp[27] adopted a classification which is essentially that of W. L. Bragg, except that they divide the first group into two parts:

I. Separate tetrahedra including other than O anions also
II. Separate tetrahedra not including other than O anions
III. Finite groups of tetrahedra
IV. Two-dimensional extended sheet of tetrahedra
V. Three-dimensional extended structures of tetrahedra.

(7) In 1937 H. Berman[28] presented a classification which was based on the close relationship between the chemical and physical characteristics of silicates. His types are:

I. Silica type	X:O	1:2
II. Disilicate type	X:O	2:5
III. Metasilicate types		
(a) chains	X:O	3:8
	X:O	4:11
	X:O	1:3
(b) rings	X:O	n:3n

IV. Pyrosilicates	X:0	3:7
V. Orthosilicates	X:0	1:4

He subdivided these types into divisions according to chemical and structural similarities between different structures of the same type. For example, in the silica type he listed groups like: Petalite, Silica, Feldspar, Nepheline, Canorinite, Sodalite and other groups. Some of these groups were further subdivided into members. The Feldspar group, for example, was subdivided into monoclinic and triclinic members.

(8) Also in 1937 C. Swartz[29] came out with another chemical modification of the already accepted scheme of crystallographic classification. His types which he called families are:

I. Orthosilicates (single tetrahedra)
II. Orthodisilicates (pairs of tetrahedra)
III. Metasilicates (chains and rings of tetrahedra)
IV. Metadisilicates (sheets of tetrahedra)
V. Dioxide types

He divided all these "families" of silicate structures into subdivisions according to their association with hydrous and anhydrous combinations of bi-, tri- and quadrivalent cations. He stressed these chemical characteristics more than the geometrical characteristics of silicates.

(9) In 1937, again, H. Strunz[30] presented a classification which differed from the principles of Machatschki's classification only in details. He recognized the following types:

I. Three-dimensional networks of tetrahedra
II. Sheets of tetrahedra
III. Chains of tetrahedra
IV. Groups of tetrahedra
V. Islands of tetrahedra (i.e. singles)
VI. Mixed structures of tetrahedra

He accepted other than Si and Al tetrahedra in the tetrahedral structures of silicates, such as P, As, Fe, B, Be, Zn, and Mg tetrahedra. He subdivided his types into "normal types" and "subtypes" according to the presence or absence of additional anions which are not connected with the tetrahedrally coordinated cations. He provided further subdivisions according to the presence of other than O anions, and to the variations in the cation-anion ratio in the structural-chemical formula of the silicates.

Between 1937 and 1954 no significant changes were proposed in the classification of the silicates or other tetrahedral structures. Most textbook authors and teachers of mineralogy accepted one or another of these classifications or a combination of two or more of them. It became a general practice, however, to separate the ring structures from the group structures and associate them with the chain structures. This was done because of the similarity of the cation-anion ratios in the structural formula of the chain and ring structures. Similarly, the chemical aspects of these classifications received considerably less attention than their geometric principles.

The system of classification started by Machatschki and Bragg was homogeneous. It involved no other than crystallographic principles. The other properties of silicates were explained through their structures. Later, however, other authors started to involve chemical principles and the original classification lost its power. The non-homogeneous nature of the later classifications is, probably, responsible for their unpopularity. In other words, the development of the classification of silicates became side-tracked and stopped. A revision of Machatschki's and Bragg's system, however, became essential due to the rapid increase of the determined silicate and other tetrahedral structures, especially of the three-dimensional network types.

In 1954 and in 1956 Wells and Liebau presented new advances in the development of the classification of tetrahedral structures. Both used different, but purely crystallographic principles, and as far as they went, they brought in healthy ideas. These two contributions are described below in more detail.

Review of Liebau's and Wells' classification of certain tetrahedral structures.

In his classification of silicates F. Liebau[4] accepts the Machatschki-Bragg classification and recognizes five types of silicate structures:

I. Silicates with single tetrahedra

II. Silicates with groups of tetrahedra

III. Silicates with single or double chains and rings of tetrahedra

IV. Silicates with sheets of tetrahedra

V. Silicates with three-dimensional networks of tetrahedra.

For the subdivisions of these types he introduces a new term which may be translated as 1-, 2-, 3-, 4-, and 5-fold repeat-units. This term refers to the number of tetrahedra in the periodic unit of the tetrahedral structure of silicates. For example, if, in a chain, each tetrahedron is translation equivalent of the other, the chain has a 1-fold repeat-unit, but if only every second tetrahedron is translationally identical, the chain has a 2-fold repeat-unit. An example of a chain with 2-fold repeat-unit is the pyroxene chain, and a 3-fold repeat-unit chain is the wollastonite chain. By the same principle double chains and rings can be broken down to such units and be subclassified according to them. An infinite number of chains welded together in a plane produce a sheet, and, consequently a sheet can be subclassified according to repeat-units. Furthermore, a three-dimensional network of tetrahedra can be resolved into a collection of sheets and can also be subclassified according to the number of tetrahedra in the periodic unit. Table 3-3. is a reproduction of Liebau's table of classification.

This classification subclassifies the simpler tetrahedral structures, such as the chains, rings and sheets, but is very awkward in the subclassification of the three-dimensional networks, In some structures it is hard to visualize subsheet structures and select the units. These units are not equivalent to the tetrahedral motif of the structure, which latter represents the number of tetrahedra which is repeated by the symmetry of the structure. Furthermore, it gives only two or three subdivisions for the three-dimensional networks. In principle, however, he introduced a good idea which can be worked into a practical classification.

A.F. Wells[3] classifies the two- and three-dimensional networks of polyhedra. His classification will be reviewed here with respect to the classification of tetrahedral structures only.

He derives the possible networks analytically, using the definition that in a two-dimensional network of tetrahedra the centers of the tetrahedra are connected to three other centers of tetrahedra through the corners. He calls such a network a three-connected net. Similarly a three-dimensional network of tetrahedra is a four connected net. The connections between tetrahedra form different loops of tetrahedra. If $\underline{\varphi_n}$ is the fraction of the total number of polygons (loops) which are $\underline{n}$-gons then

$$\varphi_3 + \varphi_4 + \varphi_5 + \varphi_6 + \dots\dots + \varphi_n = 1,$$

In a three-connected net:

$$3\varphi_3 + 4\varphi_4 + 5\varphi_5 + 6\varphi_6 + \dots\dots + n\varphi_n = 6,$$

and in a four-connected net:

$$3\varphi_3 + 4\varphi_4 + 5\varphi_5 + 6\varphi_6 + \dots\dots + n\varphi_n = 4.$$

The solutions of these equations give the possible combinations of polygonal loops of tetrahedra in two- and three-dimensional networks. The first 15 solutions for the two-dimensional networks are given in Table 3-4. N in this table refers to the number of tetrahedra in the tetrahedral motif. For example, No. 1. net is the mica or clay sheet, and No. 3. net is the apophyllite sheet.

The derivation of the three-dimensional networks is more complicated. The three-dimensional networks are regarded as collections of two-dimensional networks put together. The first 20 solutions of the four-connected nets are listed in Table 3-5. In actual structures, No.1. net is the cristobalite structure, No. 5. the quartz and No. 6. the tridymite structure.

This classification certainly subclassifies the two- and three-dimensional networks, but it has several drawbacks. First of all, it is too complicated and the determination of the place of a structure in this classification is a tedious undertaking. Structures with uneven sharing coefficients in the type of three-dimensional networks can not be classified in this system, unless the combinations of different n-connected nets is worked out. This would make the system even more complicated and would hide simple features in abstract expressions. In conclusion, Wells' classification gives the impression that he overcomplicated a simple problem. However, he discovered new principles of subclassification, namely the use of n-membered loops.

Determination of the possible sharing coefficient ranges.

It has been recognized by earlier authors that each type of the tetrahedral structure has a definite range of possible cation-anion ratios. Some silicate structures are even described by their silica radicals. Due to the relationship between the cation-anion ratio and the sharing coefficient it is obvious that each type and subtype must have a definite range of sharing coefficients. These possible ranges of sharing coefficients can be defined by the aid of geometrical and mathematical logic, keeping the previousely defined assumptions A and B in mind.

1,(a). In a single tetrahedron all the four corners are unshared and consequently, each corner belongs to one tetrahedron only. The sharing coefficient is therefore, 1.00.

1,(b). In a pair of tetrahedra six corners are unshared and two corners are joined, out of the eight corners of the two tetrahedra. Consequently, six corners belong to only one tetrahedron and two corners to two tetrahedra. These latter two corners are joined into one corner. The sharing coefficient can be expressed as an average:

$$\text{sharing coefficient} = \frac{6x1 + 2x2}{8} = 1.25 \qquad (3\text{-}1)$$

1,(c),(d). In the larger and in the mixed groups of tetrahedra the number of corners shared is a function of the number of tetrahedra in the group. If it is assumed that the groups do not form closed rings, then if there are n tetrahedra in a group, there are (n-1) shared corners, which represents 2(n-1) joined corners. Since there is a total of 4n corners in a group, there are 4n - 2(n-1) corners left unshared. Since the joined corners belong to two tetrahedra at the same time, they are asigned double weight and the unshared corners are assigned single weight.

$$\text{Sharing coefficient} = \frac{1[4n - 2(n-1)] + 2[2(n-1)]}{4n} =$$

$$= \frac{4n - 2n + 2 + 4n - 4}{4n} =$$

$$= \frac{6n - 2}{4n} = \frac{3n - 1}{2n} \qquad (3\text{-}2)$$

A quick look at the equation reveals that the sharing coefficient tends to but never reaches 1.50. Consequently, the sharing coefficient ranges from 1.00 to 1.50 for mixed groups and from 1.25 to 1.50 for larger groups, if there are no loops in the groups.

If there are loops of tetrahedra in the group, the number of loops should be added to the numerator of equation (3-2). If the group consists of closed loops only, it is obviously a ring structure, but if in addition to the rings there are tetrahedra which are not part of a loop, the structure is a group structure. It is possible that such a group structure contains a collection of small loops. The maximum sharing coefficient for such group structures would be 1.75.

2,(a),(b). In a single chain or ring of tetrahedra there is one shared corner per tetrahedra. The number of shared corners can not either be more or less than one. If it would be less the chain would break into groups. If it would be more the chain would either contain loops and would become a double or multiple chain, or would involve the sharing of edges.

Consequently, in a single chain or ring there are *n* tetrahedra and *n* shared corners:

$$\text{sharing coefficient} = \frac{1(4n - 2n) + 2(2n)}{4n} =$$

$$= \frac{4n - 2n + 4n}{4n} =$$

$$= \frac{6m}{4n} = \frac{3n}{2n} = 1.50 \qquad (3\text{-}3)$$

2,(c),(d). When two chains or rings are welded together the sharing coefficient increases according to the frequency of connection between the tetrahedra of the two single chains or rings. If the number of tetrahedra in the periodic unit of a chain, or the number of tetrahedra in a ring, is *n* and the number of connections between the two chains or rings is *k* per periodic unit of the chain, or per ring, the number of joined corners changes from $2n$ to $(2n+k)$ in the sharing coefficient equation of (3-3).

$$\text{Sharing coefficient} = \frac{1[4n - (2n+k)] + 2(2n+k)}{4n} =$$

$$= \frac{4n - 2n - k + 4n + 2k}{4n} =$$

$$= \frac{6n + k}{4n} \qquad (3\text{-}4)$$

The lower limit of the sharing coefficient range for double chains and rings is obviousely 1.50 +, and the upper limit is

1.75 where three corners are shared.

2,(e),(f),(g). Multiple chains and rings can be constructed by any number of connections between the single chains or rings. Consequently, the lower limit of sharing coefficient is that of the double chains and rings. At the upper limit all the four corners are shared and the sharing coefficient is 2.00. The smae limitations are obviously true for mixed chains and rings.

3,(a). A single sheet of tetrahedra can be constructed if more than two but less than three corners are shared. This gives the same upper and lower limits as (3-4).

3,(b),(c),(d). Theoretically two or more sheets can be welded together. In this case more than two corners have to be shared per tetrahedra, up to the maximum of four. In terms of sharing coefficient that is a range from 1.50 to 2.00.

4,(a). A three-dimensional network of tetrahedra can be constructed by sharing three or more corners between two tetrahedra. Such a network has a sharing coefficient from 1.75 to 2.00. More than two tetrahedra can also share a corner in three-dimensional networks. The upper limit for this subtype is a sharing coefficient of 4.00. Since the corners of a tetrahedron represent atoms whose radii are about half of the length of the edge of a tetrahedron, it is therefore geometrically impossible to join more than four tetrahedra together through their corners without sharing an edge.

4,(b). Sharing coefficients higher than 4.00 require the sharing of edges. Consequently the lower limit of three-dimensional networks with one or more edges shared is the sharing coefficient of 4.00. The upper limit is defined by a geometrical limitation. Since no more than eight tetrahedra can be placed together around a corner by allowing only edges to share, the upper limit of sharing coefficient is obviously 8.00.

4,(c). Any three-dimensional network with a sharing coefficient above 8.00 requires the sharing of faces. The maximum possible sharing coefficient is 25.00 where all the tetrahedral faces are shared.

In practice most of the sharing coefficient ranges defined above can be restricted by energy considerations. For example, groups of tetrahedra having a sharing coefficient between 1.50 and 1.75 require the presence of 3-membered loops. Such a configuration represents too high an energy concentration and, consequently, is highly improbable. Similarly, a double sheet of tetrahedra with the low sharing coefficient of 1.50 would require long stretches of single chains within the sheet, which represents a higher energy than a more frequently connected double chain. These improbable sharing coefficient ranges are placed between parentheses in Table 3-1.

(It might be necessary to define two terms used in the determination of the sharing coefficient ranges. These terms are "shared corners" and "joined corners". The former refers to a corner which is shared between several tetrahedra, while the latter refers to the several tetrahedral corners which are joined in this "shared corner".)

Definition of an n-membered loop in three-dimensional networks of tetrahedra.

The n-membered tetrahedral loops are easy to define in double chains, rings and sheets. A simple observation reveals the unmistakable loops. In multiple sheet structures and especially in three-dimensional networks of tetrahedra, however, the loops may require a definition in order to avoid possible misunderstanding. In the sodalite structure for example, 4- and 6-membered loops build up the so called ultramarine basket. But 10- and 12-membered loops can also be visualized. The 10-membered loop could be visualized where two 6- and one 4- membered loops are beside each other and have one common tetrahedron. If this common tetrahedron is neglected, the rest of the 6- and 4-membered loops give a complete 10-membered loop. The 12-membered loop could be similarly visualized around the equator of the spherical outline of the ultramarine basket. These loops are not accepted as loops, since they are only the descriptions of possible paths which are directed through a number of tetrahedra and end up with the original tetrahedron. Such paths are not considered as loops in the literature and are similarly disregarded in the subclassification of tetrahedral structures. However, to avoid any possibility of a mistake, the loops can be defined:

The n-membered loops accepted in the classification of tetrahedral structures are the regular or irregular closed loops of tetrahedra which are the smallest possible loops in the structure and their sizes can not be decreased by the inclusion of one or more neighbouring tetrahedra.

Table 3-3.

Liebau's classification of silicates.

	One-fold	Two-fold	Three-fold	Five-fold	Seven-fold
Single chain	$(CuGeO_3)_x$	Pyroxene	Wollastonite	Rhodonite	Pyroxmanganite
Double chain	Sillimanite	Amphibole	Xenotlite	Rabingtonite	
Sheets		Mica and clay	Apophyllite		
Networks		Quartz Tridymite Cristobalite	Feldspar		

Table 3-4.

Wells' classification of simple three-connected two-dimensional nets.

Net No.	N	Number of polygons in net									
		3	4	5	6	7	8	9	10	11	12
1	2	-	-	-	6	-	-	-	-	-	-
2	8,12	-	-	5	-	7	-	-	-	-	-
3	4	-	4	-	-	-	8	-	-	-	-
4	4	3	-	-	-	-	-	9	-	-	-
5	6	3	-	-	-	-	-	-	-	-	12
6	6	-	4	-	-	-	-	-	10	-	-
7	6	-	-	5	-	-	8	-	-	-	-
8	6	-	4	-	-	7	-	-	-	-	-
9	6	3	4	-	-	-	-	-	-	11	-
10	6	3	-	5	-	-	-	-	10	-	-
11	12	3	-	-	6	-	-	9	-	-	-
12	6	3	-	-	-	7	8	-	-	-	-
13	12	-	4	5	-	-	-	9	-	-	-
14	6	-	4	-	6	-	8	-	-	-	-
15	12	-	-	5	6	7	-	-	-	-	-

Table 3-5.

Wells' classification of simple four-connected three-dimensional nets.

Net No.	N	Number of polygons in net									
		3	4	5	6	7	8	9	10	11	12
1	2	-	-	-	6	-	-	-	-	-	-
2	3	3	-	-	-	7	8	-	-	-	-
3	3	-	4	-	6	-	8	-	-	-	-
4	3	-	-	-	6	-	8	-	-	-	-
5	3	-	-	-	6	-	8	-	-	-	-
6	4	-	-	-	6	-	-	-	-	-	-
7	4	-	4	-	6	-	8	-	-	-	-
8	4	-	4	-	6	-	8	-	-	-	-
9	4	3	-	-	-	-	8	-	10	-	-
10	4	3	-	-	-	-	8	9	-	-	-
11	4	3	4	-	-	7	8	-	10	-	-
12	4	3	-	5	6	-	-	9	10	-	-
13	4	-	4	-	6	-	8	-	-	-	-
14	4	-	4	5	-	-	8	-	-	-	-
15	4	-	4	-	-	-	8	-	-	-	-
16	4	3	-	5	-	-	8	-	-	-	-
17	4	3	4	-	-	-	8	-	-	-	-
18	4	-	4	-	-	-	8	-	-	-	-
19	4	3	-	-	-	-	-	9	-	-	-
20	4	3	-	-	6	-	-	-	-	-	-

Additional references.

24 W. L. Bragg: The structure of silicates. Zeit. Krist. B. 74, (1930) 237-305.

25 St. v. Naray-Szabo: Ein auf der Kristallstruktur basierendes Silikatesystem. Zeit. Phys. Chem. B.9,(1930) 356-377.

26 F. Machatschki: Kristallchemie der Silikate. Geol. Förenigens I. 54,(1932) 447-470.

27 C. Hermann, O. Lohrmann, H. Philipp: Table of content, Strukturbericht II. (1937) XX.

28 H. Berman: Constitution and classification of the natural silicates. Amer. Miner. 22, (1937) 342-408.

29 C. Swartz: Classification of the natural silicates. Amer. Miner. 22 (1937) 1073-1087; 1161-1174.

30 H. Strunz: Systematik und Struktur der Silikate. Zeit. Krist. B.98, (1937) 60-83.

Supplement to Chapter IV.

Classification of silicates.

Historical notes and added discussion.

In 1937 H. Strunz[5] presented the first silicate classification in which other than Si and Al tetrahedra were accepted in the tetrahedral frame of the silicates. The influence of his work was considerable in Germany. For example, W. Eitel[13] of the Kaiser Wilhelm Instituts für Kristallforschung accepted his theory completely. But Strunz's suggestion was either ignored or rejected in this continent. There were but a few arguments against his consideration of other than Si and Al tetrahedra in the tetrahedral frame of the silicates. One of the arguments stressed the different ionic radii of the other possible cations. Another argument criticized the different behavior of Si and other cations in infrared reflection spectrum and in x-rays. It is true that such differences exist, but they are no more severe than the difference between Si and Al. With one exception. Si and Al behave similarly in structure investigations using x-rays, while the other cations behave differently. But such an argument is immaterial, since the total number of electrons in a cation has no importance in the bonding of a tetrahedron.

Where could one draw the line between the acceptance and the rejection of a cation when such examples as the melilites exist? In hardystonite Si and Zn tetrahedra make up the sheet of tetrahedra, while in akermanite Si and Mg tetrahedra and in gehlenite Si and Al tetrahedra. By all standards gehlenite would be accepted as a tetrahedral sheet structure, but the others would be rejected by most mineralogists. Such a separation of otherwise almost identical structures in a classification would certainly sound artificial.

This irrational treatment of the different cations is recognized by several authors. Wyckoff, for example, writes the following in the introduction of his presentation of the silicate structures[15]:

"The classification that has been accepted is the conventional one based on the character of the silicon-oxygen associations which prevail - isolated silicate groups, silicate chains, and sheets, and silicate nets. To a degree, this is clear enough but with the borosilicates and aluminosilicates it becomes artificial and correspondingly unsatisfactory."

It seems reasonable to suggest that all tetrahedrally coordinated cations, with a previously described minor restriction, should be accepted in the tetrahedral frame of a silicate. This would certainly dissolve the "artificial" taste of the conventional classification and would permit a crystallographic and natural system of classification.

Additional references.

[13] W. Eitel: Physikalische Chemie der Silikate. J. A. Barth, 1941.

[14] J. W. Gruner: Progress in silicate structures. Amer. Miner. 33, (1948) 679-691.

[15] R. W. G. Wyckoff: Crystal Structures. Vol. III. (1953) XII, 1.

Supplement to Chapter V.

Simple technique for the construction of polyhedral models.

Possible improvement of the polyhedral model construction technique.

It is possible to improve the previously described technique to enable one to construct completely permanent polyhedral models. Instead of making the tetrahedra of acetate sheets they could be molded of liquid plastic, and then cured. These tetrahedra would be all solid and more decorative than the ones made of acetate sheets. A hole could be drilled in each apex of the tetrahedron, perpendicular of the oposite face. Small brass rods, with corresponding diameter, could be bent to a precalculated angle and placed into the corresponding holes of the tetrahedra. The calculation of the bending angle of the brass rods is relatively simple and most structures require the calculation of less than ten different angles. Such an improved model would be more elaborate to construct, but the extra effort would be justified if the model is expected to be used in classwork.

An attempt was made to construct such models. The molds for the tetrahedra were completed, but due to the lack of appropriate plastic the development of the technique has been temporarely suspended.

Biographical notes.

Tibor Zoltai was born in Gyor, Hungary on October 17, 1925. He attended public schools and highschools in Hungary and was enrolled in the Polytechnical University in Budapest. In 1945 he left Hungary with his parents as a political refugee. He attended the University of Graz, in Austria and the Sorbonne in Paris, France. In 1950 he immigrated to Canada and graduated from the University of Toronto in 1955 with a B.A.Sc. degree in Applied Geology.

He entered the Graduate School at Massachusetts Institute of Technology in the fall of 1955, and he was appointed half time teaching assistant from 1955 to 1958 and half time research assistant from 1958 to 1959.

He is a member of the Society of Sigma Xi, the American Crystallographic Association, the Mineralogical Society of America and the Association of Professional Engineers of the Province of Ontario.

He married Olga Wagner in 1950 and they have two children, Peter and Kathrina Zoltai.